JOURNAL OF STRUCTURAL
CHEMISTRY
VOLUME 2 NUMBER 6 1961

Volume 2 Number 6
1961

JOURNAL OF STRUCTURAL CHEMISTRY

ЖУРНАЛ СТРУКТУРНОЙ ХИМИИ
(ZHURNAL STRUKTURNOI KHIMII)

TRANSLATED FROM RUSSIAN

CONSULTANTS BUREAU, NEW YORK

NIKOLAI VASIL'EVICH BELOV (On His Seventieth Birthday)

Translated from Zhurnal Strukturnoi Khimii, Vol. 2, No. 6,
pp. 659-670, November-December, 1961

The eminent Soviet crystallographer and crystal chemist, Nikolai Vasil'evich Belov, was 70 years old on December 15, 1961. N. V. Belov was born in the town of Yanov, in the former Lyublin province (now in Poland), in the family of a doctor. His father, a Kiev man, was directed to work there after graduating from Kiev University. One year after the birth of their son the family returned to the Ukraine, where they lived at first in Rovno, and then in Ovruch in the former Volynsk province. On his mother's insistence N. V. Belov was sent to the First (Russian) School in Warsaw, which numbered V. I. Vernadskii, S. F. Ol'denburg, and the well-known revolutionary I. P. Kalyaev among its former pupils. There was no secondary school in Ovruch at that time.

Having graduated from his school with a gold medal, in 1910 Belov entered the metallurgical department of the Peterburg Polytechnic Institute. During those years the professors of the Polytechnic Institute included many eminent scientists of that time (N. S. Kurnakov, A. A. Baikov, V. A. Kistyakovskii, M. A. Pavlov, V. E. Grum-Grzhimailo, F. Yu. Levinson-Lessing, P. P. Fedot'ev, V. F. Mitkevich, and M. A. Shatelen), but the one to impress the students most was A. F. Ioffe to whom N. V. Belov always refers to as the man who determined his outlook. Belov carried out his diploma work on electrochemistry in the laboratory of V. A. Kistyakovskii.

During the first years of the Revolution, while still a student, Belov took a vigorous part in the building of industry in his native town of Ovruch, where he worked in the local council of national economy, and was its chairman in 1920-21. In 1921 Belov presented his diploma thesis, but continued to work in the Ovruch council of national economy. After the abolition of district councils of national economy he was for some time the authorized agent of the provincial council of national economy and the provincial trade association.

In 1924 Belov returned to Leningrad, where for ten years he worked in analytical chemical laboratories associated with the giant "Skorokhod" footwear factory.

In 1928 Belov was invited by A. E. Fersman to work on the academic journal "Priroda," and remained an active contributor for four years. From 1930, again at A. E. Fersman's invitation, he took part in work on the Khibinskii problem. The adoption of nepheline as a tanning agent for the leather industry, proposed and put into effect by Belov, led to a number of analogous investigations on other applications of nepheline, primarily in the light industry. For this work Belov was awarded in 1931 the prize of the Leningrad Soviet, which at that time had control of the Murmansk province.

His membership of the Academy of Sciences was confirmed in 1933 by his appointment as a part-time member of the staff of the Lomonosov Institute; in 1934 he was appointed to full-time work.

In 1934 O. Hassel's Crystal Chemistry was published in Germany; A. E. Fersman decided to have it published in Russian, but at first he could not find a suitable translator. However, remembering Belov's linguistic abilities, Fersman asked him to undertake this translation. Although Belov refused at first, Fersman's insistence won the day. The Russian translation proved to be twice the size of the German original, while the number of figures rose from six to 60. Belov studied an enormous amount of literature for this translation and as a result became a crystallographer. During this period he also became closely associated with the crystallographic structure laboratory established by A. K. Boldyrev in the Leningrad Mining Institute and was able to construct models of crystal structures, without which modern chemical crystallography is impossible.

Hassel's Crystal Chemistry was followed by the publication, under A. E. Fersman's editorship, of the third volume of "Fundamental Ideas of Geochemistry," which included Belov's translations of the fundamental work of Machatschki, Bragg, Schiebold, and Taylor on the crystal chemistry of silicates. From that time the crystal chemistry of silicates was for many years the main trend of Belov's work.

After moving from Leningrad to Moscow in 1936, Belov continued for some time to work in the Geochemical Section of the Lomonosov Institute, and in the following year he joined the Crystallographic Section of the Institute, which was headed by A. V. Shubnikov.

In 1938 Belov became head of the x-ray structural laboratory of this section, which by that time had become an independent institution—the Crystallography Laboratory of the Academy of Sciences of the USSR. After the reorganization of the laboratory as the Institute of Crystallography of the Academy of Sciences in the USSR, N. V. Belov has been the permanent head of its Structure Division.

In 1938-40 Belov led a new scientific trend in the USSR, associated with the transition of x-ray structural crystallography from the former method of trial and error to the new and more direct methods based on the use of Fourier series. The first strips for calculation of Fourier series were prepared in his laboratory; copies have gone to all structural laboratories of the Soviet Union. During all his subsequent scientific career Belov, together with his associates, worked successfully on methods for interpretation of x-ray diffraction data with the aid of various modifications of Fourier series.

During the years of the Great Patriotic War, when experimental work was difficult, Belov developed certain general, purely crystal-chemical, methods of structure analysis. One of these is the method of closest packings. This rigorous theory formed the basis of Belov's widely known book: "Structure of Ionic Crystals and Metallic Phases," which is a revised version of his doctorate dissertation, presented at the N. S. Kurnakov Institute of General and Inorganic Chemistry of the Academy of Sciences of the USSR in 1943.

In addition to developing the theory of closest packings, Belov was the prime mover of the adoption of Fedorov space groups in the training of future crystallographers. This initiative met with a warm response from the Department of Crystal Chemistry and Crystallography of the Moscow State University, headed by G. B. Bokii. The appropriate courses were started there and in the Gor'kii University, and experienced teachers were trained. Graduates of these two universities are now as competent in 230 space groups as classical crystallographers are in the 32 classes of symmetry.

From 1943 Academician A. V. Shubnikov has been actively introducing into crystal chemistry the principles of black and white symmetry, confining himself to point groups. At first these groups were regarded by Shubnikov as the crystallography of the future. However, in 1958 one of Belov's students in Gor'kii University (B. A. Tavger) showed that the phenomena of magnetism in general and of ferromagnetism in particular conform to black and white groups. Even before this W. Cochran and B. K. Vainshtein demonstrated the role of black and white groups in various forms of Fourier structure analysis. However, this involved space groups. At A. V. Shubnikov's request, these groups were derived in Leningrad by A. M. Zamorzaev, without an indication of their number. The derivation was radically simplified by Belov, together with his pupils N. N. Neronova, T. S. Smirnova, and others. The groups themselves were described with the use of the generally accepted "international" symbols. Their exact number (1651) was determined, and the symbols proposed by Belov are now universally accepted. The theory of black and white groups was subsequently developed into the theory of color groups. During the last few years this theory has developed rapidly as the result of fruitful competition between the Soviet crystallographic school headed by Belov, and the British school of W. Cochran.

The main direction of Belov's creative scientific work has always been in the crystal chemistry of silicates. His initial intention was to increase the numbers of examples in the classification established by W. L. Bragg and his school, which usually contain only one or two representatives. The first determination achieved by Belov, that of the structure of dioptase, provided the second example of a silicate with a six-membered ring. In the second determination, that of the structure of ramsayite, it was shown that the metasilicate chain radical SiO_3 and free oxygen atoms are contained in the silicate with the ratio $O:Si = 4\frac{1}{2}$, which is higher than the orthosilicate ratio ($O:Si = 4$). The very next interpretation (that of milarite) revealed an entirely new silicon–oxygen motif—a "double-deck" hexagonal ring.

Very unexpected was the discovery of diorthosilicate groups, Si_2O_7, together with oxygen atoms not involved in silicon–oxygen radicals, in minerals which had been regarded as classical orthosilicates—ilvaite, epidote, and zoisite. The last two minerals contain both ortho groups and diortho groups simultaneously. It was shown that whereas the main silicate building block in Mg, Fe, and Al silicates is the SiO_4 group, in silicates with large cations (Ca, Na, and the rare earths) the building block is the Si_2O_7 group. New metasilicate chains of the same general formula SiO_3 but with larger units were discovered in Ca and Na chain silicates: $Si_{2+1}O_6$ in wollastonite, $Si_{2+1+2}O_{15}$ in rhodonite. Subsequently this series was augmented ($Si_{2+3}O_{12}$ radicals in narsarsukite). In just the same way, in addition to the classic Si_4O_{11} amphibole chain, analogous chains cut with eight-membered Si_6O_{17} rings were found in xonotlite.

A very interesting fact is that the chemistry of alkali titano- and zirconosilicates proved to be very similar to the crystal chemistry of Ca and Na silicates, including those in cements. Thus, the relatively simple structure of

cuspidine, $Ca_4Si_2O_7(F, OH)_2$, now "heads," on purely geometrical grounds, the series of titano- and zirconosilicates, in which the silicate protion remains the same as in cuspidine; in the four columns corresponding to the four Ca atoms in the cuspidine formula "white" Ca or Na ions alternate with "colored" cations, which may be Zr, Ti, Mn, and Fe in different columns (lovenite, wöhlerite, seidozerite, and rosenbuschite).

All this brilliant work of Belov and his direct pupils in the field of silicate structure gained much recognition both in the USSR and abroad. In 1946 he was elected Corresponding Member of the Academy of Sciences USSR, and in 1953 he became Academician. In 1952 he was awarded a State Prize of the first class.

Nikolai Vasil'evich Belov celebrates his 70th birthday in full vigor and creative activity. He is now the universally accepted leader of the Soviet structural school, the chairman of the National Committee of Soviet Crystallographers, and Vice-President of the International Union of Crystallography. He has published more than 300 papers, more than one half of which has appeared since 1953.

The Editorial Board of Zhurnal Strukturnoi Khimii cordially wishes him many years of fruitful work and sound health for the good of Soviet science.

A list of N. V. Belov's publications from 1954 to 1961 is given below. A list of publications before 1954 was given in Trudy instituta Kristallografii, No. 9, pp. 13-19 (1954).*

1954

168. "Essays in structural mineralogy, Vol. 17. Some characteristics of the geochemistry of boron in the light of its crystal chemistry. 18. The structure of chrysotile–antigorite. 19. Chloritoid–an orthosilicate? 20. Bornite, Cu_5FeS_4. 21. The structure of realgar and orpiment and some aspects of the geochemistry of sulfur and arsenic. 22. Rutile–anatase–brookite–ilmenite–hematite–columbite. 23. Cassiterite." Mineralog. sb. L'Vovsk. geol. obshch., 8, AN SSSR 13-40.

169. "The structure of nepheline." Tr. Inst. kristallogr., No. 10, 6-9 (15-18) (in French, pp. 19-23).

170. Editorship of the book: Transactions of the Institue of Crystallography, Academy of Sciences USSR, No. 10, pp. 1-408 [in Russian and French] (jointly with A. V. Shubnikov).

171. "At the Third International Congress of Crystallography." Vestn. AN SSSR, 11, 75-80.

172. Review of the book by H. Lipson and W. Cochran: Determination of Crystal Structures (London, 1953). Novye knigi za rubezhom, 10, 3-8.

1955

173. "Crystal structure of zoisite." Dokl. AN SSSR, 102, 2, 275-278 [with E. G. Fesenko and I. M. Rumanova].

174. "Crystal structure of cuspidine." Zap. Mineralog. obshch., pt. 84, 2, 159-169 [with R. F. Smirnova and I. M. Rumanova].

175. "Physics of the solid state." Gazeta Gor'kovsk. univ., 19-20.

176. Review of the book by H. P. Klug and R. E. Alexander: X-ray Diffraction Procedures for Polycrystalline and Amorphous Materials (New York, 1954). Novye knigi za rubezhom, 7, 3-7.

177. "Shubnikov group 1651." Tr. Inst. kristallogr., vyp. AN SSSR, 11, 33-67 [with N. N. Neronova and T. S. Smirnova].

178. "Crystal structure of jeremejevite." Dokl. AN SSSR, 104, 1, 78-80 [with N. I. Golovastikov and E. N. Belov].

179. "Crystal structure of jeremejevite." Zap. Mineralog. obshch., pt. 84, 4, 405-414 [with N. I. Golovastikov and E. N. Belova].

* Three Publications were omitted from that list:

1926

165. Translation of J. A. Wilson's book: Chemistry of Leather Manufacture (Leningrad, Izd. "Myl' ") [jointly with I. A. Syrkin].

1948

166. Editorship of G. G. Lemmlein's book: Sectorial Structure of Crystals [in Russian] (Izd. AN SSSR, Moscow-Leningrad).

1953

167. "The founder of modern crystallography. On the 100th anniversary of the birth of E. S. Fedorov." Leningradskaya Pravda, 300 (11791), December 22, 1953 [jointly with D. V. Nalivkin].

180. "Geometrical interpretation of the Zachariasen statistical equation." Dokl. AN SSSR, 104, 1, 540-542 [with N. I. Golovastikov].

181. "Crystal structure of xonotlite." Dokl. AN SSSR, 104, 4, 615-618 [with Kh. S. Mamedov].

182. "Weak and strong relationships between the signs of structure amplitudes." Dokl. AN SSSR, 105, 5, 978-980 [with N. I. Golovastikov].

183. "Closest Packings." Great Soviet Encyclopedia [in Russian] 33, 289-290.

184. "Essays in structural mineralogy. VI. 24. More about the mechanism of polarization effects. The role of the f-hole. 25. Relationship between the external form and atomic structure of certain silicates." Mineralog. sb. L'vovsk. geol. obshch., 9, 3-14.

185. "The atomic structure of glass." In the collection: Structure of Glass, Conference Proceedings, November 23-27, 1953, p. 344-350.

186. Editorship of and comments on the book: A. E. Fersman, Selected Works, Vol. 3 [in Russian] (Izd. AN SSSR, Moscow).

187. "In the Department of Crystallography and Metal Physics." Gazeta Gor'kovskogo Univ., 37-38.

1956

188. "Characteristics of Patterson syntheses for centrosymmetric structures." Dokl. AN SSSR, 106, 3, 462-463 [with Kh. S. Mamedov].

189. "Crystal structure of minerals of the wollastonite group. I. Xonotlite." Zap. Mineralog. obshch., pt. 85, 1, 13-38 [with Kh. S. Mamedov].

190. "Crystal structure of wollastonite." Dokl. AN SSSR, 107, 3, 463-466 [with Kh. S. Mamedov].

191. "X-ray investigation of the crystal structure of chkalovite." Dokl. AN SSSR, 108, 6, 1077-1080 [with Yu. A. Pyatenko and G. B. Bokii].

192. "Color symmetry groups." Kristallografiya, 1, 1, 6-13 [with T. N. Tarkhova].

193. "Strip methods for Fourier synthesis calculations." Kristallografiya 1, 1, 132-136 [with T. N. Tarkhova].

194. "Crystal structure of zolsite." Kristallografiya, 1, 2, 165-196 [with E. G. Fesenko and L. M. Tarkhova].

195. "Nomographic method for calculation of structure factors." Kristallografiya, 1, 2, 236-239 [with T. N. Tarkhova].

196. "The group of the 48-faced polyhedron." Kristallografiya, 1, 3, 360-361 [with T. N. Tarkhova].

197. "Unidimensional infinite crystallographic groups." Kristallografiya, 1, 4, 474-476.

198. "Rational methods for calculating various close packings of spheres." Kristallografiya, 1, 5, 491-494 [with V. V. Bakakin].

199. "Symmetry of Patterson syntheses (functions)." Kristallografiya, 1, 5, 594-595 [with N. I. Shulepova].

200. "Medieval Moorish ornamentation in the framework of symmetry groups." Kristallografiya, 1, 5, 610-613.

201. Corrections to the paper: "Color symmetry groups." Kristallografiya, 1, 5, 615 [with T. N. Tarkhova].

202. "Color symmetry groups." Kristallografiya, 1, 6, 619-620 [with T. N. Tarkhova].

203. "Three-dimensional mosaics with color symmetry." Kristallografiya, 1, 6, 621-626.

204. "Guide for modeling of crystal structures and crystal-chemical motifs." Kristallografiya, 1, 6, 733-734.

205. "Methods for representing cubic space groups." Kristallografiya, 1, 6, 764-768.

206. "Peculiarities of the crystal chemistry of group IV elements of the periodic system." In the collection of the Institute of Metallurgy of the Academy of Sciences, USSR: Theory and Investigation of Semiconductors and Processes in Semiconductor Metallurgy [in Russian] (Izd. AN SSSR, Moscow) pp. 5-13.

207. "Essays in structural mineralogy. VII. 26. Pyroxenes, pyroxenoids, and their condensation products. 27. Interfarded structures. 28. More about the role of close packing in the external characteristics of minerals and their combinations. The Curie principle. 29. Mineral structures based on the rod principle. 30. Prod domo sua. 31. High-temperature cordierites. Mineralog. sb. L'vovsk. geolog. obshch., 10, 10-32.

208. Editorship, introduction, and comments on the translation of the book by H. Lipson and W. Cochran: Determination of Crystal Structures (Izd. inostr. lit., Moscow) [Russian translation by E. N. Belova, N. I. Golovastikov, and L. M. Rumanova].

209. N. W. Bielow. Krystallografia strukturalna. Translated into Polish by T. Volno. (State Scientific Press, Warsaw) 145 pp.

210. N. V. Belov. Structural Crystallography [Chinese translation] (Peking) 82 pp.

1957

211. "Alekseĭ Vasil'evich Shubnikov." Kristallografiya, 2, 1, 5-8 [with G. B. Bokii].

212. "Mosaics for 46 plane (Shubnikov) antisymmetry groups and for 15 color (Fedorov) groups. Kristallografiya, 2, 1, 21-22 [with E. N. Belova].

213. "Structure of silicates." Abstracts of papers at the Second Conference on Crystal Chemistry [in Russian] (Izd. AN SSSR, Moscow) pp. 10-16.

214. "Structure of silicates." Zap. Mineralog. obshch., pt. 86, 2, 239-244.

215. "New silicate structures." Kristallografiya, 2, 3, 366-370.

216. "Shubnikov groups." Kristallografiya, 2, 3, 315-325 [with N. N. Neronova and T. S. Smirnova].

217. "Energy sources of geochemical processes." Priroda, 5, 11-20 [with V. I. Lebedev].

218. "Crystal structure of hederite, datolite, and gadolinite." Dokl. AN SSSR, 114, 4, 884-887 [with P. V. Pavlov].

219. "A course of geometrical crystallography for physicists." Kristallografiya, 2, 5, 678-685.

220. "Tetartohedral and gyrohedral groups." Kristallografiya, 2, 6, 722-724.

221. "Theorem of the emptiness of a reduced elementary parallelepiped." Kristallografiya, 2, 6, 725-727.

222. "Essays in structural mineralogy. VIII. 32. Hypomorphism. 33. Specific symmetry of atoms. 34. 'Tendencies' of atoms in crystal structures and methods of satisfying them. 35. Silicon–oxygen chains (bands) of the simple formula $[Si_2O_5]_\infty$. 36. Carbonate apatites. 37. Miscellanea. 38. More about peculiarities of rutile crystallization." Mineralog. sb. L'vovsk. geol. obshch., 11, 3-21.

223. "On O. P. Mchedlov-Petrosyan's criticism of the hypothesis of accumulation of solar energy by crystalline matter." Mineralog. sb. L'vovsk. geolog. obshch., 11, 371-374 [with V. I. Lebedev].

224. "Crystal chemistry of the fundamental petrological process." In the Symposium on Geochemistry of Rare Elements in Relation to the Petrogenesis Problem [in Russian] (Izd. AN SSSR, Moscow).

225. Review of the book by M. J. Buerger: Elementary Crystallography. Novye knigi za rubezhom, 7, 56-64.

226. "Chemical Energy and Metamorphism." Geochim. et Cosmochim. Acta, 12, 348 [with V. I. Lebedev].

227. N. V. Belov. "New Silicate Structures." IV. International Congress of Crystallography. Montreal, 10-19 July, 1957. Abstracts of Communications, 29-30.

228. N. V. Belov, N. N. Neronova, and T. S. Smirnova. The 1651 Shubnikov groups. Ibidem, 120.

229. N. V. Belov. "A Classroom method of derivation of the 230 spacegroups." Proc. Leeds Philosophical and Literary Society. VII, part III, 19-66.

230. N. V. Belov. "New Silicate Structures." Acta crystallogr., 10, 757-759.

231. N. V. Belov, N. N. Neronova, and T. S. Smirnova. "The 1651 Shubnikov Groups." Acta crystallogr., 10, 848.

1958

232. "Crystal structure of amblygonite." Dokl. AN SSSR, 119, 2, 351-356 [with V. I. Simonov].

233. "The quartz extinction law." Kristallografiya, 3, 1, 89-90.

234. "Graphical method of solving the fundamental Harker–Kasper inequalities." Kristallografiya, 3, 1, 90-92 [with S. V. Borisov and P. V. Pavlov].

235. "Structure of silicates." Khimicheskaya nauka i promyshlennost', 3, 1, 46-56.

236. "Morphology of crystal faces in the light of the fine structure of crystals." Kristallografiya, 3, 2, 225-227

237. "Ways of creating a complete Soviet course of crystallography." Kristallografiya, 3, 2, 246-249.

238. "Structure analysis in the Gor'kii State University." Gazeta "Gor'kovskii universitet," 7 (401), March 15 1958.

239. Review of the book by P. Terpstra: Introduction to Space Groups (Groningen–Jakarta, 1955). Novye knigi za rubezhom, 11A, 2, 48-52.

240. Review of the book by A. Guinier: Theory and Practice of X-ray Structural Analysis (2nd edition, Paris, 1956). Novye knigi za rubezhom, 11A, 3, 57-62.

241. "Congress of Crystallography in Montreal." Vestn. AN SSSR, 3, 64-67 [with B. K. Vainshtein].

242. "Fourth International Congress of Crystallography." Kristallografiya, 3, 2, 250-260 [with L. M. Belyaev, G. B. Bokii, E. G. Bronnikova, B. K. Vainshtein, G. S. Zhdanov, V. I. Iveronova, A. I. Kitaigorodskii, and Z. G. Pinsker].

243. "Arbitrarily assigned signs in direct methods of interpretation of crystal structures." Kristallografiya, 3, 2, 269-276 [with S. V. Borisov and V. P. Golovachev].

244. "Crystal chemistry of the fundamental (petrological) process of magma crystallization." In collection: Geochemistry of the Rare Elements [in Russian] (Izd. AN SSSR, Moscow) pp. 95-99.

245. New Silicate Structures. USSR Section, Brussels Universal and International Exhibition, 1958.

246. "Crystal structure of mica-like Ca hydrosilicates: okenite, nekoite, truscottite, and gyrolite. The new silicon-oxygen radical $[Si_6O_{15}]_\infty$." Dokl. AN SSSR, 121, 4, 720-723 [with Kh. S. Mamedov].

247. "Crystal structure of foshagite, $Ca_4[Si_6O_{17}](OH)_2$." Dokl. AN SSSR, 121, 5, 901-903 [with Kh. S. Mamedov].

248. "Essays in structural mineralogy. IX. 39. Tabular forms of corundum crystals and individuality in corundum. 40. Concretions of garnets with micas and corundum. 41. Another characteristic feature of orthosilicates and island silicates in general. 42. A metal phase with garnet structure. 43. The structure of type of eulytin. 44. Cubic structures with nonintersecting threefold axes: analcime-garnet-pyrite. 45. Hydrated monazite. Its structural relation to zircon, thorite, anhydrite, and simultaneously to quartz. 46. Crystal structure of prehnite. 47. Sphene, durangite, and amblygonite. 48. The spinel and olivine structure types of the geochemical role of their respective transitions. 49. Rhombic analogs of feldspars. 50. Palygorskite and sepiolite. 51. Structural glaciology. Borax. 52. Smithite, a new (rhombohedral) iron sulfide. 53. More about the structures of realgar and orpiment. 54. The 'acid' function of lithium." Mineralog. sb. L'vovskogo geol. obshch., 12, 15-42.

249. "Determination of the crystal structure of amblygonite by the minimalization method." Kristallografiya, 3, 4, 427-437 [with V. I. Simonov].

250. Review of the book by D. McLachlan: X-ray Crystal Structure (New York, London, and Toronto). Novye knigi za rubezhom, 11A, 9, 29-36.

251. "Charles Mauguin." Kristallografiya, 3, 4, 497-498.

252. "Shunikov groups." Kristallografiya, 3, 5, 635-636 [with G. Donnay, N. N. Neronova, and T. S. Smirnova].

253. "More about color symmetry groups." Kristallografiya, 3, 5, 618-620 [with T. N. Tarkhova and E. N. Belova].

254. "Crystal structure of seidozerite." Dokl. AN SSSR, 122, 3, 473-476 [with V. I. Simonov].

255. "Crystal structure of tobermorite (the tobermorites)." Dokl. AN SSSR, 123, 1, 163-165 [with Kh. S. Mamedov].

256. "Crystal structure of hillebrandite." Dokl. AN SSSR, 123, 4, 741-743 [with Kh. S. Mamedov].

257. "Synthesis and structure of hydrosilicates containing simple and complex heavy-metal ions." Proceedings of the Fifth Conference on Experimental and Technical Mineralogy and Petrography, March 26-31, 1956 [in Russian] pp. 38-43 [with V. S. Molchanov and N. E. Prikhid'ko].

258. "Project for a university course on Fedorov groups." Kristallografiya, 3, 6, 765-772.

1959

259. "Crystal structure of hurlbutite." Dokl. AN SSSR, 125, 2, 383-385 [with V. V. Bakakin].

260. "Hexagonal Fedorov groups." Kristallografiya, 4, 2, 268-276.

261. "Isomorphous relationships between zirconium and titanium." Dokl. AN SSSR, 125, 4, 888-889 [with V. I. Simonov].

262. "Crystal structure of seidozerite." Kristallografiya, 4, 2 [with V. I. Simonov].

263. "Crystal structure of tricalcium silicate hydrate." Dokl. AN SSSR, 126, 1, 151-154 [with Kh. S. Mamedov and R. F. Klevtsova].

264. "The wochlerite and rinkite groups." Dokl. AN SSSR, 126, 2, 379-381 [with Kh. S. Mamedov and V. I. Simonov].

265. "Determination of the crystal structure of herderite, datolite, and gadolinite by direct methods." Kristallografiya, 4, 3, 324-340 [with P. V. Pavlov].

266. "Concerning the paper by A. A. Beus: Position of the alkali metals in the structure of beryl." Geokhimiya, 4, 3, 282-284.

267. "E. S. Fedorov (on the 40th anniversary of his death)." Collected Papers of the Fedorov Session on Crystallography, 1959 [in Russian] pp. 5-8 (in English, pp. 9-12).

268. "Simplest method for derivation of Fedorov (space) groups." Kristallografiya, 4, 3, 289-292 [with R. F. Klevtsova].

269. "D. P. Serdyuchenko's calciotalcite." Zap. Mineralog. obshch., pt. 88, 3, 305-308.

270. "More about the simplest method for derivation of Fedorov groups." Kristallografiya, 4, 4, 473-476 [with R. F. Klevtsova].

271. "Covariant and contravariant relationships between derived and original structures." Kristallografiya, 4, 4, 608-612.

272. Contribution to the Development of Crystallography. Moscow News, 44 (353), June 3, 1959. (Interview).

273. Essays in structural mineralogy. X. 55. The second chapter in the crystal chemistry of silicates. 56. Two mineralogical groups with Si_2O_7 island groups (radicals): a) wochlerite-lovenite; b) rinkite-lamprophyllite. 57.

Isomorphous relationships between zirconium and titanium. 58. Silicon–oxygen chains and bands in the second chapter of the crystal chemistry of silicates. 59. Crystal structure of rhodonite. 60. Silicon–oxygen networks based on wallastonite chains and xonotlite bands." Mineralog. sb. L'vovsk. geol. obshch., 13, 23-52.

274. "Conference of the Crystallography Section of the German Mineralogical Society." Vestn. AN SSSR, 7, 88-89.

275. "Georgii Borisovich Bokii." Kristallografiya, 4, 4, 463-465.

276. "Max Laue." Kristallografiya, 4, 5, 639-640.

277. "Crystal structures of danburite and hurlbutite." Dokl. AN SSSR, 129, 2, 420-423 [with V. V. Bakakin and V. B. Kravchenko].

278. "Crystal structure of epididymite. A new type of infinite silicon–oxygen bands." Dokl. AN SSSR, 129, 4, 900-903 [with E. A. Pobedimskaya].

279. "International Fedorov Session on crystallography in Leningrad." Kristallografiya, 4, 5, 796-800 [with B. K. Vainshtein, A. L. Kitaigorodskii, M. A. Porai-Koshits, S. A. Semiletov, and N. N. Sheftal'].

280. "Nomenclature of 80 plane groups in three dimensions." Kristallografiya, 4, 5, 775-778.

281. "The symmetry of ferroelectric materials." Dokl. AN SSSR, 129, 3, 556-557 [with N. N. Neronova].

282. "The fundamental theorem of the close packing theory." Kristallografiya, 4, 6, 918-919.

283. "Ferromagnetic and ferroelectric space groups." Kristallografiya, 4, 6, 807-812 [with N. N. Neronova].

284. "Expanded formulas of Beryl." Geokhimiya, 4, 8, 734-736.

285. "On the arbitrarily chosen signs in direct methods of solving crystal structures." Proc. National Inst. Sci. India, 25A, 4, 220-229 [with S. V. Borisov and V. P. Golovachev].

1960

286. "Cayley squares for cubic groups." Kristallografiya, 5, 1, 129-134 [with T. N. Tarkhova].

287. "Problems in the crystal chemistry of silicates." Kristallografiya, 5, 1, 15-18.

288. "Crystal structure of lovozerite." Dokl. AN SSSR, 130, 6, 1333-1336 [with V. I. Simonov].

289. "Crystal structure of lovozerite." Dokl. AN SSSR, 131, 1, 176-179 [with V. V. Ilyukhin].

290. "The structure of glass in the light of the crystal chemistry of silicates." Proceedings of the Third All-Union Conference on the Glassy State, Leningrad, November 16-20, 1959 [in Russian] pp. 91-98.

291. "The second chapter of the crystal chemistry of silicates." Zh. strukt. khimii, 1, 1, 39-56.

292. "Sodium borosilicate glasses." Proceedings of the Third All-Union Conference on the Glassy State, Leningrad, November 16-20, 1959 [in Russian] p. 524.

293. "False symmetry in the structure of lawsonite." Kristallografiya, 5, 2, 215-217 [with L. M. Rumanova].

294. "The so-called 'sulunite.'" Zap. Mineralog. obshch., pt. 89, 3, 367-369 [with D. P. Serdyuchenko].

295. "Chapter B of the Crystal Chemistry of Silicates." Fortschr. Mineral., 38, 1, 4-6 (Stuttgart, April 1960).

296. "Determination of the structure of lovozerite from sections of a three-dimensional Patterson function." Kristallografiya, 5, 2, 200-214 [with V. V. Ilyukhin].

297. "Structure of thiocyanopentamminecobaltinitrate $[Co(NH_3)_5 \cdot NCS](NO_3)_2$." Dokl. AN SSSR, 130, 6, 1327-1329 [with T. L. Malinovskii and L. D. Samus].

298. "Crystal structure of baddeleyite." Kristallografiya, 5, 3, 460-461.

299. "Max Laue (obituary note)." Kristallografiya, 5, 2, 460.

300. "Essays in structural mineralogy. IX. 61. New pages of the second chapter of the crystal chemistry of silicates. 62. More about the crystallographic approach to the problem of the nature of titano- and zirconosilicates. 63. More about the specific behavior of silica in native silicates and in analogous synthetic products. 64. One page in the first chapter of the crystal chemistry of silicates: sphene (durangite), ambylgonite, and kieserite; and one page of the second–narsarsukite. A new type of silicon–oxygen band. 65. The missing link in the crystal chemistry of silicates-the quaternary metasilicate ring $[Si_4O_{12}]$. 66. An atomic cellular gel (structure of lovozerite). 67. Molecular sieves. 68. Ferromagnetic garnets. 69. Structure of baddeleyite (monoclinic ZrO_2). 70. Hoentite, $CaMg_3(CO_3)_4$, an intermediate mineral between dolomite and magnesite." Mineralog. sb. L'vovsk. geol. obshch., 14, 3-33.

301. "Point groups of color symmetry (color classes." Kristallografiya, 5, 4, 497-500 [with V. L. Indenbom and N. N. Neronov].

302. "The Crystal Structure of Silicates. Chapter 2." Fifth International Congress of the International Union of Crystallography. Sec. 9. General Lectures, p. 8.

303. "The Berlin symposium on silicates with uni- and bivalent cations." Khim. nauka i prom-st', 5, 686-688.

304. "Consideration of the isomorphous presence of boron in silicates within the framework of crystal chemistry." Geokhimiya, 5, 5, 564-569.

305. "The second V. I. Vernadskii scientific lecture." Geokhimiya, 5, 5, 570-571 [with the assistance of the Editorial Board].

306. "Leonid Mikhailovich Belyaev." Kristallografiya, 5, 5, 674-676.

307. "The structure of epididymite, $NaBeSi_3O_7OH$. A new type of infinite silicon-oxygen chains (bands)." Zh. strukt. khimii, 1, 51-63 [with E. A. Pobedimskaya].

308. "Crystal structure of hurlbutite." Dokl. AN SSSR, 135, 3, 587-590 [with V. V. Bakakin].

309. "Crystal structure of paracelsian." Kristallografiya, 5, 6, 864-888 [with V. V. Bakakin].

310. "Crystal structure of sperrite." Kristallografiya, 5, 5, 689-697 [with R. F. Klevtsova].

311. "Neue Seiten aus dem zweiten Kapitel der Kristallchemie der Silikate." Silikattechnik, 11, 8, 389-390.

312. "To the memory of V. I. Vernadskii." Vestn. AN SSSR, 6, 147-148.

313. "Tables of magnetic space groups. A joint project." International Union of Crystallography. Fifth International Congress. Abstracts of Communications, p. 111 [with N. N. Neronova, J. D. H. Donnay, and G. Donnay].

314. "The crystal structure of silicates. Chapter 2." Acta crystallogr., 13, 980.

315. "Tables of magnetic groups. A joint project." Acta crystallogr., 13, 1085 [with N. N. Neronova, J. D. H. Donnay, and G. Donnay].

316. Minerals. Handbook. Part 1 [in Russian] (Izd. AN SSSR) [Descriptions of known structures and crystal chemistry, jointly with a team of associates, edited by F. V. Chukhrov and E. M. Bonshtedt-Kupletskaya].

317. "Symposium on silicates with uni- and bivalent cations." Zh. prikladnoi khimii, 33, 11, 2598-2600 [with N. E. Prikhid'ko, V. I. Simonov, V. A. Fleisinskaya, and O. P. Mchedlov-Petrosyan].

1961

318. "Unified scheme of classic and black-white crystallographic groups." Kristallografiya, 6, 1, 3-12 [with N. N. Neronova].

319. "Crystal structure of hopeite, $Zn_3(PO_4)_2 \cdot 4H_2O$." Kristallografiya, 6, 1, 114-117 [with Kh. S. Mamedov and R. Gamidov].

320. "Crystal structure of eudidymite, $NaBeSi_3O_7OH$." Dokl. AN SSSR, 136, 6, 1448-1450 [with E. A. Pobedimskaya].

321. "Crystal structure of brandisite." Dokl. AN SSSR, 137, 1, 167-170 [with Yu. A. Akhundov and Kh. S. Mamedov].

322. "Neutron-diffraction investigation of the cubic modification of PbF_2." Dokl. AN SSSR, 138, 1, 110-111 [with I. I. Yamzin and Yu. Z. Nozik].

323. "The position of quartz in the system of natural and synthetic silicon-oxygen compounds." Zap. Vses. mineralog. obshch., pt. 90, 2, 168-171.

324. "The Friedel theorem." Zap. Vses. mineralog. obshch., pt. 90, 3, 257-259.

325. "Essays in structural mineralogy. XII. 71. Epididymite-eudidymite. 72. Natural and synthetic zeolites--molecular sieves. 73. The position of quartz in the system of natural and synthetic silicon-oxygen compounds. 74. The melilite-okermanite group. 75. Datolite-apophyllite. 76. Keatite (kitite) a new tetragonal modification of silica. 77. Vlasovite. Another type of the chain silicon-oxygen radical $[Si_4O_{11}]_\infty$. 78. Kousite (koesite)-another modification of silica of high density. Its structural relationship to orthoclase. 79. Danburite-hurlbutite-paracelsian. 80. The analogy between phosphates and silicates. Mineralog. sb. L'vovsk. geol. obshch., 15, 5-44.

326. Editorship, introduction, and notes to the translation of the book by M. J. Buerger: Crystal Structure and Vector Space (translated by E. N. Belova and V. I. Simonov). (Izd. inostr. lit., Moscow) pp. 1-385.

327. "Crystal structure of bertrandite, $Be_4Si_2O_7(OH)_2$." Dokl. AN SSSR, 140, 3, 685-688 [with L. P. Solov'eva].

328. "Crystal structure of rubidium di(meta)fluoberyllate, $RbBe_2F_5$." Dokl. AN SSSR, 140, 5, 1066-1069 [with V. V. Il'yukhin].

329. "Crystal structure of praseodymium nitrate hydrate, $Pr(NO_3)_3 \cdot 6H_2O$." Kristallografiya, 6, 6, 919-922 [with G. F. Volodina and L. M. Rumanova].

330. "Crystal chemistry of silicates with large cations." Second V. I. Vernadskii Lecture [in Russian] (Izd. AN SSSP, Moscow) p. 68.

331. "Specific character of isomorphous presence of small atoms, in particular boron, in alien lattices." Geokhimiya, 6, 10, 942-945.

332. "Colored antisymmetrical mosaics." Kristallografiya, 6, 6, 831-839 [with N. N. Neronova].

333. Editorship. Introduction and notes to the translation of the book by A. Guinier: X-ray Crystallography. Theory and Practice [Russian translation by E. N. Belova, S. S. Kvitka, and V. P. Tarasov]. (Fizmatgiz, Moscow) 604 pp.

334. "The morphological aspect of hopeite." Kristallografiya, 6, 6, 825-827 [with V.Kliber].

335. "Trends in the development of modern crystallography." (Review of the 5th International Congress of Crystallography)." Vestn. AN SSSR, 4, 99-104 [with B. K. Vainshtein].

336. "Crystal structure of rubidium di(meta)fluoberyllate $RbBe_2F_5$ and its model relationships to laminar silicates with the $[Si_2O_5]$ radical." Kristallografiya, 6, 6, 847-858.

POTENTIOMETRIC STUDY OF THE STRUCTURE OF HYDRATED IONS IN SOLUTIONS

A. M. Golub and A. A. Baran

T. G. Shevchenko Kiev State University
Translated from Zhurnal Strukturnoi Khimii, Vol. 2, No. 6,
pp. 671-676, November-December, 1961
Original article submitted April 17, 1961

It is shown that the coordination numbers of metal ions in solution can be determined potentiometrically. Investigations of mixed water–dioxane, water–acetone, and water–alcohol solutions showed that the coordination numbers of the hydration shells of lead and silver approximate to 4 and 3 respectively.

One of the most important problems in the physical chemistry of solutions is determination of the nature and degree of ion solvation. Various methods have been proposed for determination of the coordination number of hydrated ions in aqueous and mixed (mainly aqueous alcohol) solutions.

Zaidel' and Rotshtein [1] studied the absorption spectra of aqueous alcoholic solutions of neodymium chloride and found that addition of six to eight molecules of water per neodymium ion in alcoholic solution results in complete replacement of the solvating alcohol molecules by water molecules. Rotshtein [2] measured the optical density of aqueous alcoholic $NdCl_3$ solutions and calculated the coordination number of the hydration shell of the neodymium ion; it was found to be four. These authors deny the possibility that mixed solvation shells can be formed around ions. On the other hand, Pominov [3] concluded that neodymium ions solvated by alcohol and water simultaneously exist in aqueous alcoholic solutions if not enough water is present for complete hydration. Usanovich et al. [4], who studied vapor pressure variations in the $CoCl_2–CH_3OH–H_2O$ system, refer to the simultaneous interaction of bivalent cobalt ions with both components of the mixed solvent.

Mishchenko [5] showed, from calculations of the solvation energies of ions and on spatial considerations, that the coordination numbers of ions lie within fairly narrow limits, between 4 and 8. This conclusion is confirmed by the data of Mishchenko and Pominov [6], who studied the absorption spectra of Cu^{2+}, Co^{2+}, and Nd^{3+} ions in aqueous alcoholic solutions and found that the coordination numbers in hydration of these ions are four, four, and six respectively, the maximum coordination number being six. They attribute this discrepancy to simultaneous coordination of water molecules and anions around these ions if the concentration of the nonaqueous solvent is high and the salt in it is predominantly in the undissociated state. Bjerrum and Jörgensen [7] also found that the coordination number of the solvation shells of neodymium and praseodymium ions in aqueous alcoholic solutions is six. Samoilov [8] showed by a thermochemical method that the coordination numbers of the hydration shells of Li^+, Na^+, K^+, Cl^-, Br^-, I^-, Mg^{2+}, Ca^{2+}, Sr^{2+} and Ba^{2+} ions in aqueous solutions are 3,8; 3,7; 3,8; 4,4; 4,8; 5,3; 3,8; 4,0; 4,4; and 4,8 respectively; i.e., that they lie in a relatively narrow range.

Pasynskii [9] determined the numbers of water molecules bound by ions in solutions (hydration numbers) and found the following values: 5-7 for alkali metals, 8 for Be^{2+}, 16 for Mg^{2+} and Ba^{2+}, and 31 for Al^{3+}. Some workers [10] consider that in general one cannot speak of a definite hydration number because the energy of hydration progressively decreases for successive molecules attached to a given ion.

In a study of mixed solutions one of us [11,12] observed increases of the electrode potential of a metal in equilibrium with an aqueous nitrate or perchlorate solution if alcohol, acetone, or dioxane was added to this solution. This was attributed to the so-called negative complex formation effect [13] involving dehydration of the metal ion as the result of formation of compounds between water and donor-active molecules of nonaqueous solvents. Others [14] have also referred to the possible dehydration of ions in solution.

Accordingly, and in view of the fact that the data cited above on ion hydration are contradictory even when determined for the same substance, we attempted to study ion solvation by a potentiometric method.

Starting Materials and the Solutions Used

Metal perchlorates were used for the investigation, as the ClO_4^- ion is the least active complex former. Moreover, perchlorates are less liable to hydrolysis than other salts [15].

Lead perchlorate was synthesized as described in [16]. Alcoholic solutions were prepared from anhydrous $Pb(ClO_4)_2$, which was obtained by drying of the hydrated salt in a vacuum drying oven over phosphoric anhydride at 170-180° [16]. Silver perchlorate was prepared from excess silver oxide and the chemically pure acid. Sodium perchlorate of analytical-reagent grade was recrystallized twice. Dilute lead amalgam (used as the indicator electrode) was prepared by saturation of pure mercury with metallic lead made by electrolysis of c.p. $Pb(NO_3)_2$.

The nonaqueous solvents were dioxane, methanol, and acetone. Dioxane was left to stand and boiled with $KMnO_4$ for purification, and was dehydrated by treatment with metallic sodium on standing followed by distillation over sodium. Acetone and methyl alcohol were dried by the usual method [17]. The anhydrous nonaqueous solvents were kept in waxed bottles or sealed ampoules before the experiments.

The circuits used for the investigation consisted of a saturated calomel electrode (the reference electrode) and a silver (for $AgClO_4$) or lead amalgam [for $Pb(ClO_4)_2$] indicator electrode. The salt concentrations of the solutions were constant while the concentrations of the nonaqueous solvents were varied. The measurements were performed by the balancing method with the PPTV-1 high-resistance potentiometer. The null instrument was a sensitive galvanometer of the GZP-47 type. The experiments were performed at 20 ± 0.05°.

Results and Discussion

The results of the potentiometric measurements are given in Tables 1-4. The sensitivity in the measurements of the potentials of silver and lead electrodes at not excessively high concentrations of the nonaqueous solvents in the mixtures (up to 8 M dioxane and up to 15 M methyl alcohol) was 0.0002 v. The equilibrium potentials became established in an average time of 20-40 minutes. With higher contents of these solvents the sensitivity fell to 0.001 v. The time for establishment of the equilibrium potential was then 40-80 minutes (for alcohol and dioxane mixtures) or 2-4 hours (for acetone solutions).

TABLE 1. Results of Potentiometric Investigation of the System $Pb(ClO_4)_2-H_2O-$Dioxane (salt concentration 0.02007 M)

Water concentration in mixture, M	Dioxane concentration in mixture, M	$\lg [H_2O]^a$	Potentials, v	$\lg \frac{[Pb^{2+}]}{[Pb^{2+}]_{nonhydr}}$ hydr / nonhydr
5,56	10,56	—	—0,337	—
8,33	9,95	0,921	—0,349	0,200
11,11	9,36	1,046	—0,358	0,623
13,89	8,77	1,143	—0,367	0,991
16,67	8,19	1,222	—0,3778	1,389
22,22	7,02	1,347	—0,3919	1,886
27,78	5,85	1,447	—0,4018	2,232
33,34	4,68	1,523	—0,4103	2,525
38,89	3,51	1,590	—0,4170	2,758

The following must be pointed out before a discussion of these results. It has been shown by us and others [16,18] that dioxane forms molecular compounds with perchlorates of the above-named metals: $AgClO_4 \cdot 3C_4H_8O_2$ and $Pb(ClO_4)_2 \cdot 2C_4H_8O_2$. Therefore it might have been expected that the potentials of these metals in aqueous dioxane mixtures should decrease with increasing concentration of the nonaqueous solvent as the result of complex formation. In reality (see Tables 1-4) the potentials increase appreciably in aqueous dioxane and in the other mixed solutions. It is therefore likely that in aqueous solutions metal complexes with such organic ligands as dioxane, alcohol, and acetone are not formed. Moreover, increase of the nonaqueous-solvent concentration in the system results in the formation of ions of a lower degree of hydration, and this leads to the observed increase of potentials.

For quantitative interpretation of our results we assume that at the maximum concentration of the nonaqueous solvent the Ag^+ and Pb^{2+} ions are in the "bare" or nonhydrated state. This assumption is obvious for pure alcoholic solutions, while for dioxane and acetone mixtures it is justified as follows. The very fact that the potentials increase

on introduction of the organic solvents indicate that the latter interact with water molecules. It is also known from the literature that the dioxane molecule (like the acetone molecule) can bind three, four, or even six water molecules [19]. In our experiments the concentrations of dioxane and acetone in the first mixtures were approximately double the water concentration. Therefore, in this case we can postulate nonhydrated ions and, starting with the potential of the metal in this mixture (taking this as the standard value), we can use the Nernst equation for calculating the concentration of the "bare" metal ions. The concentration of hydrated ions is found by difference. We then plot the relationship

$$\lg \frac{[Me^{n+}]_{hydr}}{[Me^{n+}]_{nonhydr}} = f(\lg [H_2O])$$

(as for determination of the composition of complexes [20]), and l from the slope of the line we find the coordination number of the hydration shell of the given ion. The results are presented in this form in Figs. 1-4.

TABLE 2. Results of Potentiometric Investigation of the System $Pb(ClO_4)_2-H_2O-$Acetone (salt concentration 0.01003 M)

Water concentration in mixture, M	Acetone concentration in mixture, M	$\lg [H_2O]$	Potentials, v	$\lg \frac{[Pb^{2+}]_{hydr}}{[Pb^{2+}]_{nonhydr}}$
5,56	12,28	—	—0,334	—
6,49	11,98	0,814	—0,355	0,635
8,33	11,59	0,921	—0,364	0,993
11,11	10,91	1,046	—0,378	1,504
16,67	9,55	1,222	—0,390	1,927
22,22	8,14	1,347	—0,4079	2,517
27,78	6,82	1,447	—0,4152	2,801
33,34	5,46	1,523	—0,4213	3,011
33,89	4,09	1,530	—0,4258	3,166

TABLE 3. Results of Potentiometric Investigation of the System $Pb(ClO_4)_2-H_2O-CH_3OH$ (salt concentration 0.0199 M)

Water concentration in mixture, M	Alcohol concentration in mixture, M	$\lg [H_2O]$	Potentials, v	$\lg \frac{[Pb^{2+}]_{hydr}}{[Pb^{2+}]_{nonhydr}}$
—	31,25	—	—0,335	—
8,33	25,56	0,921	—0,353	0,438
11,11	25,00	1,046	—0,365	0,954
13,89	23,43	1,143	—0,374	1,313
15,28	22,65	1,184	—0,383	1,635
16,67	21,87	1,222	—0,389	1,844
22,22	18,75	1,347	—0,394	2,019

TABLE 4. Results of Potentiometric Investigation of the System $AgClO_4-H_2O-$Dioxane (salt concentration 0.02055 M)

Water concentration in mixture, M	Dioxane concentration in mixture, M	$\lg [H_2O]$	Potentials, v	$\lg \frac{[Ag^+]_{hydr}}{[Ag^+]_{nonhydr}}$
5,56	10,58	—	0,546	—
8,33	9,95	0,921	0,525	0,123
11,11	9,36	1,046	0,510	0,492
13,89	8,77	1,143	0,498	0,755
16,67	8,19	1,222	0,4895	0,925
19,45	7,60	1,289	0,4822	1,043
22,22	7,02	1,347	0,4751	1,195
26,14	6,15	1,422	0,4658	1,404

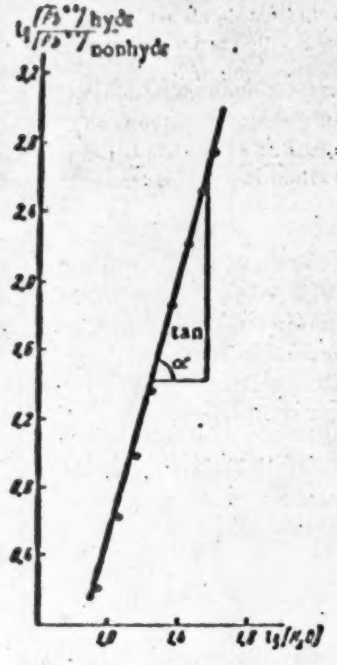

Fig. 1

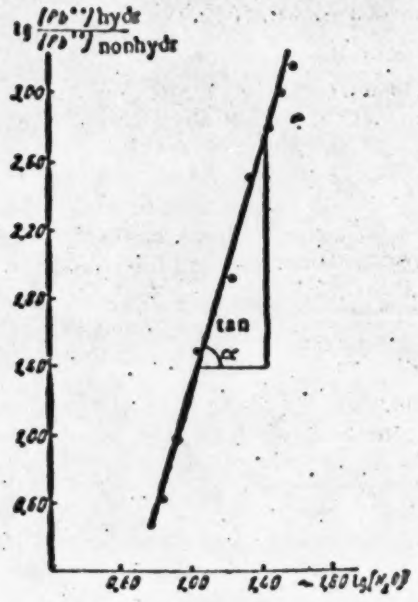

Fig. 2

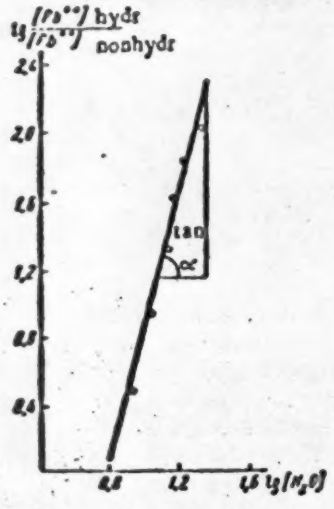

Fig. 3

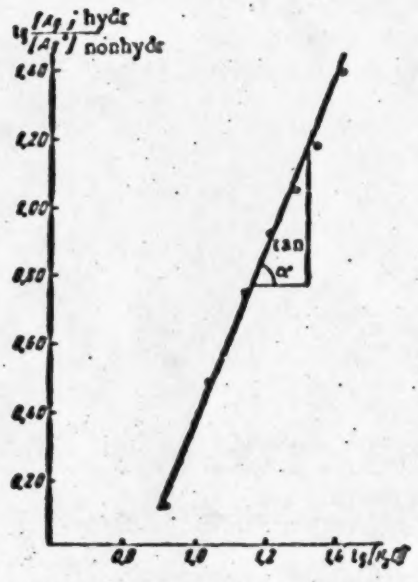

Fig. 4

Fig. 1. Variation of $\log \frac{[Pb^{2+}]\ \text{hydr}}{[Pb^{2+}]\ \text{nonhydr}}$ with $\log [H_2O]$ for dioxane–water solvent.

Fig. 2. Variation of $\log \frac{[Pb^{2+}]\ \text{hydr}}{[Pb^{2+}]\ \text{nonhydr}}$ with $\log [H_2O]$ for acetone–water solvent.

Fig. 3. Variation of $\log \frac{[Pb^{2+}]\ \text{hydr}}{[Pb^{2+}]\ \text{nonhydr}}$ with $\log [H_2O]$ for methanol–water solvent.

Fig. 4. Variation of $\log \frac{[Ag^{+}]\ \text{hydr}}{[Ag^{+}]\ \text{nonhydr}}$ with $\log [H_2O]$ for dioxane–water solvent.

These results show that the coordination number of the hydration shells of lead and silver ions approximates to the values of four and three respectively in all the solvents studied. Our results therefore confirm the view that the coordination numbers of ion hydration comprise only a few units, most often three or four. The coordination numbers of the hydration shells of many other metal ions can be found similarly.

Unfortunately we were unable to measure the emf of the system $AgClO_4-H_2O-CH_3OH$, because silver perchlorate is readily reduced in aqueous alcoholic mixtures.

LITERATURE CITED

1. A. Zaidel' and V. Rotshtein, Dokl. AN SSSR, 57, 587 (1947).
2. V. Rotshtein, Dokl. AN SSSR, 71, 335 (1950).
3. L. S. Pominov, Zh. fiz. khimii, 21, 1926 (1957).
4. M. L. Usanovich, V. R. Sergeeva, and M. B. Bakeev, Uch. zap. Kazakhsk. Univ., 22, 130 (1956).
5. K. P. Mishchenko, Zh. fiz. khimii, 26, 1736 (1952); 27, 26 (1953).
6. K. P. Mishchenko and L. S. Pominov, Zh. fiz. khimii, 21, 2026 (1957).
7. J. Bjerrum and H. Jörgensen, Acta chem. scand., 7, 6, 951 (1953).
8. O. Ya. Samoilov, Structure of Aqueous Electrolyte Solutions and Ion Hydration [in Russian] (Izd. AN SSSR, Moscow, 1957).
9. A. G. Pasynskii, Zh. fiz. khim., 2, 606 (1938).
10. E. Glueckauf and G. P. Kitt, Nature, 171, 1010 (1953).
11. A. M. Golub, Nauk. shchorichnik. Kiivs'k. Univ., 380 (1957).
12. A. M. Golub, Nauk. zap. Kiivs'k. Univ., Khim. zbirn., 8, 13 (1957).
13. A. M. Golub, Dokl. AN SSSR, 120, 6, 1255 (1958).
14. R. Matuura and Y. Koga, Met. Fac. Sci. Kyushu Univ., C3, 1, 21 (1928); cited through RZhKhim., 30628 (1959).
15. L. V. Tananaev and M. Ya. Bokmel'der, Zh. neorg. khimii, 3, 1273 (1958).
16. A. M. Golub, A. A. Baran, and T. L. Tsitsurina, Ukr. khim. zh., 27, 443 (1961).
17. A. Weissberger et al. Organic Solvents [Russian translation] (Izd. inostr. lit., Moscow, 1958).
18. A. E. Comyns and H. J. Lucas, J. Amer. Chem. Soc., 76, 1019 (1954).
19. J. K. Coates and R. L. Sullivan, J. Phys. Chem., 62, 183 (1958).
20. A. M. Golub, Ukr. khim. zh., 19, 205 (1953); 19, 486 (1953).

All abbreviations of periodicals in the above bibliography are letter-by-letter transliterations of the abbreviations as given in the original Russian journal. *Some or all of this periodical literature may well be available in English translation.* A complete list of the cover-to-cover English translations appears at the back of this issue.

CHANGES OF STRUCTURE IN AQUEOUS SOLUTIONS OF NONELECTROLYTES

V. A. Mikhailov

Institute of Inorganic Chemistry, Siberian Division of the Academy of Sciences, USSR

Translated from Zhurnal Strukturnoi Khimii, Vol. 2, No. 6, pp. 677-681, November-December, 1961
Original article submitted April 1, 1961

Breaks were found in solubility isotherms of sparingly soluble nonelectrolytes in water–ethyl alcohol and water–acetone mixtures and in viscosity isotherms of aqueous alcohol mixtures. In every case the break is found when the mole fraction of ethyl alcohol or acetone is close to 0.1. This effect is probably caused by a sharp change in the solution structure as the result of filling of the cavities in the water structure by molecules of the second component.

In 1938 Martin and Brown [1] discovered a sharp break, corresponding to a mole fraction of about 0.1 of alcohol in the water–ethyl alcohol system, in the plot of the logarithm of the activity coefficient of water against $(D-1)/(2D+1)$ (where D is the dielectric constant of the mixture). They attributed this break to the persistence of the quasicrystal lattice of water in dilute ethyl alcohol solutions. Later Mitchell and Wynne-Jones [2], using D. I. Mendeleev's density data for aqueous ethyl alcohol solutions, found a break in the curve for the partial molar volume of the alcohol at the same alcohol concentration. It must be pointed out that the composition $x_{alcohol} \approx 0.1$ is close to the composition of the most distinct "special point" noted by Mendeleev [3], corresponding to the hypothetical compound $C_2H_5OH \cdot 12H_2O$ ($x_{alcohol} \approx 0.08$), which was detected by Mendeleev from the break in the ds/dp curve (where s is the density and p is the percentage of alcohol by weight), i.e., essentially by the same method. A similar curve for the partial molar volume of alcohol, calculated by Hildebrand from other data, is given without comment in the well-known book by Lewis and Randall [4]. Mitchell and Wynne-Jones attributed the unusual course of the curve for the partial molar volume to a change in the structure of the solution in the region of low ethyl alcohol concentrations. At a low alcohol concentration its molecules remain outside the water lattice, but as the alcohol concentration increases the solution structure undergoes a sharp change accompanied by breakdown of the original structure of liquid water. Similar effects were discovered recently in aqueous solutions of higher alcohols [5,6].

We have discovered breaks at the same ethyl alcohol concentration in several solubility isotherms of a sparingly soluble nonelectrolyte in mixtures of water and ethyl alcohol and on solubility isotherms of acetanilide in water–acetone mixtures. It should be pointed out here that the solubility of a sparingly soluble substance in a mixed solvent may be regarded as one of the properties of the mixed solvent.

We showed earlier [5] that solubility isotherms of nonelectrolytes in binary mixed solvents conform to the equation

$$\lg(x_1/s_{12}) = x_3^0 \lg(s_{13}/s_{12}) + x_2^0 x_3^0 (a + bx_3^0 + cx_3^{0\,2}). \qquad (1)$$

where x_1 is the mole fraction of nonelectrolyte 1 in its saturated solution; s_{12} and s_{13} are the solubilities, in mole fractions, of nonelectrolyte 1 in the pure solvents 2 and 3; x_2^0 and x_3^0 are the mole fractions of components 2 and 3 in the mixed solvent; a, b, and c are constants. Equation (1) was verified with the aid of extensive literature data. For most systems the relationship between $\log(x_1/s_{12})$ and x_3^0 is represented by a smooth curve; only four systems of the type nonelectrolyte–water–ethyl alcohol, and the system acetanilide–water–acetone, give curves with breaks which cannot be attributed to transitions in the solid phase. Two such anomalous curves are given in Fig. 1.

The existence of inflections (breaks of the first derivative) in these curves may be doubted. We therefore used the method developed jointly with A. N. Kirgintsev for revealing inflections, based on substitution of a new function $\Phi(x)/x$ for the function $\Phi(x)$ passing through the origin. It can be shown that the break in the $\Phi(x)/x$ curve appears at the same value of the variable, but is much sharper than in the $\Phi(x)$ curve (compare curve 1 in Fig. 1 with curve 1 in Fig. 2, and curve 2 in Fig. 1 with the curve for 20° in Fig. 4). This method is henceforth used without additional explanations.

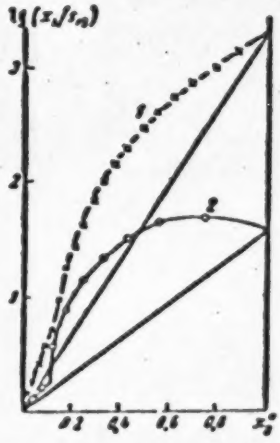

Fig. 1. Anomalous solubility isotherms: 1) $I_2-H_2O-C_2H_5OH$, 15° [7]; 2) acetanilide$-H_2O-(CH_3)_2CO$, 20° [9].

Fig. 2. Breaks on solubility isotherms: 1) $I_2-H_2O-C_2H_5OH$, 15° [7]; 2) dimethylglyoxime$-H_2O-C_2H_5OH$, 25° [8].

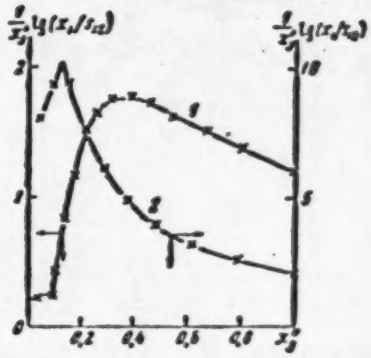

Fig. 3. Breaks in solubility isotherms: 1) $HgCl_2-H_2O-C_2H_5OH$, 25° [10]; 2) salicylic acid$-H_2O-C_2H_5OH$, 70° [9].

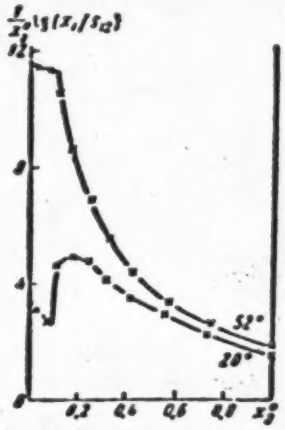

Fig. 4. Breaks in solubility isotherms of acetanilide in $H_2O-(CH_3)_2CO$ mixtures at 20 and 52° [9].

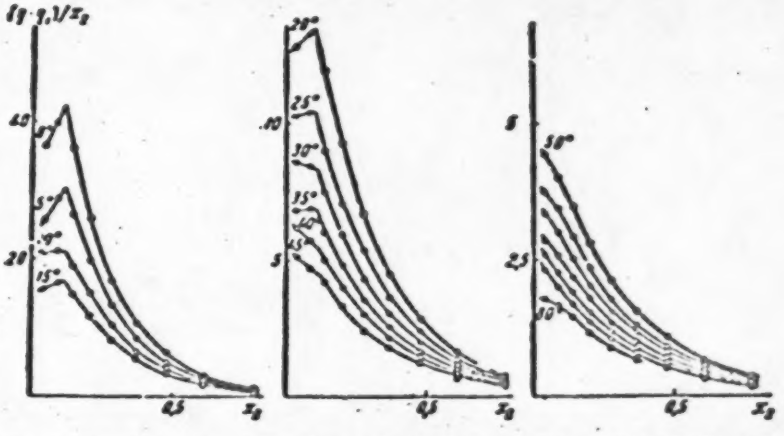

Fig. 5. Breaks in viscosity isotherms for the system $H_2O-C_2H_5OH$ [11]. In the right-hand diagram the isotherms correspond to temperature at intervals of 5°.

In Figs. 2-4 $1/x_3^0 \log(x_1/s_{12})$ is plotted against x_3^0 for the five ternary systems which are given in the table and which have breaks in their solubility isotherms. We did not find any other systems with breaks in an examination of data available in the literature.

Since in four of these five systems the mixed solvent is aqueous ethyl alcohol, it is reasonable to assume that the mixed solvent itself is responsible for the occurrence of the break, especially as the break occurs at a mole fraction of 0.10-0.12 of the alcohol (see table) in all the systems. In the system acetanilide–water–acetone the break is also found when the mole fraction of acetone is 0.10.

TABLE. Systems with Breaks in Solubility Isotherms

System	t°, C	s_{12}	s_{13}	x_3^0 at break	Literature
I_2(1)–water(2)–ethyl alcohol (3)	15	$1.78 \cdot 10^{-5}$	0.0366	0.12	[8]
Dimethylglyoxime(1)–water(2)–ethyl alcohol(3)	25	$8.4 \cdot 10^{-5}$	$7.2 \cdot 10^{-3}$ (91%-C_2H_5OH)	0.10	[9]
Salicylic acid(1)–water(2)–ethyl alcohol(3)	70	$2.66 \cdot 10^{-3}$	0.267	0.12	[10]
$HgCl_2$(1)–water(2)–ethyl alcohol (3)	25	$4.82 \cdot 10^{-3}$	0.0755	0.10	[11]
Acetanilide(1)–water(2)–acetone(3)	20	$3.0 \cdot 10^{-3}$	0.115	0.10	[10]
Same	52	$3.4 \cdot 10^{-3}$	0.278	0.10	[10]

Viscosity isotherms of water–ethyl alcohol mixtures also exhibit breaks at a mole fraction of about 0.10 of alcohol [12] (Fig. 5). The breaks on the viscosity isotherms are gradually leveled out with rise of temperature and are apparently shifted slightly toward higher alcohol contents. Each of the above effects individually might be regarded as doubtful, but the combination of all the above data indicates that in the system water–ethyl alcohol (and, with somewhat less certainty, in the system water–acetone) a certain point near $x_2 = 0.1$ does have special properties.

It is difficult to interpret these facts except by introduction of the concept of a sudden change in the solution structure. Dilute solutions of ethyl alcohol and water can probably be regarded as solutions with an interstitial type of structure. Bokii [13] put forward the idea of the possible existence of aqueous nonelectrolyte solutions of the interstitial type. As the alcohol or acetone concentration increases the cavities in the water structure become filled and the possibilities of deformation of the original structure are exhausted; in consequence, there is an abrupt transition to a different type of structure which subsequently undergoes gradual deformation. The structural change may be manifested in various properties of the solution in the form of breaks in the first or higher derivative of the property with respect to composition. The solubility of a third substance in the solution may be such a property. Low solubility of the third substance is an essential condition here because high solubility must evidently involve considerable distortion of the structure of the mixed solvent itself.

Persianova and Tarasov [14] have shown that in studies of the compressibility of aqueous solutions of nonelectrolytes it is also necessary to introduce the concept that solute molecules fill the cavities in the quasicrystalline lattice of water. Radchenko and Shestakovskii [15] found in direct x-ray structural investigation that water retains its original structure even in aqueous solutions containing methyl alcohol at relatively high concentrations (up to 30% by weight).

As already noted, the breaks in the property isotherms are gradually leveled out and may even disappear with rise of temperature; evidently this is because the structure of water becomes progressively more diffuse. The composition corresponding to the break depends little on temperature, and in composition–temperature plots the line separating regions of different structures, which could be named the heterostructural line, is almost vertical. The differences between the properties of the solutions on each side of this line are gradually leveled out with rise of temperature and vanish entirely at a certain point (which is reminiscent of the critical point).

It seems likely that effects associated with sharp changes in the structure of binary solutions should be fairly common, especially if water is one of the solution components. It is possible that these effects may also appear on the solubility curves of sparingly soluble electrolytes in mixed solvents, although here, because of stabilization of the water structure by the ions present in solution, the break point may be shifted toward higher nonelectrolyte concentrations. Studies of the solubility of a third component may thus provide a method for investigating the structure of solutions.

LITERATURE CITED

1. A. R. Martin and A. C. Brown, Trans. Faraday Soc., 34, 742 (1938).

2. A. G. Mitchell and W. F. K. Wynne-Jones, Disc. Faraday Soc., 15, 161 (1953).
3. D. I. Mendeleev, "Investigation of aqueous solutions by density." In the book: D.I. Mendeleev, Solutions [in Russian] (Izd. AN SSSR, Moscow, 1959).
4. G. N. Lewis and M. Randall, Chemical Thermodynamics [Russian translation] (ONTI, Leningrad, 1936) p. 28.
5. J. Kenttämaa, E. Tommila, and M. Martti, Some thermodynamic properties of the system t-butanol-water. Suomalaisen tiedekatemian toimituksia annales academiae scientiarum Fennica, Ser. A, Chemica, No. 93, Helsinki (1959).
6. K. Nakanishi, Bull. Chem. Soc., Japan, 33, 793 (1960).
7. V. A. Mikhailov, Izv. SO AN SSSR, 5, 51 (1961).
8. N. Schoorl and A. Regenbogen, Pharm. Weekblad, 56, 538 (1919); cited through A. Seidell and W. F. Linke, Solubilities of inorganic and metal-organic compounds, Vol.1, D. Van Nostrand Co., Inc., Princeton, New Jersey, Toronto, London, and New York (1958).
9. A. G. Stromberg, Zh. fiz. khimii, 23, 962 (1949).
10. A. A. Volkov, Candidate's Dissertation [in Russian] (Perm' State University, 1950).
11. R. Abe, J. Tok. Chem. Soc., 33, 1087 (1912); cited through A. Seidell and W. F. Linke, Solubilities of inorganic and metal-organic compounds, vol. 1, D. Van Nostrand Co., Inc., Princeton, New Jersey, Toronto, London, New York (1958).
12. Chemist's Handbook [in Russian] (Goskhimizdat, Moscow-Leningrad, 1952) Vol. 3, p. 422.
13. G. B. Bokii, Usp. khimii, 23, 605 (1954).
14. L. V. Perslanova and V. V. Tarasov, Izv. vyssh. uch. zaved., Khimiya i khim. prom-st', 3, 4 (1960).
15. L. V. Radchenko and F. K. Shestakovskii, Zh. fiz. khimii, 29, 1456 (1955).

All abbreviations of periodicals in the above bibliography are letter-b letter transliterations of the abbreviations as given in the original Russian journal. *Some o. all of this periodical literature may well be available in English translation.* A complete list of the cover-to-cover English translations appears at the back of this issue.

INTERMOLECULAR INTERACTION IN THE SYSTEM $(C_4H_9O)_3PO - HNO_3 - H_2O$

M. F. Pushlenkov, E. V. Komarov, and M. E. Shurenkova

Translated from Zhurnal Strukturnoi Khimii, Vol. 2, No. 6,
pp. 682-689, November-December, 1961
Original article submitted April 12, 1961

Mutual solubility in the ternary system TBP–HNO_3–H_2O was studied and certain characteristics of the solubility isotherm were considered. It was shown by means of infrared spectroscopy that at low HNO_3 concentrations a compound of TBP with HNO_3 in 1:1 ratio is formed; its structure should be represented by the formula $(C_4H_9O)_3PO$ ...$HONO_2$, rather than $[(C_4H_9O)_3POH^+]\cdot[NO_3^-]$. Addition of further nitric acid molecules to the monosolvate apparently proceeds by the following mechanism:

$$(C_4H_9O)_3PO\ldots HO-N\begin{matrix}O\ldots HONO_2\\ O\ldots HONO_2\ldots HONO_2\ \text{etc.}\end{matrix}$$

Participation of the ester oxygen of TBP in bond formation with nitric acid was not detected experimentally. The assumption of the so-called "nonchemical" distribution of nitric acid between water and TBP is contrary to the experimental results obtained. Water dissolved in pure TBP and in mixtures of TBP with HNO_3 forms hydrogen bonds either with phosphoryl groups of TBP or with oxygen in nitrate groups of HNO_3. The following mechanism is postulated for addition of water to the nitric acid solvate: $(C_4H_9O)_3PO\ldots HONO_2\ldots HOH$.

There have been many investigations [1-10] of the interaction of tributyl phosphate (TBP) with nitric acid. The vast majority of these investigations were concerned with distribution of nitric acid between water and TBP. All investigators conclude that nitric acid and TBP form the compound $TBP\cdot HNO_3$.

The fact that nitric acid enters the organic phase in amounts exceeding a 1:1 ratio of HNO_3:TBP prompted certain authors to postulate formation of the compounds $TBP\cdot 2HNO_3$ [4,5, and 8], $TBP\cdot 3HNO_3$, and $TBP\cdot nHNO_3$ where $n>3$ [7,8]. Others, such as Alcock, Grimley, Healy, Kennedy, and McKay [2] assume the possibility of simple dissolution of nitric acid in $TBP\cdot HNO_3$ solution without formation of chemical compounds. Sheka and Kriss [7] also assume the possibility of "nonchemical" dissolution, but only after the HNO_3:TBP mole ratio has reached the value of 3.

There is no proof in the literature of the existence of the compound $TBP\cdot 2HNO_3$. The experimental data of Fomin and Malorova [1,5] do not provide such proof, because they used the law of mass action in terms of concentrations. The validity of this assertion does not follow from general considerations only: it follows from the data in [6] that the magnitude of the apparent solvation number depends on the TBP concentration, the nature of the diluent, and the ionic strength of the aqueous solution.

Very little information is available on the mechanism whereby molecules of nitric acid are added to the TBP molecule. It is suggested in [2] that in the formation of a compound of 1:1 composition bonding of HNO_3 and TBP molecules is effected as follows:

$$(C_4H_9O)_3PO\ldots HONO_2.$$

Korpak and Deptula [8] interpreted their experimental data on the assumption that all four oxygen atoms of the TBP molecule are involved in formation of bonds with HNO_3.

In this investigation we studied mutual solubility in the ternary system TBP–HNO_3–H_2O and determined infrared spectra of the solutions in the 2.5-11 μ region. In discussion of the experimental data the main attention is devoted to intermolecular interaction in this system.

EXPERIMENTAL

The nitric acid used in the experiments was 100% pure, prepared as described in [11]: $d^{20} = 1.529$, $n_D^{20} = 1.4043$.

The tributyl phosphate after the usual treatment contained $6 \cdot 10^{-5}$ M of monobutyl phosphate (MBP) and $2 \cdot 10^{-4}$ M of dibutyl phosphate (DBP). The tributyl phosphate used in the experiments ($n_D^{20} = 1.4242$), was distilled under vacuum. Twice-distilled water was used.

After layer formation both phases were analyzed for TBP, DBP, MBP [12] and nitric acid. In addition, water was determined in the organic phase with the Fischer reagent. Nitric acid was determined in both phases by titration.

The mutual solubility determinations were performed in a thermostat at 25° ± 0.1°. The time of mixing was 1 hour. Each experiment was repeated two or three times.

The infrared spectra were measured with the IKS-12 spectrometer, with rock salt and lithium fluoride prisms. The calculated spectral slit width was 3 cm^{-1} in the 1200 cm^{-1} region, and about 5 cm^{-1} in the 3000 cm^{-1} region.

The cell materials (LiF and KBr) were protected against the action of the solutions by means of polyethylene and Teflon films a few microns thick.

Mutual Solubility in the System TBP – HNO_3 – H_2O

The results of mutual solubility determinations in this system are given in Fig. 1. The compositions are given in molar percentages. Data of two kinds were used for plotting of the solubility isotherms. The experimental points represented by black circles were found by complete chemical analysis of the coexisting phases. The points represented by white circles were found by determinations of the volume concentration of nitric acid and solution densities. In the latter case the molar percentages of water and TBP were calculated from our data in conjunction with the data in [2].

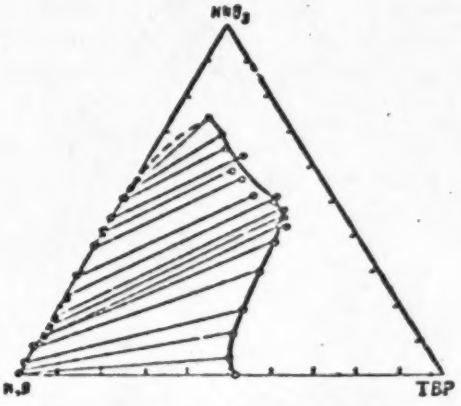

Fig. 1. Mutual solubility isotherm. The straight lines are conodes.

Analyses of the solutions for their DBP and MBP contents showed that under our experimental conditions hydrolysis of TBP was slight (the DBP content varied in the range of $\cdot 9 \cdot 10^{-4}$ – 0.033 M, and the MBP content in the range of 10^{-3} – 10^{-4} M).

Figure 1 shows that the solubility isotherm is of very peculiar form. The simplest and most acceptable explanation of the complex form of Fig. 1 is based on the assumption that the associated groups formed in the aqueous and organic solutions differ in composition. The spectrometric data presented below indicate the complex character of molecular interaction in the organic phase.

Results and Discussion of the Infrared Spectrum Determinations

Table 1 contains certain vibrational frequencies of TBP, HNO_3, and H_2O, and their interpretations adopted in this investigation.

The results of the spectrometric determinations are given in Table 2 and in Figs. 2 and 3. It follows from Table 2 that when pure nitric acid is dissolved in "dry" TBP the spectra of nitric acid itself and of TBP undergo substantial changes. In the spectrum of the solution with the molar ratio TBP: HNO_3: H_2O = 1 : 1 : 0 the absorption band with a maximum at 1272 cm^{-1}, characteristic of the phosphoryl group, is no longer present. It is replaced by a new strong band with a maximum at 1204 cm^{-1}. The situation here is similar to that observed during dissolution of various uranyl salts in TBP [14].

The appearance of a new band in the region of lower wave numbers is associated with strong perturbation of the valence vibrations of the phosphoryl group. The total disappearance of the band at 1272 cm^{-1} evidently indicates that virtually all the TBP is bound by nitric acid molecules; i.e., that a compound of the composition TBP·HNO_3 is formed quantitatively. The spectrum of a solution of nitric acid in TBP with the molar proportions of TBP: HNO_3: H_2O = 1 : 0.5 : 0 (see Table 2) contains both absorption bands, with maxima at 1272 and 1204 cm^{-1}. This is because part of the TBP remains free and part is combined in TBP·HNO_3.

This conclusion is confirmed by the changes in the absorption spectrum of nitric acid. The strong broad band with a maximum near 3380 cm^{-1}, assigned to valence vibrations of the hydroxyl group in liquid nitric acid, does not appear in the spectra of solutions A and B (Fig. 2). Instead there is an absorption band with a maximum near 3050 cm^{-1}. The pronounced shift of this band into the long-wave region of the spectrum indicates that the bonding between the nitric acid molecule and the phosphoryl group is effected through hydroxylic hydrogen. Accordingly, the formula of the compound formed must be written as $(C_4H_9O)_3PO...HNO_3$. Attempts to represent the structure of this compound by the formula $[(RO)_3POH^+][NO_3^-]$ cannot be regarded as justified. The intense absorption band in the 1380-1400 cm^{-1} region, characteristic of ionic nitrate [13], is not found in the spectra of any of the solutions studied by us. The presence of a strong absorption band with a maximum at about 1650 cm^{-1} (Table 2) indicates that the nitrate group has the C_{2v} point symmetry group [21]. In other words, the bond between the oxygen atom of the nitrate group and the hydrogen atom is not disrupted in the compound TBP·HNO_3. This is tantamount to the absence of the oxonium cation $(RO)_3POH^+$ as a structural unit in monosolvated nitric acid. This conclusion is consistent with electrical conductivity data for solutions of nitric acid in TBP [22]. According to Table 2, the relative shift of the absorption band of the phosphoryl group is large (5.4%) and is outside the limits of the usual shifts with small perturbations. Solvation of uranyl salts by TBP results in an even greater shift of the absorption band due to the phosphoryl group [14,23]. This effect is probably attributable to peculiarities of the P→O bond. According to [24] in compounds of phosphorus in fourfold coordination in addition to four σ-bonds (sp^3 hybridization) π-bonds are also formed, and the latter are, in general, distributed nonuniformly. Although the participation of π-electrons is greatest in the phosphoryl bond, their participation in the other three bonds is also considerable. Therefore the P→O bond cannot be regarded as either a double or a single bond. Such a large relative displacement of the phosphoryl group absorption band may be due to an approach of the P→O bond to the single bond type (decreased participation of π-electrons) in interactions of the type of $(RO)_3PO...B$, where B is a metal atom or acidic hydrogen. This effect should lead to the appearance of additional charges on the atoms of the phosphoryl group and to an increase in the strength of P–O (butyl) bonds. The mutual influence of the bonds should be strong owing to the participation of π-electrons in all the bonds. This reasoning provides a satisfactory explanation of the increased intensity and the strong shift of the phosphoryl group absorption band into the long-wave region of the spectrum, and the increased intensity and the shift of the P–O (butyl) absorption band into the short-wave region.

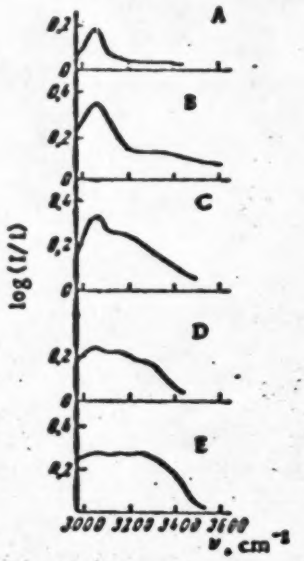

Fig. 2

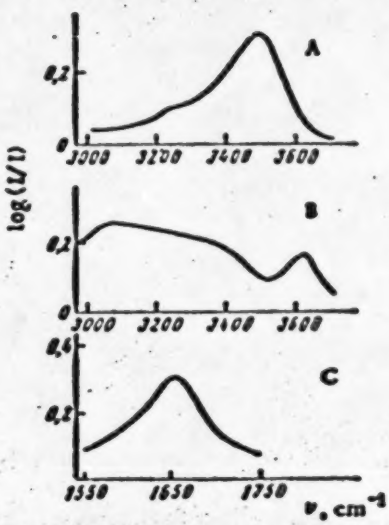

Fig. 3

Fig. 2. Absorption spectra of solutions with molar TBP: HNO_3 ratios of: A) 2:1; B) 1:1; C) 1:2; D) 1:3; E) 1:4.

Fig. 3. Absorption spectra of solutions with molar TBP: HNO_3: H_2O ratios of: A) 1:0:0.96; B) 1:1:0.38; C) 1:0:0.5.

Changes in vibrations of NO_3 and N–(OH) groups as the result of formation of the molecular compound TBP·HNO_3 are of definite interest. The frequency of the antisymmetrical valence vibration of the NO_3 group falls to 1649 cm^{-1}

(Table 2). The corresponding vibration frequencies are 1710 cm^{-1} in nitric acid vapor and 1676 cm^{-1} in liquid nitric acid. The frequency of the N–(OH) valence vibration rises to 943 cm^{-1} (886 cm^{-1} in the vapor, 920 cm^{-1} in liquid HNO_3). The observed shifts of these absorption bands are probably caused by mutual influence of the bonds in the nitric acid molecule. The formation of a strong hydrogen bond between the nitric acid hydroxyl and the phosphoryl group in TBP leads to weakening of the O–H bond; this, in its turn, increases the strength of the N–(OH) bond and weakens the other bonds between the nitrogen atom and oxygen atoms. In other words, formation of a hydrogen bond should bring the N–(OH) and N–O distances (in NO_2) closer together. This type of mutual bond influence is fully consistent with the changes observed in the vibrational spectrum of nitric acid in the transition from vapor to liquid [25] and in formation of the monohydrate [25] and the ether solvate [26].

TABLE 1. Vibrational Frequencies (cm^{-1}) of TBP, HNO_3, and H_2O

Substance	Wave number (cm^{-1})	State of aggregation	Interpretation	Literature
TBP	1272	Liquid	Valence vibration of phosphoryl group	[13,14]
	1026	"	Valence vibration of P–O(butyl)	Same
	3560	Gas	Valence vibration of OH	[15,16]
	3380	Liquid	Same	Same
HNO_3	1710	Gas	Antisymmetrical valence vibration of NO_2 group	*
	1675	Liquid	Same	*
	886	Gas	Valence vibration of N–(OH)	*
	920	Liquid	Same	*
H_2O	3750	Gas	Antisymmetrical valence vibration of OH	[17,18]
	3650	"	Symmetrical valence vibration of OH	Same
	3425	Liquid	Valence vibration of OH	[19,20]
	1637	"	Deformational vibration	[20]
	1595	Gas	Same	[18]

TABLE 2. Wave Numbers (cm^{-1}) of Absorption Bands of Solutions of HNO_3 and H_2O in TBP

Interpretation	TBP : HNO_3 : H_2O molar ratio								
	1:0:0	0:1:0	0:0,5:0	1:1:0	1:1,5:0	1:2:0	1:4:0	0:0:1	1:1:0,39
Valence vibrations of →PO	1272	—	1272	—	—	—	—	—	—
	—	—	1204	1204	1196	1194	—	1263	1196
Valence vibrations of P–O (butyl)	1026	—	1029	1033	1033	1032	1034	1027	1034
Antisymmetrical valence vibrations of NO_2 group	—	1676	1646	1649	1664	1670	1674	—	1645
Valence vibrations of N–(OH)	—	920	914	943	927	930	920	—	?*

* Wave number not determined.

On further addition of nitric acid to TBP above the 1:1 molar ratio the absorption band of phosphoryl group in the spectrum of the solutions undergoes a further (although small) shift toward smaller wave numbers (Table 2). The P–O (butyl) absorption band does not change appreciably with increase of nitric acid concentration up to the molar ratio TBP: HNO_3 = 1:4. This shows that there is no appreciable interaction between the nitric acid molecules and ester oxygen in TBP. The nitric acid absorption bands in the 920-943 and 1646-1676 cm^{-1} frequency ranges in the spectra of solutions with molar TBP: HNO_3 ratios of 1:1.5, 1:2, and 1:4 should probably be regarded as the results of superposition of the absorption bands of nitric acid molecules directly bound to the phosphoryl group of TBP and the bands of the additional nitric acid molecules. Indeed, these frequency ranges are narrow, whereas the half width of the absorption bands is considerable (under our experimental conditions the half width of the absorption band of

the NO_2 group was ~70 cm^{-1}, and that of the N–(OH) group was ~20-25 cm^{-1}). Moreover, the TBP concentration in solution falls with increase of acid concentration and the intensity of the absorption bands of nitric acid bonded directly to the phosphoryl group in TBP diminishes accordingly.

The data in Table 2 show that with increase of the HNO_3:TBP molar ratio the vibrational frequencies of the NO_2 and N–(OH) groups approximate to the corresponding frequencies in pure nitric acid, while in the 3050-3400 cm^{-1} range, as Fig. 2 shows, there is total absorption. This is probably due to absorption by hydroxyl groups of nitric acid, which interact in different ways with their environment. This can be represented more clearly as follows. In hydrogen bonding the oxygen in nitrate groups in liquid nitric acid acts as a proton acceptor. In accordance with this, the interaction mechanism of nitric acid molecules is represented by the formation either of dimers *

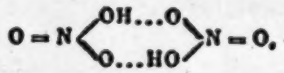

or of chains

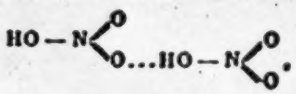

which may be branched [27, 28, 29].

Figure 2 shows that in solutions of nitric acid in TBP nearly all the nitric acid hydroxyls are involved in the formation of hydrogen bridges. The spectra do not show absorption by free hydroxyl groups, which occurs at about 3550 cm^{-1}. Therefore, in view of the absence of interaction between nitric acid and ester oxygen in TBP, the following mechanism may be assumed for intermolecular interaction in these solutions:

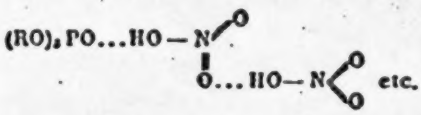

This is all the more probable because the proton-acceptor properties of oxygen in the NO_2 group should be intensified as the result of formation of the TBP·HNO_3 complex, as the frequency of the antisymmetrical valence vibration of the NO_2 group falls appreciably when nitric acid dissolves in TBP. An analogous lowering of frequency is observed in ether solutions of nitric acid [26].

As the HNO_3 molecules take up positions progressively further from the phosphoryl group in TBP so the absorption by nitric acid should approximate to the absorption spectrum of pure nitric acid; this is in full agreement with experimental data. Therefore searches for a boundary between "chemical" and "nonchemical" dissolution of nitric acid in TBP are unjustified. The assertion that formation of a hydrogen bridge of the $\geqslant$PO...HO– type is formation of a chemical bond, whereas the formation of a bridge of the type

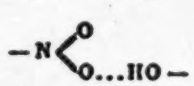

is not equivalent to chemical bonding is not sound in principle.

When water dissolves in TBP the absorption band with a maximum at 1272 cm^{-1}, assigned to the valence vibration of the phosphoryl group, is shifted by 9 cm^{-1} in the direction of lower wave numbers. A broad absorption band with a maximum near 3484 cm^{-1} appears in the region of valence vibrations of water (Fig. 3). The maximum of the absorption band due to deformational vibration of water dissolved in TBP has a value (1647 cm^{-1}) close to the corresponding maximum in the spectrum of pure water (1637 cm^{-1}).

In accordance with [18, 30-34] the above experimental data must be regarded as indicating the formation of hydrogen bonds between H_2O and TBP. It is seen in Fig. 3 that addition of water to a solution of nitric acid in TBP results in increased absorption in the 3200-3600 cm^{-1} region; this is probably caused by direct absorption by the bound water.

* Here and subsequently the structure of the nitrate group is indicated by means of five valence lines for the sake of simplicity, although the actual electron distribution between the bonds is more complex.

The small shift of the maximum of the phosphoryl group absorption band caused by addition of water to a solution with the molar ratio TBP: HNO_3 = 1:1 can be explained with the assumption of the following mechanism of addition of water molecules to the complex:

$$(RO)_3PO\ldots HONO_2\ldots HOH$$

or

An analogous mechanism was postulated for the formation of nitric acid hemi- and monohydrate [29,35]:

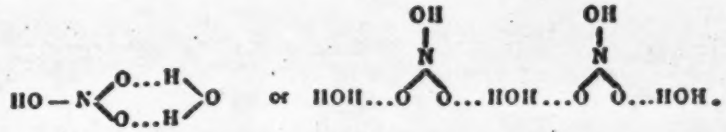

The formation of a nitric acid hydrate intensifies the acidic properties of the complex [29]. Accordingly, hydration of the TBP·HNO_3 complex or solvation by additional nitric acid molecules should produce a further decrease in the vibrational frequency of the phosphoryl group; this is found to be the case (Table 2).

The above results show that in the solutions studied the molecules are joined by hydrogen bridges. Whereas at not very high nitric acid concentrations in solution we can still speak of the existence of discrete particles, such as TBP·HNO_3, TBP·HNO_3·H_2O, TBP·HNO_3, HNO_3, and others, at high nitric acid concentrations and with an increased amount of water in the organic phase it is impossible to identify discrete (isolated) aggregates of simple composition. In this case it is appropriate to refer to structural order in the liquid.

Having elucidated certain details on intermolecular interaction in the TBP–HNO_3–H_2O system, we can discuss in more concrete terms the peculiarities of the data represented by Fig. 1. The unlimited miscibility of TBP with anhydrous nitric acid favors formation of strong hydrogen bonds between TBP and HNO_3 and subsequent continuous solvation. The absence of ion pairs helps the solution to remain homogeneous in the region of low concentrations of HNO_3 in TBP. Water has considerable solubility both in TBP and in TBP + HNO_3 mixtures. Phase separation of the ternary system is evidently the result of competition between water and TBP for HNO_3. Excess water causes ionization of the acid and separation of water with the ionized acid in an independent phase. The decrease of the solubility of water in the organic phase with increase of nitric acid concentration is due to the lower stability of the $HONO_2$... ...HOH bond in comparison with the $(RO)_3PO\ldots HOH$ bond. The other possible mechanism of water addition

$$(RO)_3PO\ldots H_2O\ldots HNO_3,$$

apparently should not lead to a decrease of the solubility of water with increasing HNO_3 concentration. The fact that the solubility of water in the organic phase remains roughly constant after the molar ratio TBP: HNO_3 = 1:1 has been reached is consistent with a chain solvation mechanism of monosolvated nitric acid.

LITERATURE CITED

1. V. V. Fomin and E. P. Malorova, Zh. neorgan. khimii, 1, 8, 1703 (1956).
2. K. Alcock, S. S. Grimley, T. V. Healy, J. Kennedy, and H. A. C. McKay, Trans. Faraday Soc., 52, 1, 39 (1956).
3. T. V. Healy and H. A. C. McKay, Trans. Faraday Soc., 52, 5, 633 (1956).
4. R. L. Allen and M. A. Desesa, Nucl. Sci. Abstr., 11, 2, ref. 931 (1957).
5. V. V. Fomin and E. P. Malorova, Zh. neorgan. khimii, 3, 2, 540 (1958).
6. V. B. Shevchenko, N. S. Novitskii, et al. Zh. neorgan. khimii, 3, 9, 2109 (1958).
7. Z. A. Sheka and E. E. Kriss, Zh. neorg. Khimii, 4, 11, 2505 (1959).
8. W. Korpak and C. Deptula, Nucleonics, 5, 1-2, 63 (1960).
9. T. V. Collopy and L. F. Blum, J. Phys. Chem., 64, 9, 1324 (1960).
10. T. V. Collopy and L. H. Cavendish, J. Phys. Chem., 64, 9, 1328 (1960).
11. V. A. Palauzov, Chemical Reagents: Their Properties and Methods of Preparation [in Russian] (Gos. nauchno-tekhn. izd. Ukrainy, Khar'kov, 1935) p. 247.
12. J. Kennedy and S. Grimley, Harwell AERE CE/R, 968 (1957).
13. L. J. Bellamy, Infrared Spectra of Complex Molecules [Russian translation] (Izd. inostr. lit., Moscow, 1957) p. 301.

14. E. V. Komarov and M. F. Pushlenkov, Radiokhimiya, 3, 567 (1961).
15. C. K. Ingold, D. J. Millen, and H. G. Poole, J. Chem. Soc., 2576 (1950).
16. H. Cohn, C. K. Ingold, and H. G. Poole, J. Chem. Soc., 4272 (1952).
17. M. M. Vol'kenshtein, M. A. El'yashevich, and B. I. Stepanov, Molecular Vibrations [in Russian] (GTTI, Moscow, 1949) Vol. 2, p. 429.
18. Landolt-Börnstein, Zahlenwerte und Funktionen, Bd. 2, S. 334.
19. M. O. Bulanin, Optika i spektroskopiya, 2, 5, 557 (1957).
20. E. Greinacher, W. Luttke, and R. Mekke, Z. Elektrochem., 59, 1, 23 (1955).
21. B. M. Gatehouse and A. E. Comyns, J. Chem. Soc., 3965 (1958).
22. E. Hesford and A. C. McKay, J. Inorg. and Nucl. Chem., 13, 1-2, 156 (1960).
23. E. V. Komarov and M. F. Pushlenkov, Radiokhimiya, 3, 575 (1961).
24. L. R. Van Wasser, J. Amer. Chem. Soc., 78, 22, 5709 (1956).
25. A. Simon and H. Hoppner, Kolloid-Z., 85, 1, 8 (1938).
26. J. Desmaroux, J. Chédin, and R. Dalmon, Compt. rend., 209, 455 (1939).
27. J. Chédin and S. Fénéant, Compt. rend., 228, 242 (1949).
28. R. Dalmon and R. Freymann, Compt. rend., 211, 472 (1940).
29. J. Chédin and S. Fénéant, J. Chim. Phys., 45, 4-5, 66 (1948).
30. W. Gordy, J. Chem. Phys., 8, 7, 516 (1940).
31. W. Gordy and L. Stanford, J. Chem. Phys., 9, 3, 204 (1941).
32. W. Gordy, J. Chem. Phys., 9, 3, 215 (1941).
33. V. M. Vdovenko and D. N. Suglobov, Zh. fiz. khimii, 34, 1, 51 (1960).
34. J. Goubeau and W. Berger, Z. anorgan. und allgem. Chem., 304, 3-4, 147 (1960).
35. J. Chédin, J. Chim. Phys., 49, 3, 109 (1952).

All abbreviations of periodicals in the above bibliography are letter-by-letter transliterations of the abbreviations as given in the original Russian journal. *Some or all of this periodical literature may well be available in English translation.* A complete list of the cover-to-cover English translations appears at the back of this issue.

COMPUTER CALCULATIONS ON ESR SPECTRA

1. SPECTRA WITH SYMMETRICAL HYPERFINE STRUCTURE

Ya. S. Lebedev, D. M. Chernikova, and N. N. Tikhomirova

Institute of Chemical Physics, Academy of Sciences of the USSR
Translated from Zhurnal Strukturnoi Khimii, Vol.2, No. 6,
pp. 690-695, November-December, 1961
Original article submitted July 7, 1961

Calculations of ESR spectra with hyperfine structures are presented; various ratios of component width to splitting are used. Results are presented for equal components (1:1, 1:1:1, 1:1:1:1, 1:1:1:1:1, 1:1:1:1:1:1) and for binomial intensity distributions (1:2:1, 1:3:3:1, 1:4:6:4:1). The calculations have been made for gaussian and lorentzian line shapes. Nomograms are given for deriving the true line parameters from the observed ones. Methods of analyzing actual spectra are presented.

Spin-resonance techniques are now extensively used in physics, chemistry, and biology; in particular, ESR spectra are used in studies on radicals and ions, on reaction kinetics, and on interactions in and between molecules. The parameters that can be measured are 1) the area under the absorption curve, 2) the hyperfine structure (HS), number and strengths of components, 3) line widths, and 4) line shapes.

It is usually difficult to determine these parameters (except the first) on account of overlap between components, anisotropy in the g-factor, or hyperfine splitting [1,2]. It is rare to find an ESR spectrum fully resolved; analysis of such spectra is still difficult, and the results are often not unique (or even correct). Line shapes admit of analytic treatment only in the simplest cases (singlet [3] and doublet [4] lines). The best test of any interpretation is to compare the theoretical spectrum with the observed one, as has been done in some cases [5-7] with very good results. Experience has shown, though, that the volume of calculations can be very large.

Here we give some calculations on ESR spectra performed on a high-speed computer; many parameters have been varied in order to cover the majority of spectra actually encountered. It is shown below that these calculations enable one to interpret spectra comparatively readily.

The problems to be handled in order to cover all practical cases are as follows.

1) ESR spectra with unresolved HS must be calculated for various line numbers, intensity distributions, and ratios of component width to splitting on the assumptions that the components are symmetrical and have the same width and splitting. This is so for many free radicals and ion-radicals in the liquid state (see [8], for example).

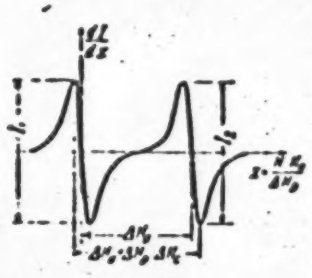

Fig. 1. Theoretical parameters of an ESR spectrum showing HS: H_0 is the center for the extreme components, ΔH_i is the width (between points of maximum slope) of a component, and ΔH_c is the width of the composite spectrum.

2) ESR spectra as above must be calculated on the assumption that the components differ in width (as for ions and radicals in structured liquids [9], amorphous polymers [10], etc.).

3) ESR spectra as above also occur with anisotropic g-factors (ions and radicals in solids, biological objects, etc. [2, 4-6, 10]).

Here we give results for some of these problems. ESR spectra were considered for HS components from two to six in number, the intensity ratios being 1:1, 1:1:1, 1:1:1:1, 1:1:1:1:1, 1:1:1:1:1:1, 1:2:1, 1:3:3:1, 1:4:6:4:1, and the forms being gaussian and lorentzian.

A very general form for the line shape in universal coordinates (Fig. 1) is

$$I(x) = \sum_{k=1}^{n} a_k / \left[\frac{x - k + 1}{\beta}\right]. \qquad (1)$$

Here n is the number of components, the a_k are the intensity factors, and k is the number of the component reckoned from the edge of the spectrum:

$$f(x) \sim \begin{cases} (1 + 1{,}335x^2/\beta^2)^{-1} & \text{Lorentzian form} \\ \exp(-2x^2/\beta^2) & \text{Gaussian form} \end{cases}$$

$\beta = \Delta H_i/\Delta H_p$, $x = H - H_0/\Delta H_p$, ΔH_p – is the partial splitting between components, ΔH_i is the width between points of maximum slope, H_0 is the field corresponding to the middle of an extreme component, and H is the varying maguetic field.

Thus all parameters, if referred to ΔH_p, are dimensionless.

The β used range from 0.3 to 6.0 by intervals of 0.2 (or smaller in the critical range) and for x from -5β to $(n-1)\beta/2$ [lorentzian form] or from -2.5β to $(n-1)\beta/2$ [gaussian form] by steps of 0.1. The derivative curve $I'(x)$ was computed, for this is the most usual form for ESR recordings at present.

The calculations were performed on the high-speed computer in the mathematics section of this institute. The results were drawn up as graphs and nomograms representing the experimentally observed parameters as functions of the true parameters. Actual spectra may be analyzed in two ways, namely 1) by direct comparison with theoretical spectra and 2) by the use of nomograms.

1. Direct Comparison

Figure 2 shows theoretical results for six identical lorentzian lines for several β. Clearly, if an actual spectrum coincides (apart from scale) with one of these, the parameters may readily be computed by reference to the theoretical ones.

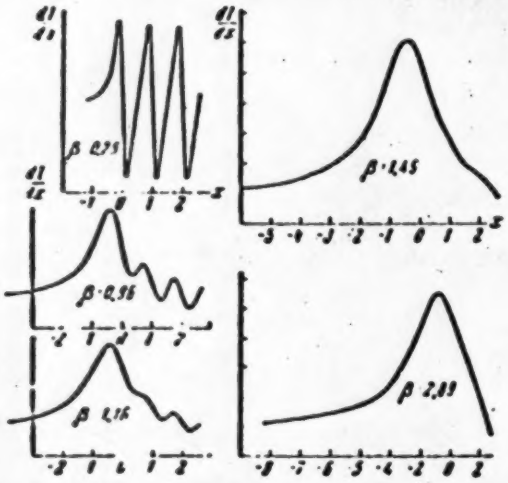

Fig. 2. Theoretical ESR spectra with six HS components whose intensity ratios are 1:1:1:1:1:1; line shape lorentzian, β variable. Only half of each spectrum is given here and in Fig. 3, because the second half is a mirror image of the first.

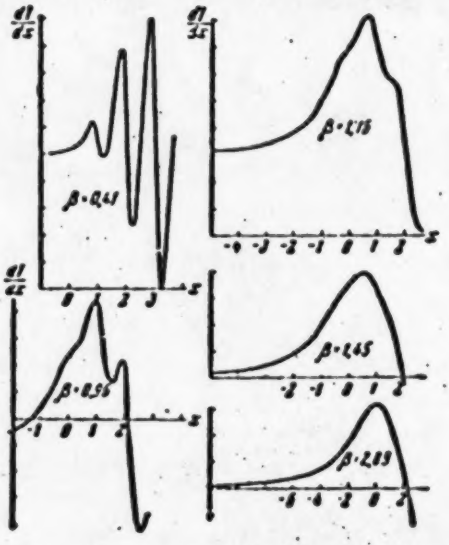

Fig. 3. Theoretical ESR spectra with five HS components in the intensity ratio 1:4:6:4:1; lorentzian shape, β variable.

Our results enable us to draw some general conclusions of value in the analysis of unresolved ESR spectra (even if the spectra are not comparable with any theoretical ones).

a) The HS is lost when $\Delta H_i = 1.16\Delta H_p$ (lorentzian form) or $\Delta H_i = 1.41\Delta H_p$ (gaussian form).

b) The positions of the HS components in a partly resolved spectrum are very nearly those at which the first-derivative curve cuts the baseline (components of symmetrical surroundings should be used for this).

c) Poor resolution of the HS, if this consists of identical components, results in a partial loss of the central components; a binomial intensity distribution causes a partial loss of the side components, whose apparent position is moved outwards.

d) Incorrect interpretations may be reached for β in the critical range (1.0-1.7); here point c) is useful, and so is the observation that the side components are resolved at lower β than the central ones and are raised above the baseline if the distribution is binomial (Fig. 3).

2. Use of Nomograms

Figures 4 and 5 show nomograms for use with unresolved ESR spectra. The abscissa is β, the ordinates being $\Delta H^*_c/\Delta H_p$ (part a), β (part b), $\Delta H^*_{p(k-l)}/\Delta H_p$ (parts c-e of Fig. 4) I^*_k/I^*_l (part f of Fig. 4 and e of Fig. 5). Here an asterisk denotes measured quantities, k and l being the numbers of components, I^*_k and I^*_l the amplitudes of those components as measured on the first derivative (Fig. 1). The broken lines represent the relations for perfectly resolved spectra. The spectra are resolved to the left of the hatched vertical line, while to the right the β are such that the spectra are completely unresolved.

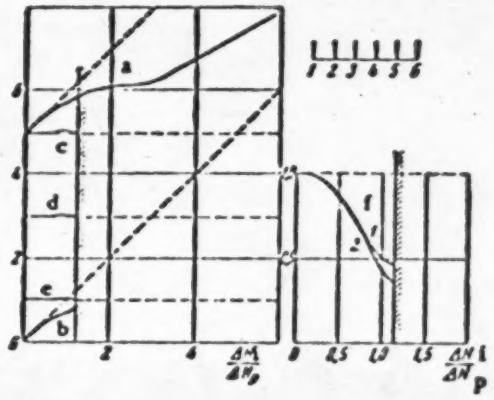

Fig. 4. Nomograms for analyzing any unresolved ESR spectrum consisting of six lorentzian components equal in strength: a) $\Delta H^*_c/\Delta H_p$, in which ΔH^*_c is measured between the maximum for the first component and the minimum for the sixth; b) $\Delta H^*_i/\Delta H_p$ in which ΔH_i is twice the distance from the center to the point of maximum slope for the first component; c) $\Delta H^*_{p(1-6)}$, as measured between centers for the first and sixth components; d) $\Delta H^*_{p(2-5)}/\Delta H_p$, in which $\Delta H^*_{p(2-5)}$ is measured between the centers of the second and fifth components; e) $\Delta H^*_{p(3-4)}$, as measured between the centers of the third and fourth components; f) I^*_2/I^*_1 (curve 1) and I^*_3/I^*_1 (curve 2), in which the I^* are the amplitudes of the derivatives for the corresponding components.

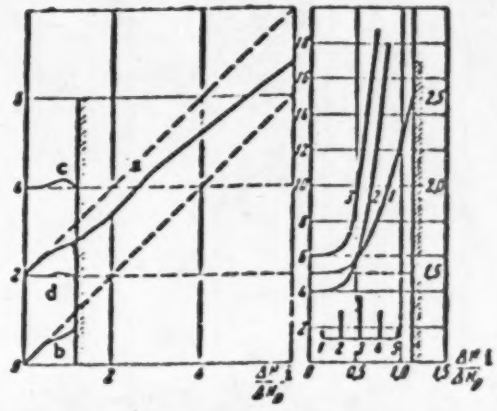

Fig. 5. Nomograms for analyzing any unresolved ESR spectrum consisting of five lorentzian components having a binomial intensity distribution: a) $\Delta H^*_c/\Delta H_p$, in which ΔH^*_c is measured between the maximum for the second component and the minimum for the fourth; b) $\Delta H^*_i/\Delta H_p$, in which ΔH^*_i is measured between the maximum and minimum for the central component; c) $\Delta H^*_{p(1-5)}/\Delta H_p$, in which $\Delta H^*_{p(1-5)}$ is measured between the centers of the second and fourth components; d) I^*_2/I^*_1 (curve 1), I^*_3/I^*_1 (curve 2), and I^*_3/I^*_1 (curve 3), in which the I^* are the amplitudes of the derivatives for the corresponding components.

Figures 4 and 5 enable one to establish how far the measured parameters deviate from the true values; clearly, the deviation is the greater the poorer the resolution. Table 1 lists the maximal errors of ΔH^*_i, ΔH^*_p, and ΔH^*_c; ΔH^*_p is assumed to be measured between the centers of components having the most symmetrical surroundings. The errors relate to the case in which the HS is somewhat resolved (k is the number of the components, as reckoned from the center, that are used in measuring ΔH^*_p). Then

$$\Delta H_e = k\Delta H_p + \Delta H_i. \qquad (2)$$

We have $\Delta H_c = (n-1)\Delta H_p + \Delta H_i$ if all components are the same, so ΔH_p can, as a rule, be estimated accurately for a partly resolved spectrum. Formula (2) gives ΔH_i to 10-15% or so.

Now we consider how the nomograms may be used to interpret unresolved spectra. Here there are several problems, which differ in complexity.

a) The structure and ΔH_p are known. This case is a common one, for the resolution may be dependent on temperature or concentration by virtue of variation in ΔH_i [4]. The ratios of the intensities give $\Delta H_i/\Delta H_p$ if the spectrum is partly resolved (part f of Fig. 4 or part e of Fig 5), so ΔH_i is known; error about 2%. Nomogram gives $\Delta H_i/\Delta H_p$ from ΔH_c^* if the spectrum is not resolved; error about 10%.

b) Only the structure is known (on the basis of structural chemistry or from comparison with theoretical spectra). We find ΔH_p as the distance between the centers of central lines if the spectrum is partly resolved; then the procedure is as above. Error about 10%; this can be reduced if ΔH_p is corrected by reference to parts c, d, and e of Fig. 4. We cannot determine ΔH_i and ΔH_p if the spectrum is not resolved at all.

c) ΔH_p is known (e.g., from quantum-mechanical considerations). Various structures are tested and the $\Delta H_i/\Delta HP$ are determined from the intensity ratios and ΔH_c^* if the spectrum is partly resolved. The structure giving the best agreement is selected. A structure is assumed and $\Delta H_i/\Delta H_p$ is found as in b) above if the spectrum is unresolved. Theoretical spectron are best used in order to select a structure.

TABLE 1. Maximum Errors of Measurement in Percent for Incompletely Reduced ESR Spectra

Spectrum	Lorentz form				Gauss form			
	ΔH_i	ΔH_p	ΔH_c	k	ΔH_i	ΔH_p	ΔH_c	k
1:1	—15	10	—10	1	—12	12	— 4	1
1:1:1	—33	6	—10	2	—20	6	— 9	2
1:1:1:1	—25	2	— 7	3	—25	2	— 7	3
1:1:1:1:1	—25	2	— 7	4	—20	2	— 7	4
1:1:1:1:1:1	—33	2	— 6	5	—25	2	— 3	5
1:2:1	—20	6	—17	2	—16	20	— 5	2
1:3:3:1	—35	2	—13	1	—25	10	— 7	1
1:4:6:4:1	—50	3	—15	2	—25	8	—10	2

d) No details of the spectrum are known, but it is partly resolved; all the above methods (including that of comparison with theoretical spectra) are brought to bear in order to determine the structure and parameters.

CONCLUSIONS

These computations on ESR spectra provide useful general suggestions for approximate analyses of unresolved ESR spectra; means of more rigorous analysis are also indicated. It is probable that the theoretical spectra and nomograms will provide a means of facilitating the various methods of analysis as applied to ESR spectra; this should make ESR methods all the more valuable for a variety of purposes.

We are indebted to V. V. Voevodskii for valuable advice and assistance, and also to Professor A. Ya. Povzner and others of the mathematics section of this institute for performing the calculations.

LITERATURE CITED

1. V. V. Voevodskii, Kinetika i kataliz, 1, 45 (1960).
2. A. A. Chirkov and A. K. Kokin, Zh. éksperim. i teor. fiz., 39, 1381 (1960).
3. N. N. Tikhomirova and V. V. Voevodskii, Optika i spektroskopiya, 7, 829 (1959).
4. G. M. Zhidomirov, Yu. D. Tsvetkov, and Ya. S. Lebedev, Zh. strukt. khimii, 2, 6, 696 (1961).
5. W. Gordy and H. Schields, Proc. Nat. Acad. Sci. USA, 46, 1124 (1961).
6. D. Libby and M. G. Ormerod, J. Phys. Chem. Solids, 18, 316 (1961).
7. E. J. Cochran, F. J. Adrican, and V. A. Bowen, J. Chem. Phys., 34, 1161 (1961).
8. A. L. Buchachenko, M. B. Neiman, and Ya. S. Lebedev, Tr. po khimii i khim. tekhnol., 1, 39 (1961).
9. J. G. Powles and M. H. Mosley, Proc. Phys. Soc., 77, 729 (1959).
10. Yu. D. Tsvetkov, Yu. N. Molin, and V. V. Voevodskii, Vysokomolek. soed., 1, 1805 (1959).

INVESTIGATION OF INTERNAL MOTIONS IN POLYISOBUTYLENE BY THE METHOD OF ELECTRON PARAMAGNETIC RESONANCE

G. M. Zhidomirov, Yu. D. Tsvetkov, and Ya. S. Lebedev

Institute of Chemical Physics, Academy of Sciences, USSR
Institute of Chemical Kinetics and Combustion, Siberian Division
of the Academy of Sciences, USSR
Translated from Zhurnal Strukturnoi Khimii, Vol. 2, No. 6,
pp. 696-699, November-December, 1961
Original article submitted January 26, 1961

A method has been developed for determining the width of an individual EPR line from an unresolved doublet. The effect of temperature on individual line width in the EPR spectrum of irradiated polyisobutylene was studied. Certain conclusions are drawn concerning the unfreezing of internal motions in polyisobutylene at low temperature.

Investigations by various methods (measurements of mechanical and dielectric losses, nuclear paramagnetic resonance) show that in most cases internal motions in polymers are unfrozen with increase of temperature. This unfreezing may be of different character in the crystalline and amorphous states of a polymer. According to the results of nuclear magnetic resonance (NMR), there are three characteristic temperature transitions [1]: 1) a low-temperature transition in the 100-200°K region; 2) a transition near room temperature; 3) a transition in a higher temperature region.

It should be noted that this classification of the transitions is somewhat arbitrary, as their positions vary appreciably for different polymers and as they occur over relatively wide temperature ranges. Whereas the interpretation of the latter two transitions is fairly clear (they are associated with configurational changes affecting the entire polymer chain and with transition into the viscofluid state), the nature of the motions causing the low-temperature transition is still obscure in most cases. We therefore studied this transition in the case of polyisobutylene by the electron paramagnetic resonance method (EPR) which, as was shown earlier [2], can also be used for investigation of internal motions in polymers.

Irradiation of polyisobutylene gives rise to an EPR signal consisting of two lines [3], ascribed to the radical

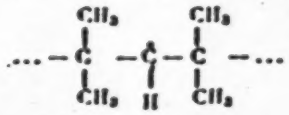

The splitting is 22 oe. The signal was studied in the temperature range between −196 and −60° (at about −50° the radicals begin to recombine rapidly). Figure 1 shows that the resolution of the spectrum depends considerably on the temperature, owing to decrease in the width of the individual components ΔH_i. The decrease of line width with rise of temperature indicates that line broadening is determined by anisotropic interactions which become leveled out as the intensity of the internal motions increases. This makes it possible to use measurements of ΔH_i for obtaining information about the character of internal movements in polymer chains.

For determinations of the values of ΔH_i from an unresolved spectrum we established the relationship between the positions of the externals on the experimental curve is represented by the following equation (the spectrum is recorded in differential form):

$$f(H) = \frac{d}{dH}\left(\exp\left(-b^2(H-\delta)^2\right) + \exp\left(-b^2(H+\delta)^2\right)\right),$$

where H is the magnetic field strength, taken from the resonance value; 2δ is the splitting between the components (measured for a spectrum with good resolution).

Let 2x be the distance between the corresponding extremals on the experimental curve; then the relationship between ΔH_i and δ is represented by the following transcendental equation:

$$\frac{((x+\delta)/\Delta H_i)^2}{1-((x-\delta)/\Delta H_i)^2} = \exp(2x\delta/\Delta H_i^2).$$

The graphical solution of this equation is given in Fig. 2. The graph is plotted in dimensionless coordinates and can be applied to the calculation of any doublet if the form of the individual line is close to the Gaussian. This graph was used for determining values of ΔH_i at various temperatures Fig. 3, curve a). This figure shows that the line width diminishes steadily over a range of 100° from 20 to 10 oe.

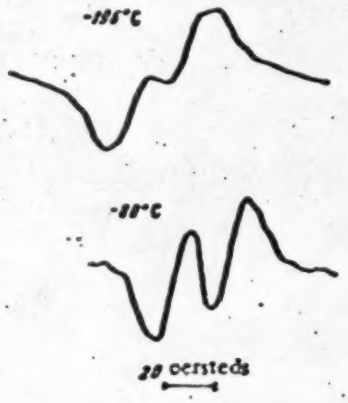

Fig. 1. EPR spectra of irradiated polyisobutylene at various temperatures.

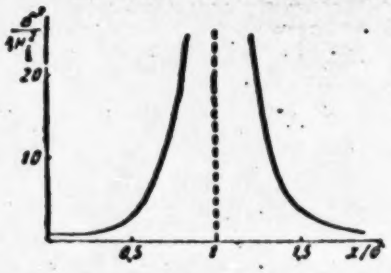

Fig. 2. Graph for calculation of the width of an individual component from an unresolved doublet.

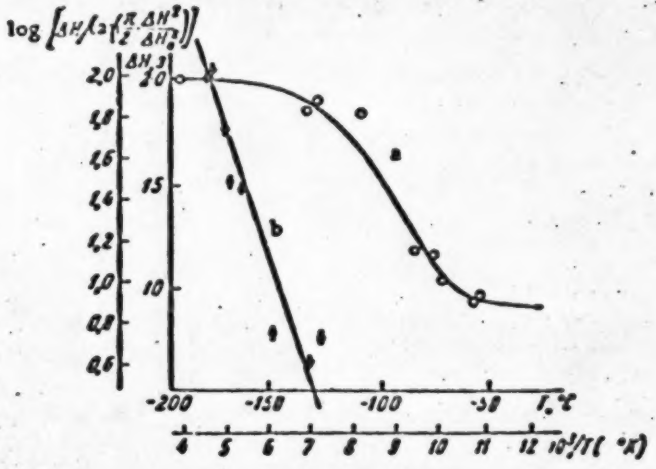

Fig. 3. Relationship between individual line width and temperature (a), and the linear anamorphosis of this relationship (b).

For analysis of the $\Delta H_i(T)$ relationships we used the formulas [4]:

$$\Delta H_i = A + \Delta H; \quad \Delta H^2 = \Delta H_0^2 \frac{2}{\pi} \arctan(\tau_c \Delta H).$$

where $A + \Delta H$ is the width of the unaveraged line (20 oe.); ΔH_0 is the contribution to the line width which is averaged during unfreezing of internal motions (10 oe.); τ_c is the correlation time of the averaging motion (correspond-

ingly, $\nu_c = 1/\tau_c$ is its frequency). Using this formula and assuming that

$$\nu_c = \nu_c^0 \exp(-\varepsilon/RT),$$

we can derive a linear anamorphosis for the relationship between the variable component of the line width and temperature:

$$\log\left[\Delta H^2 \tan\left(\frac{\pi}{2}\cdot\frac{\Delta H^2}{\Delta H_0^2}\right)\right] = \log\nu_c^0 - \varepsilon/2{,}3RT.$$

Figure 3 (curve b) shows that the relationship is satisfactorily linear. We can find from the graph that the frequency of the averaging motion (in sec^{-1}) is

$$\nu_c = 3\cdot10^{11}\exp(-2000/RT).$$

A detailed knowledge of the factors determining line width is necessary for elucidation of the character of the averaging motions. In the case of radicals (if the specimen is not a single crystal) line widths are generally associated with anisotropic spin-orbital and hyperfine interactions. In the present instance, as for most hydrocarbon radicals, the former interaction is weak in comparison with the latter; the latter comprises interaction with the nearest proton and with the protons of neighboring methyl groups (we disregard interaction with the remaining protons because of their distance). For estimation of the magnitude of these interactions we must know the wave function of the unpaired electron.

In simplified form, we can consider two extreme cases arising on removal of a proton from the polymer chain:

1. The fragment assumes a configuration corresponding to sp^2 hybridization, and the wave function of the unpaired electron becomes a pure atomic p-function.

2. The electron configuration of the fragment is unchanged. The choice between these two possibilities is determined by the magnitude of the steric hindrances associated with valence angle changes.

The results of x-ray structural analysis indicate that the tetrahedral angle in the polyisobutylene chain is distorted and is 126°; this is due to strong repulsion of methyl groups. It is therefore to be expected that steric hindrance in this case should not be great, and the fragment undergoes rearrangement. This is also consistent with the hyperfine splitting, which is 22 oe, in agreement with theoretical calculations [5]. A tentative calculation made with this assumption and with the results of [6] taken into account showed that the observed line width, at least in order of magnitude, can be explained by interactions with the nearest proton and with protons of neighboring methyl groups; the contributions of these two types of interaction are comparable.

The low-temperature transition in polyisobutylene was studied earlier by Powles [7] by the NMR method. We believe that the transitions observed by Powles and by ourselves are caused by the same movements; this is indicated primarily by the agreement between the temperature ranges, calculated with the resonance frequency differences taken into account. Powles suggested that the observed decrease of line width and of the second moment of the NMR signal is due either to unfreezing of the rotation of 15% of the CH_3 groups or to a phase transition. However, despite the appreciable contribution to line widths made by interactions with methyl groups, unfreezing of the rotations of a limited number of methyl groups cannot give rise to the large decrease of ΔH_4 observed by us, primarily because of the high symmetry of the CH_3 groups. The alternative suggestion of a phase transformation is likewise doubtful, since the transition is observed over a very wide temperature range and, moreover, intermolecular interactions should be little affected by a phase transition. It is still difficult to put forward a reasonable picture of these motions. We think it possible that this decrease of line width may be caused by certain conformations which influence a small portion of the polymer molecule by rotational oscillation of the fragment of the type with a high amplitude possibly associated with some distortion of the valence angles. It should be pointed out that with respect

to the decrease of line width rotational vibrations of 60° amplitude are equivalent to complete rotation [8]. It is interesting to note that analogous motion of methylene groups in an undistorted polymer chain can account quantitatively for the experimentally observed narrowing of the nuclear resonance line.

The hypothesis that such motion exists in polymers is in agreement with the results obtained for certain polymers, such as polyethylene [9] and polyvinyl chloride [10]. Such movements may be more pronounced in polyisobutylene because of the relatively low bonding energy in the polymer chain [11].

LITERATURE CITED

1. J. A. Sauer and A. E. Woodward, Revs. Mod. Phys., 32, 88 (1960).
2. Ya. S. Lebedev, Yu. D. Tsvetkov, and V. V. Voevodskii, Optika i spektroskopiya, 8, 811 (1960).
3. Yu. D. Tsvetkov, Yu. N. Molin, and V. V. Voevodskii, Vysokomolek. soed., 1, 1805 (1959).
4. H. S. Gutowsky and C. E. Pake, J. Chem. Phys., 18, 162 (1950).
5. H. Sternlicht, J. Chem. Phys., 33, 1128 (1960).
6. H. M. McConnel and J. Strathdee, Molec. Phys., 2, 2, 129 (1959).
7. J. G. Powles, Proc Phys., 69, 281 (1956).
8. E. R. Andrew, J. Chem. Phys., 18, 607 (1950).
9. N. Fuschillo and J. A. Sauer, Bull. Amer. Phys. Soc., Ser II, 4, 187 (1959).
10. A. Odajima, J. Soluna, and M. Koike, J. Phys. Soc. Japan, 12, 272 (1957).
11. Action of Ionizing Radiation on Natural and Synthetic Polymers, IL (Moscow, 1959) p. 66.

All abbreviations of periodicals in the above bibliography are letter-by-letter transliterations of the abbreviations as given in the original Russian journal. *Some or all of this periodical literature may well be available in English translation.* A complete list of the cover-to-cover English translations appears at the back of this issue.

NUCLEAR QUADRUPOLE RESONANCE SPECTRUM OF HEXACHLOROETHANE

N. E. Ainbinder, A. D. Gordeev, V. S. Grechishkin, Yu. G. Svetlov, and G. B. Soifer

Perm' State University

Translated from Zhurnal Strukturnoi Khimii, Vol. 2, No. 6, pp. 700-702, November-December, 1961
Original article submitted January 12, 1961

The effect of temperature on NQR frequencies in hexachloroethane was studied. The magnitude of the potential barrier for the structural transition in this compound was estimated.

Crystalline hexachloroethane at room temperature has rhombic symmetry in the group D_{2h}^{16} = Pnma [1]; the unit cell contains four molecules. Livingston [2] studied nuclear quadrupole resonance (NQR) of Cl^{35} nuclei in this compound at 77°K, using a regenerative detector with registration of the signal on an oscilloscope screen. Conclusions about the integral intensity of NQR lines cannot be drawn with the aid of this method, and line width cannot be measured with sufficient precision. The reason is that filters eliminating parasitic amplitude modulation have to be used for observation of NQR. Parasitic amplitude modulation arises during observation of signals on the oscilloscope screen when the deviation of the generator frequency is chosen to be considerably greater than the width of the absorption line. Much more accurate results can be obtained if a synchronous detector is used.

We used a regenerative detector with recording of the first derivative of the absorption line by means of the EPP-09 recording instrument [3]. Low-frequency modulation of the 90 cps frequency was effected by the HGPK-3 standard generator. For scanning of the spectra in the forward and reverse directions at a rate of 1.5 kc/min a Warren motor reversed with the aid of two additional windings on the stator was used. The depth of the frequency modulation was chosen to be considerably less than the width of the absorption line. A time constant of 10 seconds was used in the synchronous detector. The absorption spectra were recorded in the range from 77 to 196°K. Temperature variations from 77 to 90°K were effected by addition of small portions of liquid oxygen to the liquid nitrogen. Higher temperatures were obtained in a mixture of solid carbon dioxide with ethyl alcohol. Intermediate temperatures were obtained by cooling of a special refrigerant mixture (a mixture of saturated paraffins) by means of a tube through which a stream of liquid oxygen was passed. Unsaturated hydrocarbons are unsuitable for this purpose because of the explosion risk. The temperature was measured with a thermocouple to a precision of not less than ± 1°K. Specimens about 2 cc in volume were put in the coil of the generator circuit, situated at the end of a long rigid coaxial. The whole system was then placed in the refrigerant mixture. The system was cooled for one hour before each measurement in order to eliminate the influence of temperature gradients on the NQR line width. The absorption frequencies were measured with the FGFQ-353 wave meter, which gave a precision of the order of 0.01%.

Figure 1 is a record of the absorption spectrum at 90°K, and Fig. 2 represents the relationship between temperature and frequency. Similar measurements of the frequency–temperature relationship were performed earlier [4]. Line 1 is the strongest (the integral intensity is 32% of the intensity of all four lines. Line 2 has an integral intensity of 16%, line 3, 28%, and line 4, 22%. Thus, 32% of all the resonating nuclei contribute to the integral intensity of line 1, whereas only 16% contribute to the integral intensity of line 2.

The formation of a fine structure in the NQR spectrum can be attributed to the nonequivalent positions of the chlorine atoms in the crystal lattice. Indeed, according to x-ray structural data [1] the unit cell contains two chlorine atoms in the symmetry plane for each molecule, and four atoms joined in pairs by the plane symmetry for each molecule. Therefore, four lines are to be expected in the NQR spectrum, two of which should be twice as intense as the other two (in accordance with the number of equivalent atoms in unit volume). The small difference of the ratio of integral intensities of the NQR spectrum from 2:1:2:1 is due partly to experimental error and possibly also to nonequivalence of the crystal environment of the respective chlorine atoms. In fact for lines 1,2,3, and 4 the ratio

$\sqrt{S_2}/\Delta\nu_m$ (where S_2 is the second moment of the absorption line and $\Delta\nu_m$ is the half width of the line between the points of maximum and minimum slope of the absorption line) is of the same order of magnitude, but the absolute values of the moments are not equal:

	Curve no.			
	1	2	3	4
S_2	18	16	17	34
S_4	780	620	730	2600
$\Delta\nu_m$	6,5	6,5	7,0	10,0
$\sqrt{S_2}/\Delta\nu_m$	0,64	0,62	0,60	0,59
$\sqrt[4]{S_4}/\sqrt{S_2}$	1,26	1,24	1,24	1,23

All these data are in relative units for 90°K. It is easy to show that the $\sqrt{S_2}/\Delta\nu_m$ ratio for the Gaussian, Lorentz, and rectangular forms of the line is 1, ∞, and 0.58 respectively. The ratio $\sqrt{S_4}/\sqrt{S_2}$, where S_4 is the fourth moment of the absorption line, is 1.32, 1.60, and 1.16 respectively for these forms. It follows that the form of the absorption lines in hexachloroethane is close to the rectangular.

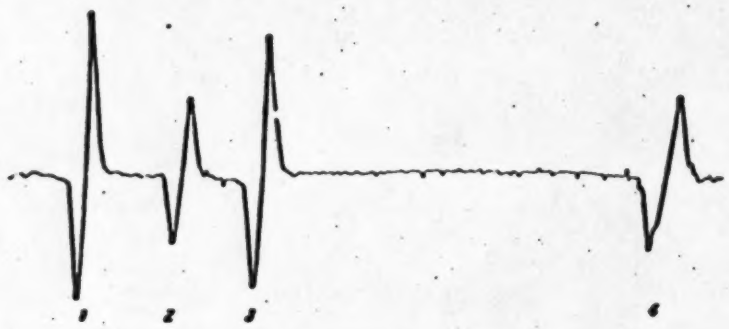

Fig. 1. Spectrum of Cl^{35} in hexachloroethane at 90°K.

At 195°K the hexachloroethane absorption lines broadened and were lost in the amplifier noise (Fig. 3). This can probably be attributed to reorientation or rotation of the molecules in the lattice (intramolecular rotation is also possible). If a reorientated or rotating molecule (including a molecule with internal rotation as the result of fluctuation) is regarded as a defect in the crystal lattice, then by the theory of heterophase fluctuations we can derive a formula representing the intensity decrease of NQR lines in processes of this kind:

$$A = A_0 \exp(-N_1 C_0 l^{V/RT}), \qquad (1)$$

where A_0 is the initial intensity of the NQR line, N_1 is a characteristic parameter (determining the number of molecules influenced by a reorientated or rotating molecule), V is the potential barrier per mole, and the constant $C_0 \approx 1$ [4]. A more detailed discussion of the mechanism of partial hindered molecular rotation state is not attained at once (primarily owing to increase in the amplitudes of rotational oscillations of the molecules in the lattice with rise of temperature) will be found in [4]. Formula (1) gives the value of about 8-9 kcal/mole for the potential barrier in hexachloroethane. Direct measurements of the relaxation time showed that the broadening of the lines cannot be explained in terms of the Buyle-Bodin relaxation mechanism [5]. This estimate of the potential barrier must be regarded as reasonable.

The NQR method is unsuitable for obtaining a final answer to the question of the nature of the rotation, because the effects of molecular reorientation and internal rotation are exactly the same: the signal intensity diminishes. If such processes are cooperative in character the potential barrier should depend on the temperature. No such dependence was observed; therefore, the cooperation of the processes is probably slight [4]. The problem of the gradual character of such transitions can now be regarded as solved by numerous experiments on nuclear magnetic resonance

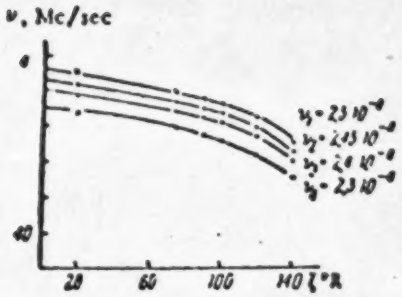

Fig. 2. NQR frequency–temperature relationship for hexachloroethane.

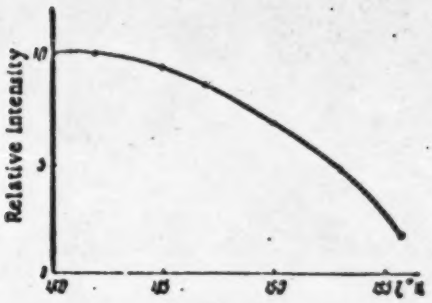

Fig. 3. Effect of temperature on line intensity I. The points on the curve represent average values from several determinations.

LITERATURE CITED

1. Y. Sasada and M. Atoji, J. Chem. Phys., 21, 145 (1953).
2. R. Livingston, J. Phys. Chem., 57, 496 (1953).
3. V. S. Grechishkin, Pribory i tekhnika éksperimenta, 2, 31 (1959).
4. V. S. Grechishkin, Candidate's Dissertation [in Russian] (Leningrad gos. Univ., 1959).
5. M. Buyle-Bodin, Ann. phys., 10, 533 (1955).

All abbreviations of periodicals in the above bibliography are letter-by-letter transliterations of the abbreviations as given in the original Russian journal. *Some or all of this periodical literature may well be available in English translation.* A complete list of the cover-to-cover English translations appears at the back of this issue.

PHASE TRANSITIONS IN THE GOLD – PLATINUM SYSTEM

V. V. Sanadze and N. I. Labartkava

V. I. Lenin Georgian Polytechnic Institute
Translated from Zhurnal Strukturnoi Khimii, Vol. 2, No. 6,
pp. 703-711, November-December, 1961
Original article submitted April 25, 1961

Gold–platinum alloys containing 10 and 25 atomic % of platinum were studied. The alloys were investigated by the method of consecutive quenching from 100 to 1000°. It was shown that in the course of mutual dissolution the phases pass through a series of ordered states.

Introduction

Studies of the Au–Pt system were started in the last century, but the phase diagram was finalized only in 1952-1953 (Fig. 1). According to this diagram, platinum and gold for a continuous series of solid solutions; in a certain concentration range these separate out into a gold-rich (α_2) and a platinum-rich (α_1) phase on decrease of temperature [1].

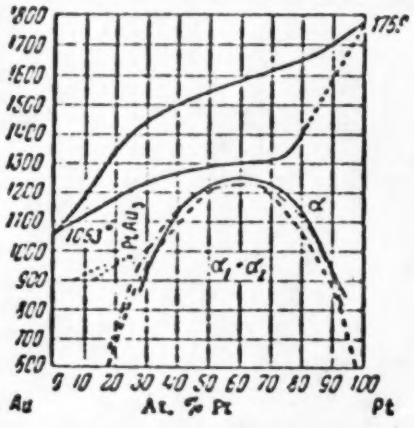

Fig. 1. Phase diagram of the platinum–gold system.

Johansson and Hagsten [2] made a detailed study of the segregation of a homogeneous solid solution in the alloy containing 30 atomic % of platinum by a thermal method and by measurements of electrical resistance. They reported certain peculiarities in the segregation; in particular, the fact that segregation of the homogeneous phase is considerably slower at high temperatures, near the upper boundary of the two-phase region (954°). In their opinion, this means that metastable regions where segregation is retarded exist near the boundary curve. Another observation of interest was that the electrical resistance of a specimen measured at different temperatures periodically approached to the lower limiting value.

Wictorin [3] investigated a series of gold–platinum alloys with 25 atomic % Pt and over. He measured resistance variations, established the boundary of the two-phase region more precisely, and showed that the rate of segregation, which is very high in the region of medium concentrations, falls considerably outside this region.

In 1951 Grube, Schneider, and Esch (cited in [1]) used the x-ray diffraction method for investigating transitions in the solid state and discovered an ordered phase of the composition Au_3Pt (α'-phase) below 1000°. The parameter of the α'-phase after annealing at 900° increases from 3.873 A for the alloy with 5 atomic % Pt to 3.918 A for the alloy with 25 atomic % Pt.

The most detailed investigation of the gold–platinum system, with measurement of lattice parameters of the alloys, was carried out by Darling et al. [4]. They showed that the parameters of alloys in the one-phase region deviate only slightly from the line corresponding to Vegard's law. As the result of this work the phase diagram assumed its final form. Subsequently Hardy [5] carried out a thermodynamic analysis of the system; comparing his results with the experimental data in [4] he noted that they were in good agreement.

Earlier [6,7] we studied the Ni–Au system and showed that mutual dissolution of the phases in the course of formation of a homogeneous solid solution proceeds by way of a series of ordered states. It is of interest in this respect to study this platinum–gold system which is analogous to the nickel–gold system, at least in the solid-phase region.

Preparation and Treatment of the Alloys

Gold–platinum alloys were prepared from gold plates 99.99% pure and platinum plates 99.8% pure. The alloys were made in a high-temperature tungsten furnace under vacuum, in corundum crucibles. The ingots were forged in the cold state and remelted. This treatment was repeated four times, and the alloys were then homogenized under vacuum at 900° for 70 hours. Cylinders of each composition, 0.4-0.5 mm in diameter, were cut from a part of the alloys; after removal of the surface layers by etching the cylinders were again annealed at 900°, for 30 hours. The other part of the alloys were used for preparation of polished sections; these were etched with aqua regia and used for microstructure investigations. The x-ray patterns showed some line broadening; the alloys were therefore annealed further at 800° for 25 hours and then cooled slowly.

The lattice parameters of the alloys were determined simultaneously with a back-reflection camera and the VRS-3 camera 142.4 mm in diameter with Cu-K_α radiation from the 333 doublet at $\theta \approx 81°20'$ for the α_2-phase, and from the 422 doublet at $\theta \approx 74°13'$ for the α_1-phase. The parameters, densities, and other characteristics of the alloy are:

Alloy no.	Pt, % by wt.	Pt, atomic %	Parameter of α_2-phase A	Paramater of α_1-phase, A	Density, ρ	Microhardness, H
1	10.2	10	4.055	3.921	19.9	5.45
2	25.15	25	4.047	3.921	20.2	6.1

The alloys were investigated by the method of consecutive quenching, described earlier in [6]. In the present instance three series of specimens were investigated simultaneously. Specimens of the first series were heated to the required temperature and quenched immediately. Specimens of the second series were heated, annealed for 3 minutes, and then quenched, while specimens of the third series were quenched after 10 minutes of annealing. Because of the high stability of these alloys they were heated in air and simultaneously in a suitable salt bath. No differences between the two sets of specimens were found in the experimental results. For the alloy with 10 atomic % Pt this process was performed between 100 and 875°, and for the alloy with 25 atomic % Pt, between 100 and 1000° with intervals of 15-25°.

Alloys with 10 Atomic % of Platinum

The x-ray diffraction patterns of alloys of this composition at room temperature contain, in addition to strong lines of the α_2 solid solution based on gold, weak lines of the α_1 solid solution of gold in platinum. According to the above data, about 9 atomic % Pt is dissolved in the gold lattice, while the platinum-based alloy contains about 3.5 atomic % of gold. This was to be expected from the phase diagram, which also shows that increase of temperature initially raises the solubility of platinum in gold sharply, whereas the gold solubility curve is almost vertical. Therefore the alloy chilled at 100° and held for 3 minutes shows a decrease of the α_1-phase parameter due to transfer of Pt atoms into the lattice of the α_2 solid solution. The value of the parameter reaches 3.916 A and after a halt at 150 and 175° continues to decrease, reaching 3.913 A after subsequent quenchings, which is lower than for pure platinum. The parameters of the α_1- and α_2-phases and of all the intermediate states for alloys with 10 and 25 atomic % Pt are shown in Fig. 2. A distinct periodicity is seen in the course of the parameters. The causes of this periodicity are discussed in detail below.

As the parameter decreases the intensity of the α_1-phase diminishes and the width of the 333 line of the main phase and the background of the x-ray pattern increase (Fig. 3). From 100° upward the solubility of gold in platinum also begins to increase slowly; this leads to formation of gold-rich zones. These layers of the new phase are formed in the planes of the Au–Pt lattice, as diffuse halos appear even at 190° near the corresponding lines in the x-ray patterns (the two-dimensional diffraction effect); the halos gradually form into lines (Fig. 4). These lines can be indexed in the cubic system with the parameter 4.065 A, i.e., with the parameter of a lattice containing only about 3 atomic % Pt. Dissolution of the gold-rich formations and appearance of the new lines corresponds to a sharp decrease in the width of the 333 line of the main phase (Fig. 3), a decrease in its intensity, and a decrease in the background of the x-ray pattern. It is seen in Fig. 2 that the parameters of the α_1- and α_2-phases diminish somewhat here, and then remain unchanged over a certain temperature range. During this period the formations of the intermediate phase are dissolved; this is accompanied by broadening of the lines and intensification of the background. All the diffuse lines

disappear. As a result of this dissolution the gold atoms pass into the platinum-rich solution increasing the parameter to 3.916 A at 260°. On the other hand, the platinum atoms enrich the gold-based alloy and thus decrease the parameter and increase the microhardness and density.

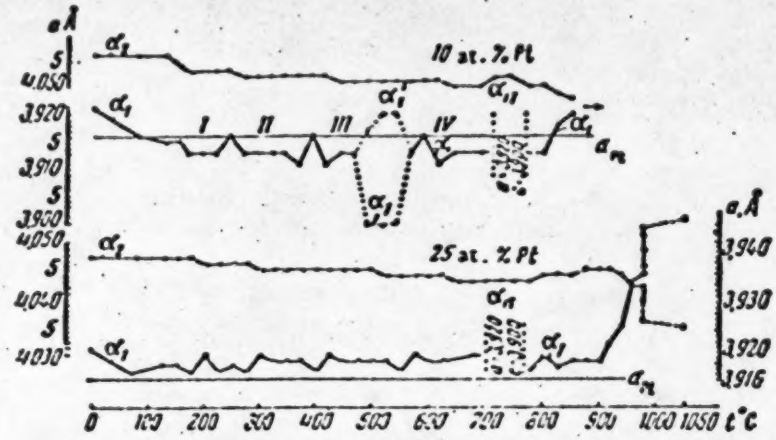

Fig. 2. Variations of the parameters of the α_1- and α_2-phases for alloys with 10 and 25 atomic % Pt with the quenching temperature.

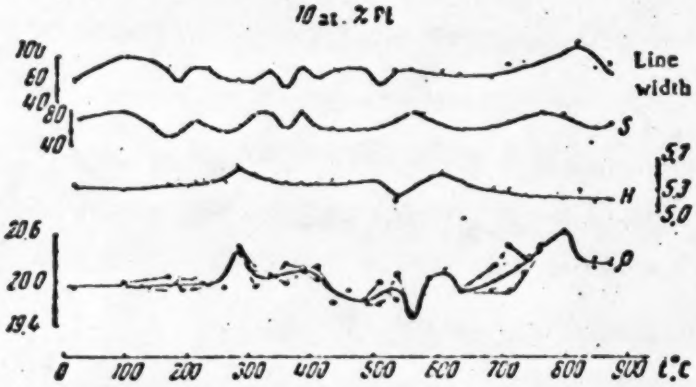

Fig. 3. Effects of the quenching temperature of the alloy with 10 atomic % Pt on the width (in mm·10^{-2}) of the 333 line, microhardness H (kg/mm^2), background S of the x-ray pattern [log I_0/I], and density ρ(g/cc) of the α_2-phase.

Thus, 265-275° corresponds to the end of period I, involving transfer of gold atoms into the platinum lattice and of platinum atoms into the gold lattice; this transfer proceeds by formation of intermediate gold-rich interlayers (zones). The curves in Fig. 3 show variations of the microhardness H, the background of the x-ray pattern S, the width of the 333 line of the α_2-phase, and the density ρ in relation to the quenching temperature. Densities were determined 5 minutes after the quenching, and then after 1, 2, 24, and 48 hours. The reason is that the alloy density changed sharply after the quenching and then slowly reached its stable value over a period of 24 hours, and sometimes 48 hours. These stable values are plotted against the quenching temperature. In addition, the density values determined soon after the quenching are shown. The distances between the two sets of values are matched for clarity. The greatest discrepancies are found if substantial changes take place in the alloy. There are virtually no differences between the densities in regions where there are no such changes.

This is especially clear for the alloy with 25 atomic % of platinum.

At about 270° transition period II begins; its course is analogous to that of the first. Dissolution of platinum atoms again causes a reduction of the parameter of the α_1-phase to 3.913 A, broadening of the lines of the main

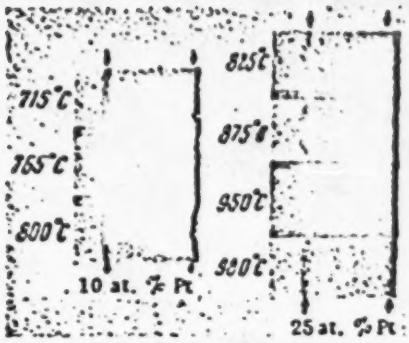

Fig. 4. Comparison of the diffuse halos in the x-ray diffraction patterns near the 422 and 333 lines of the main phase of alloys with 10 and 25 atomic % Pt.

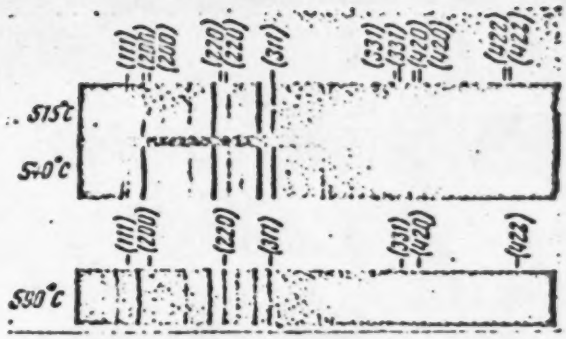

Fig. 5. X-ray diffraction pattern of alloys with 10 atomic % Pt quenched at 515, 540, and 590°.

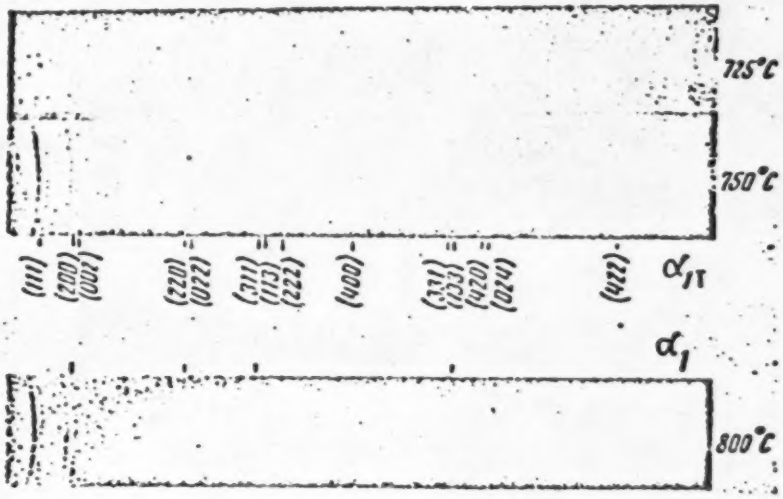

Fig. 7. X-ray diffraction pattern of alloys with 25 atomic % Pt, quenched at 725, 750, and 800°.

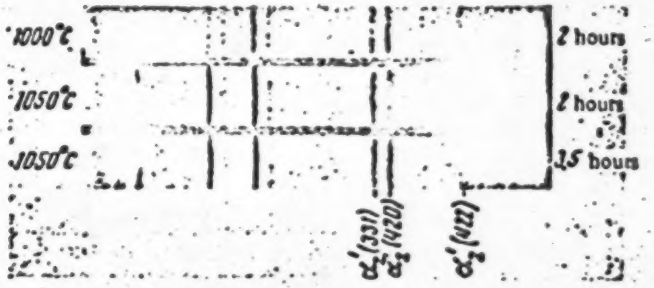

Fig. 8. X-ray diffraction patterns of alloys with 25 atomic % Pt, quenched for 2.5 hours at 1000° and for 2 and 3.5 hours at 1050°.

phase, and increase in the background of the x-ray pattern (Figs. 2 and 3). Formation of the gold-rich intermediate zones and their loss (dissolution) from the main phase occurs approximately at 360°, where the intensity and width of the line of this phase and the background fall to a minimum. Dissolution of the intermediate formations and appearance of diffuse lines lead to further dissolution of platinum and a further decrease of the parameter to 3.911 A. However, at 400-420° the diffuse halos near the main phase disappear, and the intermediate formations dissolve, enriching the α_1-solid solution with gold atoms, and the α_2-phase with platinum atoms. The parameter of the α_1-phase increases again to 3.916 A while that of the main phase undergoes the next decrease. In the x-ray patterns this dissolution process is accompanied by increase of the background and broadening of the lines of the α_1-phase. This completes period II of the redistribution of gold and platinum atoms. Mutual dissolution of the phases subsequently proceeds by the same routes as before, but now the quantitative proportions of the atoms which have diffused between the two phases become significant. Thus, in the 500-600° range the α_2-phase separates into two solid solutions, α_1 and A_1', with parameters of 3.900 and 3.920 A respectively.

The lines of these phases are so weak that any analysis of intensities is impossible. Therefore, in the table below we merely compare the squares of the sines of the reflection angles, calculated from the lattice parameters given above, with the experimental values:

hkl of α_1-phase	$\sin^2\theta$ exptl.	$\sin^2\theta$ calc.	*hkl* of α_1'-phase	$\sin^2\theta$ exptl.	$\sin^2\theta$ calc.
111	—	—	111	0,118	0,116
200	0,159	0,157	200	0,155	0,154
220	0,313	0,312	220	0,309	0,308
311	—	—	311	0,425	0,424
331	0,732	0,730	331	0,736	0,734
420	0,779	0,779	420	0,773	0,771
422	0,932	0,933	422	0,925	0,925

Figure 5, which gives the x-ray diffraction patterns of the alloy with 10 atomic % Pt quenched at 515, 540, and 590°, clearly shows the appearance of two similar systems of lines, followed by their coalescence as the result of equalization of the concentrations of the platinum-based solid solutions. While equalization of concentrations is taking place in the α_1-phase, the formation, separation, and dissolution of gold-rich interlayers proceeds in the main phase. This dissolution enriches the α_1-phase with gold atoms and its parameter reaches 3.916 A at 590°. This concludes yet another stage in the course of phase dissolution. Rise of temperature above 625° leads to a new distribution of atoms with enrichment of the platinum-based solid solution with platinum atoms by way of formation and dissolution of intermediate zones. This redistribution leads to splitting of the α_1-phase lines at 740°. The character of this splitting is such that the lattice of the α_1-phase passes into a tetragonal lattice with the parameters $\underline{a}$ = 3.920, $\underline{c}$ = 3.900 A, and $\underline{c}/\underline{a}$ = 0.99. Calculations based on the x-ray patterns of alloys quenched at 740° give the following results:

hkl of α_{1T}'-phase	$\sin^2\theta$ exptl.	$\sin^2\theta$ calc.	*hkl* of α_{1T}'-phase	$\sin^2\theta$ exptl.	$\sin^2\theta$ calc.
111	0,118	0,116	331	0,732	0,732
200	0,151	0,154	133	0,736	0,735
002	0,156	0,156	420	0,773	0,772
220	0,306	0,308	024	0,778	0,776
022	0,310	0,310	422	0,924	0,925
311	0,425	0,424	224	0,929	0,930

The formation and subsequent growth of gold-rich zones in the main phase is most distinct in this temperature range. Diffuse halos arise near the lines of this phase; they are apparently caused by two-dimensional diffraction effects gradually appearing in the lines. This may be seen especially clearly near the 333 and 422 lines of the main phase. The arrows in Fig. 4 indicate shifts of the 333 and 422 lines for alloys with 10 atomic % Pt, quenched at 715, 765, and 800°. It may be seen that the fluctuation of the parameter of the main phase in the direction of an increase at 850° is due to the presence of strong diffuse halos near the main doublet lines and to consequent errors in their measurement. Similar effects are observed for alloys with 25 atomic % Pt (Fig. 2). Dissolution of the intermediate-phase

formations leads to disordering of the α_1-phase. The lattice becomes cubic again. Its parameter increases while that of the α_2-phase decreases. Even at 575° the two parameters converge, indicating formation of a homogeneous solid solution.

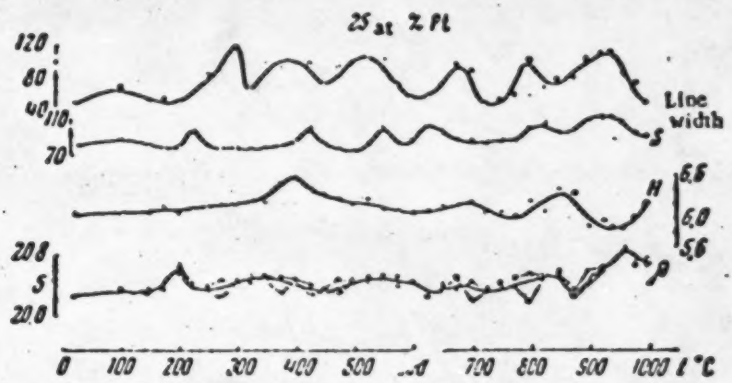

Fig. 6. Effect of the quenching temperature of alloys with 25 atomic % Pt on the width of the 333 line, the microhardness H, background of the x-ray pattern, and density ρ of the α_2-phase (for measurement units, see Fig. 3).

Alloys with 25 Atomic % of Platinum

Alloys of this composition are also two-phase at room temperature: they consist of the α_1-phase with parameter 3.921 A and the α_2-phase with parameter 4.047 A. Thus, the lattice of the platinum-based solid solution has the same gold content as the corresponding phase of the 10% alloy, whereas the gold lattice contains much more dissolved platinum. As before, rise of temperature leads to transfer of platinum atoms from the α_1-phase into the α_2-phase, accompanied by a decrease of the parameter of the first phase to 3.917 A and broadening of the lines of the second phase (Fig. 6). This is the lower limit of the decrease of the parameter. In contrast to alloys with 10 atomic % of platinum, where the parameter diminishes to 3.193 A and even less, the parameter of the α_1-phase almost reaches that of pure platinum but does not fall below that value. Every time that the parameter of the α_1-phase falls to this limiting low value the width of the 333 line of the main phase exhibits a maximum (Fig. 6), thereby indicating maximum lattice distortion. During this period gold-rich zones of the intermediate phase are formed in the crystal lattice of the α_2-phase causing additional dissolution of platinum and a decrease of the parameter of the α_1-phase at 200°.

Further rise of temperature leads to dissolution of this intermediate formation, enrichment of the platinum-based solid solution (the α_1-phase) with gold atoms, and increase of its parameter to 3.920 A. At the same time the gold-based solid solution (the α_2-phase) is enriched with platinum atoms and its parameter decreases. Accordingly, at 225° the width of the 333 line of the main phase reaches a minimum while the hardness rises slightly. The density of the alloy also increases a little in this temperature region (Fig. 6). A similar process of redistribution of gold and platinum atom with rise of temperature is repeated periodically, terminating at 325, 450, and 600°. The width of the 333 line of the main phase reaches a minimum at the same temperatures. The hardness of this phase gradually increases with increasing platinum content. It is interesting to note the course of the density variations. As stated earlier, densities were determined immediately after the quenching and then several times more at intervals. The spread of the density values was fairly considerable in the region where processes of atom redistribution and formation of intermediate zones are the most intensive. In the region where these processes terminate and the parameter of the α_1-phase reaches its maximum value all the densities converge at one point with very little scatter. This is clearly seen in Fig. 6. It must be pointed out that segregation of platinum-based solid solutions with very low values of the parameter, observed alloys with 10 atomic % Pt in the 500-600° range, does not occur in alloys with 25 atomic % Pt. However, as in the previous case, splitting of the lines of the α_1-phase occurs. The lattice of this phase becomes tetragonal, with the parameters a = 3.920, c = 3.900 A and c/a = 0.99, while the intensity becomes almost equal to the intensity of the main phase. Figure 7 shows the x-ray patterns of alloys with 25 atomic % Pt, quenched at 725, 750, and 800°. The following results were obtained for the x-ray pattern of the alloy quenched at 750° (the intensities of

the α_1-phase lines were calculated approximately with the Lorentz, polarization, and multiplicy factors taken into account:

hkl of α_1 phase	$\sin^2\theta$ exptl.	$\sin^2\theta$ calc.	$I_{exptl.}$	$I_{calc.}$	hkl of α_1 phase	$\sin^2\theta$ exptl.	$\sin^2\theta$ calc.	$I_{exptl.}$	$I_{calc.}$
111	0,117	0,116	30	50	222	0,463	0,463	20	10
200	0,154	0,154	27	18	400	0,616	0,616	15	5
002	0,157	0,156	7	10	331	0,732	0,732	40	22
220	0,308	0,308	35	18	133	0,735	0,735	5	12
022	0,312	0,310	10	15	420	0,772	0,772	45	16
311	0,424	0,424	40	22	024	0,779	0,776	5	14
113	0,470	0,427	10	12	422	0,926	0,925	50	42

The subsequent changes are similar to that already described: rise of temperature to 800° leads to coalescence of the split lines. A disordering process begins caused by the consequent enrichment of the α_1-phase with gold and loss of platinum. At 825° its parameter again reaches 3.920 A and the width of the α_1-phase line reaches a minimum. The line intensities of the two phases become almost equal. The x-ray patterns of alloys quenched above 825° exhibit intense diffuse halos near the lines of the main phase which form gradually in the line of the gold-rich phase. The parameter of the intermediate phase gradually diminishes. Therefore the diffuse lines which first appear on one side of the lines of the main phase move over to the other side and begin to disappear at 980°. This is clearly seen in Fig. 4, which shows diffuse lines near the 422 and 333 lines of the main phase in the x-ray patterns of alloys quenched at 825, 875, 950, and 980°.

Dissolution of the intermediate phase results in enrichment of the α_1-phase with gold atoms, and increases its parameter and line intensities. At the same time the parameter of the α_2-phase gradually decreases. Alloys quenched at 1000° have parameters of 3.935 and 4.012 A. Exposure at this temperature for 2.5 hours increases the parameter of the first phase to 3.942 A and decreases that of the second to 4.010 A. At 1050° segregation begins in the main phase. Very diffuse lines of a phase with a parameter of 4.020 A appear near each line of the α_2-phase, while the lines of the α_1-phase become much weaker. Annealing for 2 hours at 1050° leads to almost complete dissolution of the α_1-phase with sharp separation of the lines of the α_2- and α_2^*-phases (Fig. 8).

As the result of the dissolution of the α_1-phase, the parameter of the α_2^*-phase increases to 4.017 A. Further annealing of the alloy equalizes the concentrations of these two solid solutions with formation of an ordered phase of the Au_3Pt type.

DISCUSSION OF THE RESULTS

A general scheme representing the mutual dissolution of phases in the gold–platinum system can be postulated on the basis of the above experimental data. This scheme is shown in Fig. 9. It follows from the foregoing that at room temperature alloys containing 10 and 25 atomic % Pt are mixtures of two solid solutions (α_1 and α_2). Progressive increase of temperature results in redistribution of platinum and gold atoms between the phases. Initially the solubility of platinum in gold increases to the greater extent. As the result of dissolution of platinum the parameter of the α_1 solid solution decreases to a value smaller than that of platinum in the 10% alloy and almost down to that value in the alloy with 25 at.% Pt.

Increase of the solubility of gold leads in its turn to accumulation of gold atoms and formation of gold-rich interlayers of an intermediate phase. On further increase of temperature these intermediate formations dissolve, enriching the platinum-based solid solution with gold, and the gold-rich solid solution with platinum. This type of atom redistribution by formation and dissolution of an intermediate phase is periodically repeated on increase of temperature. This periodicity of the process not only gives rise to regular variations of the lattice parameters but also influences variations of line width, density, and other physical characteristics of the alloys. Redistribution of gold and platinum atoms between the solid solutions in the alloy with 10 atomic % Pt leads to segregation in the α_1-phase and formation of a cubic α_1^*-phase in the 500-600° range. This, like the α_1-phase, is a platinum-based solid solution but is richer in gold. Rise of temperature leads to leveling of the concentrations and disappearance of this phase. In the 715-790° range the cubic lattice of the α_1-phase becomes tetragonal. "Tetragonalization" of the α_1-phase in alloys with 25 atomic % Pt also occurs in the same temperature range. The tetragonal form disappears with rise of temperature and the parameters of the two solid solutions begin to converge. In alloys with 25 atomic % Pt the α_1-phase dissolves completely only after several hours of exposure at 1050°. As the result of this dissolution the α_2-phase becomes enriched with platinum and segregates. A solid solution with a parameter of 4.017 A (the α_2^*-

phase) is formed. Equalization of the concentrations of these two gold-based solid solutions leads to the formation of a one-phase alloy with an ordered structure of the Au_3Pt type. Superstructure lines are very difficult to observe in the Pt–Au system because they are extremely weak. However, it may be concluded on approximate geometrical grounds that the α_1^*-phase which forms in the 500-600° range is an ordered phase of the Pt_3Au type, whereas tetragonalization of the lattice occurs as the result of ordering with the composition PtAu.

Thus, mutual phase dissolution in the Pt–Au system proceeds by way of a series of ordered states in exactly the same way as was demonstrated by us in the Ni–Au system [6,7].

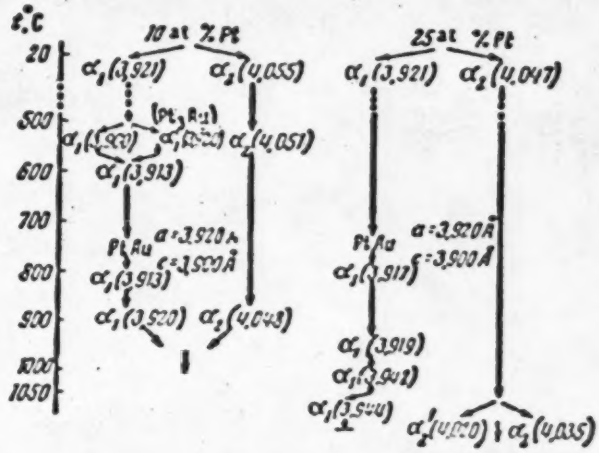

Fig. 9. Schematic diagram of the intermediate states arising during mutual dissolution of phases in the Pt–Au system.

It is interesting to note that the presence of ordered phases of the types of Au_3Pt, Pt_3Au, PtAu in the Pt–Au system was discovered as long ago as 1930 [8]. However, subsequent investigations refuted this result and only a final ordered phase of the composition Au_3Pt was found. The cause of these contradictions is clear in the light of the present investigation. The reason is that Pt_3Au, PtAu and Au_3Pt are not stable phases which exist in definite temperature ranges but are merely ordered states which arise in the course of mutual dissolution of the phases.

LITERATURE CITED

1. M. Hansen, Constitution of Binary Alloys (London, 1958).
2. C. H. Johansson and O. Hagsten, Ann. Phys., 28, 520 (1937).
3. C. G. Wictorin, Ann. Phys., 33, 509 (1938).
4. A. S. Darling, R. A. Mintern, and L. C. Caston, J. Inst. Met., 31, 125 (1952-53).
5. H. K. Hardy, J. Inst. Met., 31, 599 (1952-53).
6. V. V. Sanadze and G. V. Gulyaev, Kristallografiya, 4, 4, 526 (1959).
7. V. V. Sanadze and G. V. Luyaev, Kristallografiya, 4, 5, 637 (1959).
8. C. H. Johansson and L. O. Linde, Ann. Phys., 5, 762, (1930).

All abbreviations of periodicals in the above bibliography are letter-by-letter transliterations of the abbreviations as given in the original Russian journal. *Some or all of this periodical literature may well be available in English translation.* A complete list of the cover-to-cover English translations appears at the back of this issue.

X-RAY STRUCTURAL INVESTIGATION OF THE CRYSTALS OF THE DOUBLE SALT OF PENTAMMINECOPPER PERCHLORATE AND AMMONIUM PERCHLORATE

M. Bukovska and M. A. Porai-Koshits

M. V. Lomonosov Moscow State University
Translated from Zhurnal Strukturnoi Khimii, Vol. 2, No. 6,
pp. 712-718, November-December, 1961
Original article submitted August 31, 1960

The structure of crystals having the over-all formula $NH_4Cu(NH_3)_5(ClO_4)_3$ was investigated by the x-ray diffraction method. The crystals belong to the tetragonal system; $a = 10.59$, $c = 7.50$ A, $N = 2$. Space group $P\bar{4}2_1m$. Magnetic moment $\mu_{eff} = 1.77\ \mu_B$. The crystals exhibit a considerable piezo effect. The structure was determined from the (001) and (110) projections of the interatomic function, by geometrical analysis in conjunction with the method of trial and error, and from the (001) and (110) electron density projections with the aid of the Booth correction. The structural elements are $[Cu(NH_3)_4]^{2+}$ square complexes, NH_4^+ and ClO_4^- ions, and NH_3 groups. The Cu-NH_3 distances are 2.07 ± 0.02 A. There are numerous hydrogen bonds between the NH_3 groups and NH_4^+ and ClO_4^- ions.

In the course of studies of the crystal chemistry of complex compounds of bivalent copper (and, in particular, its amines) in the Laboratory of Crystal Chemistry of the Chemical Faculty of Moscow State University crystals of $Cu(NH_3)_4PtCl_4$ [1], $Cu(NH_3)_4 \cdot (NO_2)_2$ [2], $CuPy_2(NCS)_2$ [3] were investigated by the x-ray structural method. In this paper we present the results obtained by structure analysis of $NH_4Cu(NH_3)_5(ClO_4)_3$ crystals.

An account of the preparation of the substance and its crystallographic characteristics are given in an earlier brief communication [4]. The lattice parameters were determined from oscillation x-ray patterns along the [100], [001], and [110] directions and refined from the distant spots of zero layer lines taken with the Wessenberg x-ray goniometer. The cassette radius was determined with the aid of an NaCl standard. The following values were obtained: $a = b = 10.59 \pm 0.02$, $c = 7.50 \pm 0.02$ A; $N = 2$; $d_{x\text{-ray}} = 1.84$, $d_{pycn.} = 1.84$ g/cc. The crystals belong to the $D_{4h} = 4/mm$ diffraction class. In accordance with the extinctions found, the space groups $D_{2d}^3 = P\bar{4}2_1m$ and $D_4^2 = P4_12_1$ are possible. The absence of an inversion center is confirmed by the strong piezo effect.*

The structure was determined by recording of the zero layer lines during rotation of the crystal about the [001] and [110] axes. The reflection intensities were estimated visually on a blackening point scale. The squares of the structure amplitudes were calculated with the polarization and Lorentz factors taken into account; the absorption factor was disregarded. Crystals of approximately 0.2 × 0.2 mm square section were chosen. In some instances the crystals were elongated in the [110] direction; this was very convenient for adjustment of the crystal in that direction and diminished the errors due to absorption. After adjustment the crystals were coated with collodion.

Preliminary structure data were obtained by calculation of projections of the interatomic functions in the [110] and [001] directions [because of numerous superpositions of maxima, the projection on the (100) plane did not give any useful results]. Combined analysis of these projections gave the possible vertical (along the Z axis) and horizontal (lying in the XY plane components of the Cu–Cu, Cu–Cl_I·Cu–Cl_{II}, and Cu–NH_3 vectors (Fig. 1).

Analysis of the occurrence of general and special positions in both possible space groups reveals several structural variants different in principle. However, detailed comparison of the coordinates of the maxima and of the positions which may be occupied by Cu and Cl atoms makes it possible to reject all the variants with the exception of one which belongs to the $P\bar{4}2_1m$ group. Thus, analysis of Patterson projections gave the space group and the coordinates of most of the atoms. It was found that Cu atoms occupy the twofold position 2 (a): 000, ½ ½ 0; six Cl

* The piezo effect was measured by V. A. Koptsik (Faculty of Physics, Moscow State University).

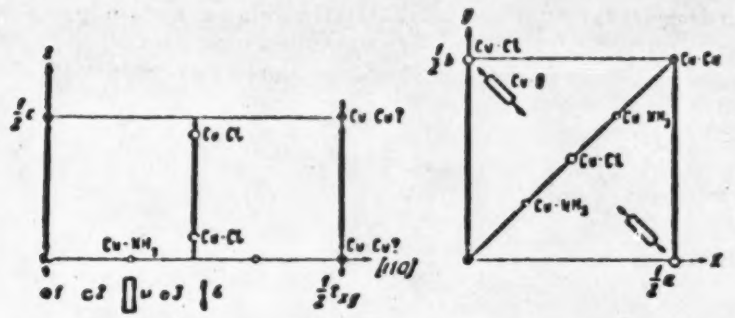

Fig. 1. Distribution of the maxima in Patterson projections (the Cu–Cu, Cu–Cl, Cu–O, and Cu–NH_3 vectors): 1) Highest maxima; 2) maxima of medium height; 3) low maxima; 4) direction of "diffusion" of the maximum and the possible vector displacement associated with it.

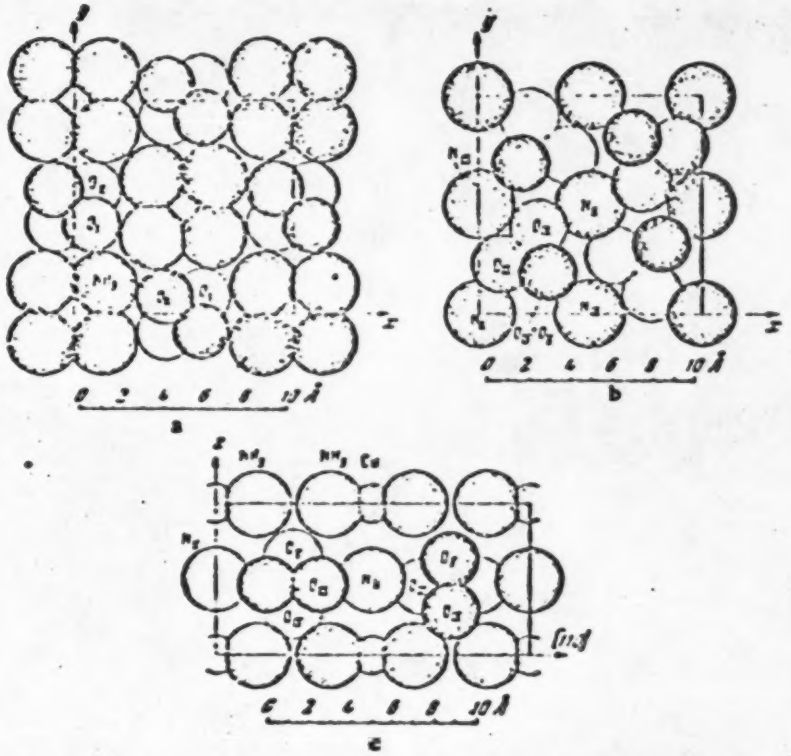

Fig. 2. Atomic packing in the structure: a) Layer parallel to (001), with z = = 0; b) layer parallel to (001), with $z = 1/2$; c) layer parallel to (110), with z=0.

atoms occupy two positions: Cl_I a twofold position 2(c): $0\ 1/2\ z$, $1/2\ 0\ z$ with z close either to zero or to $1/2$; Cl_{II} occupies the fourfold position 4(e): $x, 1/2+x, z$ with $x = 1/4$, and z close to $1/2$ or to zero; of the ten NH_3 groups, eight occupy the general position 8(f): xyz with $x = y = 0.13$ and $z = 0$. The remaining two NH_3 groups and the two NH_4^+ ions must occupy twofold positions 2(b): $1/2\ 00$, $1/2\ 1/2\ 1/2$ and 2(c): $0\ 1/2\ z$, $1/2\ 0\ \bar{z}$. As these groups are indistinguishable by the x-ray method, we use the symbol N_{II} to denote the group in position 2(b), and N_{III} for the group in position 2(c). In analysis of the positions of the oxygen atoms we took into account the obvious fact that they are in tetrahedral coordination around the chlorine atoms. This gave two positions 4(e) for the eight oxygen atoms O_I and O_{II} surrounding the Cl atoms, and three positions: 8(f), 4(e), and 4(c) for the 16 oxygen atoms O_{III}, O_{IV}, and O_V surrounding the Cl_{II} atoms. The coordinates of the O_I and O_{II} atoms are found from Patterson Projections.

Three problems remained to be solved for a complete determination of the atomic arrangement.

1. Selection of one of the two possible variants for distribution of Cl_I and Cl_{II} atoms along the height z of the cell (Cl_I with $z \approx 0$ and Cl_{II} with $z \approx 1/2$, or vice versa).

2. Determination of the coordinate z of the N_{III} atom in position 2(c).

3. Determination of the orientation of the $[Cl_{II}O_4]^-$ perchlorate group; i.e., determination of the coordinates of the atoms O_{III}, O_{IV}, and O_V.

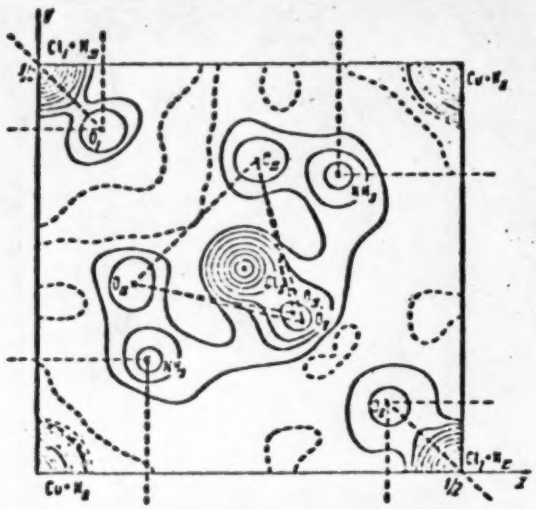

Fig. 3. Electron-density projection on the (001) plane. The curves are drawn at intervals starting at the 2 el/A² level.

These structural details were elucidated by geometrical analysis in conjunction with the method of trial and error. In analysis of the possible spatial distribution of the structural elements, the ClO_4^- tetrahedrons were assumed to be regular, and the Cl–O distances were taken as 1.50 A; the values adopted for the intermolecular radii were 1.40 A for O, and 1.70 A for NH_3 groups and NH_4^+ ions. Values of $F_{calc.}$ and $F_{meas.}$ were compared for reflections of the hk0 and 00*l* type. As the result of somewhat laborious work on rejection of geometrically improbable positions, and variations of the positional parameters for improving the agreement between $F_{calc.}$ and $F_{meas.}$, we obtained the configuration shown in Fig. 2 a,b, and c, which is a schematic diagram of the atomic packing in individual layers of the unit cell.

The final electron-density projections are given in Figs. 3 and 4. The maxima on the projections were found by interpolation from parabolic curves (electron-density sections passing through the maximum) and determinations of the points where the first derivatives are zero. The (001) centrosymmetric projection clearly reveals the maxima corresponding to all five independent oxygen atoms and the NH_3 groups surrounding the copper atoms in a square arrangement. The characteristic feature of the noncentrosymmetric projection (110) is that for many atoms (linked by the plane of symmetry parallel to the projection plane) there are maxima of double height, so that the precision in determination of their coordinates is increased considerably; moreover, the two independent chlorate groups both appear twice in different regions of the projection. The theoretical (001) and (110) projections were calculated, with the Booth correction, for determination of the displacements of the maxima due to termination of the series and superposition of maxima of atoms in close proximity in the projections. The final values were the x and y coordinates averaged over two projections and the z coordinates from the (110) projection averaged for independent maxima. In the averaging differences between the errors of the coordinates found from the centrosymmetric and noncentrosymmetric coordinates [5] and from maxima of single or double height were taken into account. The final atomic coordinates are given in Table 1.

TABLE 1. Atomic Coordinates in the Crystal Structure of $NH_4[Cu(NH_3)_4](ClO_4)_2 \cdot NH_3$

Atoms	Position	x	y	z	Atoms	Position	x	y	z
Cu	2 (a)	0	0	0	O_{IV}	4 (e)	0,392	0,191	0,696
Cl_I	2 (c)	0	1/2	0,067	O_V	4 (e)	0,397	0,193	0,368
Cl_{II}	4 (e)	1/2	1/2	0,530	NH_3	8 (f)	0,138	0,138	−0,002
O_I	4 (e)	0,092	0,418	0,187	N_{II}	2 (b)	0	0	1/2
O_{II}	4 (e)	0,085	0,585	−0,053	N_{III}	2 (c)	0	1/2	0,567
O_{III}	8 (f)	0,109	0,230	0,532					

Neither the experimental nor the theoretical (110) projection shows clearly the maxima corresponding to N_{III} atoms. In both projections they are hidden to an equal extent in the slopes of high maxima corresponding to two Cl_{II} atoms and two O_{IV} atoms. However, the small difference between the electron densities in the experimental

and theoretical projections in regions where N_{III} atoms may be present confirms that it is correct to locate them half way between the perchlorate groups, i.e., with $zN_{III} = 0.566_5$. The N_{II} maximum on the (110) projection is also in the region of the stronger Cl_{II} maximum. Here, however, the coordinate $z = 1/2$ is determined by the crystal symmetry. Nevertheless two other variants were tested involving displacement of the N_{II} atom along the z axis to a position with $z \approx 0.17$, i.e., into the region of a diffuse "spur" of one of the maxima which cannot be accounted for by the other atoms. If the twofold position of the N_{II} atom was to be retained, it was necessary to assume either a lowering of symmetry in the structure to $P2_12_12$, or a statistical distribution of N_{II} atoms over one half of the points of the fourfold position 4(d): 00z, 00z, $1/2$ $1/2$ z, $1/2$ $1/2$ z, with $z \approx 0.17$. However, both variants increased the divergence factor and worsened the general contours of the (110) projection. Moreover, a similar "spur" was found on the theoretical electron-density projection. Its existence is therefore a consequence of series termination.

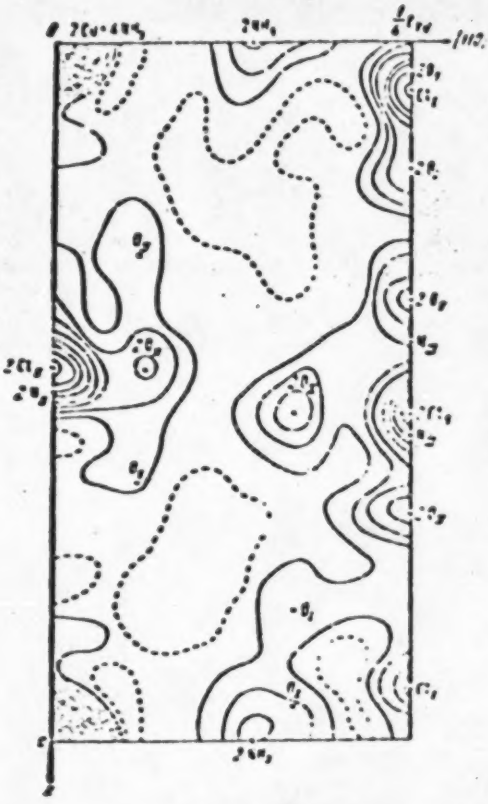

Fig. 4. Electron-density projection on the (110) plane. The curves are drawn at intervals of 4 el/A^2.

The experimental and calculated structure amplitudes are compared in Table 2. Reduction to the absolute scale and determination of the average temperature correction for all the atoms were effected by comparison of $F_{calc.}$ with $F_{meas.}$ [6]. For hk0 reflections B = 2.8 A^2, and for reflections of the hhl type B = 2.3 A^2. The divergence factor, calculated for all the reflections up to $(\sin\theta/\lambda)_{max.} = 0.63$ was found to be 0.226 for reflections of the hk0 type (0.197 without zero reflections). For reflections of the hhl type it was 0.194. The probable errors in determination of the atomic coordinates, calculated from Vainshtein's formula [7-8] for a two-dimensional electron density distribution, were:

$$\Delta(x_{Cl_I}) \quad \Delta(z_{Cl_I}) = 0.006, \quad \Delta(z_{Cl_{II}}) = 0.013,$$
$$\Delta(x_O) \quad \Delta(z_O) = 0.014, \quad \Delta(x_N) = \Delta(z_N) = 0.019 \text{ A}.$$

Description of the Structure

The most important interatomic distances in A and bond angles have the following values:

Distances and angles in ClO_4 groups

$Cl_I - 2O_I$	= 1.52 ± 0.02	$\angle O_I - Cl_I - O_I$	= 108°
$Cl_I - 2O_{II}$	= 1.55 ± 0.02	$\angle O_I - Cl_I - O_{II}$	= 110°
$O_I - O_I$	= 2.46 ± 0.03	$\angle O_{II} - Cl_I - O_{II}$	= 110°
$O_{II} - O_{II}$	= 2.54 ± 0.03		
$O_{II} - O_I$	= 2.52 ± 0.02		
$Cl_{II} - 2O_{III}$	= 1.51 ± 0.02	$\angle O_{III} - Cl_{II} - O_{III}$	= 107°
$Cl_{II} - O_{IV}$	= 1.52 ± 0.02	$\angle O_{IV} - Cl_{II} - O_V$	= 109°
$Cl_{II} - O_V$	= 1.48 ± 0.02	$\angle O_{IV} - Cl_{II} - O_{III}$	= 111°
$O_{III} - O_{III}$	= 2.42 ± 0.03	$\angle O_V - Cl_{II} - O_{III}$	= 111°
$O_{IV} - O_V$	= 2.46 ± 0.02		
$O_{III} - O_{IV}$	= 2.49 ± 0.02		
$O_{III} - O_V$	= 2.46 ± 0.02		

Environment of the NH_3 group

$NH_3 - NH_3$	= 2.92 ± 0.01 (in complex)		
$NH_3 - NH_3$	= 3.36 ± 0.01	$\angle Cu - N_I - O_{II}$	= 124°
$NH_3 - O_{IV}$	= 2.97 ± 0.02	$\angle Cu - N_I - O_{IV}$	= 127°
$NH_3 - O_{II}$	= 3.01 ± 0.02	$\angle O_{II} - N_I - O_{IV}$	= 64°

TABLE 2. Comparison of $F_{meas.}$ and $F_{calc.}$ for Reflections of the hk0 and hkl Types

hk0	$F_{meas.}$	$F_{calc.}$	hk0	$F_{meas.}$	$F_{calc.}$	hk0	$F_{meas.}$	$F_{calc.}$	hk0	$F_{meas.}$	$F_{calc.}$
200	17	+7	520	7	−18	640	40	+26	770	7	+6
300	69	+73	620	66	+61	740	10	−8	870	0	0
400	9	+6	720	10	+14	840	49	+46	970	0	+8
500	75	+58	820	18	+18	940	8	+8	10.70	0	+1
10.00	17	+20	920	16	−11	10.40	17	+13	11.70	4	+3
12.00	23	+27	10.20	33	+34	11.40	0	−4	880	49	+47
210	20	−14	11.20	0	+4	12.40	28	+26	980	5	+4
310	24	−10	12.20	13	+7	550	21	−29	10.80	9	−9
410	36	+39	13.20	0	0	650	0	0	990	9	+8
510	24	+29	330	29	+14	750	9	+6			
610	17	−35	430	15	−18	850	9	−4			
710	31	+34	530	40	+47	950	10	+6			
810	0	0	630	8	+8	10.50	0	+1			
910	12	+15	730	10	−6	11.50	0	+5			
10.10	7	+6	830	10	+10	12.50	0	−2			
11.10	5	−11	930	9	+1	660	71	+69			
12.10	0	−1	10.30	10	−7	760	0	+1			
13.10	0	+4	11.30	10	+16	860	16	+9			
220	172	+181	12.30	0	+2	960	0	−5			
320	11	+11	440	85	+89	10.60	26	+28			
420	52	+54	540	0	+7	11.60	0	+3			

hkl	$F_{meas.}$	$F_{calc.}$	Phase	hkl	$F_{meas.}$	$F_{calc.}$	Phase	hkl	$F_{meas.}$	$F_{calc.}$	Phase
002	169	189	0°	228	7	5	45°	556	28	22	35,9°
003	27	30	0°	330	34	14	0°	557	16	21	331,2°
004	66	90	0°	331	54	49	25,1°	558	20	24	19,6°
005	9	9	0°	332	59	63	21,6°	660	84	75	0
006	49	51	0°	333	18	20	19°	661	21	7	16,8°
007	0	2	0°	334	58	53	6°	662	54	54	0,7°
008	0	1	0°	335	38	33	355,1°	663	11	1	0°
009	5	8	0°	336	40	36	24,4°	664	22	33	358°
111	41	21	315°	337	24	23	0°	665	7	6	70,2°
112	72	64	26,5°	338	24	30	17,3°	666	11	19	337,7°
113	31	39	346,6°	440	102	94	0°	770	11	6	0
114	47	55	25,8°	441	64	51	348,7°	771	17	14	344,8°
115	27	45	303,4°	442	70	70	356°	772	22	21	24,4°
116	44	53	46,5°	443	38	36	340,3°	773	24	19	339°
117	38	41	318,5°	444	18	47	6,1°	774	22	24	24,4°
118	37	37	26,2°	445	14	20	16,7°	775	14	21	317,7°
119	14	19	325,6°	446	26	29	324,5°	880	54	54	0
220	169	183	0°	447	0	10	0°	881	16	5	288,2
221	21	23	272,0°	448	0	10	329,0°	882	31	33	359,3°
222	92	91	351,1°	550	31	32	180,0°	883	14	10	335,6°
223	32	28	315°	551	31	26	356,6°	990	7	8	0°
224	28	47	10,1°	552	53	50	33,1°	991	5	8	262,6°
225	19	5	249°	553	31	20	334,1°				
226	31	29	350,5°	554	31	25	29,9				
227	8	7	296,4°	555	21	22	326,3°				

Environment of the $(NH_n)_{II}$ group

$N_{II} \cdots 4O_{III} = 2.71 \pm 0.02$ $\quad \angle O_{III} \cdots N_{II} - O_{III} = 90.4°$

Environment of the $(NH_m)_{III}$ group

$N_{III} \cdots 2O_I$	= 3.10	$\angle O_I - N_{III} - O_I$	= 51°
$N_{III} \cdots 2O_{II}$	= 3.15	$\angle O_{II} \cdots N_{III} - O_{II}$	= 51°
$N_{III} \cdots 4O_{III}$	= 3.11	$\angle O_{III} - N_{III} - O_{III}$	= 51°
$N_{III} \cdots 2O_V$	= 2.92	$\angle O_V - N_{III} - O_V$	= 160°

The structure is composed of $[Cu(NH_3)_4]^{2+}$, NH_4^+, ClO_4^- ions and NH_3 groups. The complex $[Cu(NH_3)_4]^{2+}$ ions have plane square structure with Cu–NH_3 distances of 2.07 ± 0.02 A. The ClO_4^- tetrahedrons are only slightly distorted; nearly all the differences between the Cl–O and O–O distances lie within the possible error limits. The average distances are 1.52 A for Cl–O and 2.48 A for O–O.

The idealized packing pattern of the structural elements may be described as follows. The $[Cu(NH_3)_4]^{2+}$ complexes and $(ClO_4^-)_I$ ions lie in the (001) plane at height z = 0 and alternate in checkerwork order (Cu at the points 000 and $\frac{1}{2}\ \frac{1}{2}\ 0$, Cl at the points $0\ \frac{1}{2}\ 0$ and $\frac{1}{2}\ 0\ 0$). The remaining ("fifth") NH_3 groups and NH_4^+ ions are arranged in the same manner in another layer at height $z = \frac{1}{2}$. Between them (in the same layer) the four $(ClO_4^-)_{II}$ perchlorate groups are situated at the points $\frac{1}{4}\ \frac{1}{4}$, $\frac{1}{4}\ \frac{3}{4}$, $\frac{3}{4}\ \frac{1}{4}$, $\frac{3}{4}\ \frac{3}{4}$. As the NH_3 groups and NH_4^+ ions are indistinguishable by the x-ray method, it is not possible to determine which is in position N_{II} (at the point $00\frac{1}{2}$) and which at N_{III} (at the point $\frac{1}{2}\ 0\ \frac{1}{2}$); statistical distribution between these positions is not excluded. The actual coordination of $(NH_n)_{II}$ and $(NH_m)_{III}$ groups is determined by displacements of ClO_4^- ions from their "ideal" positions and by differences in the orientation of $(ClO_4^-)_I$ and $(ClO_4^-)_{II}$ groups. The $(NH_n)_I$ group is surrounded by four oxygen atoms which form a very flattened tetrahedron around it (two Cu atoms at a distance of 3.75 A are more distant neighbors). The distances $N_{II}-4O_{III} = 2.71$ A indicate the existence of stable hydrogen bonds. The $(NH_m)_{II}$ group is surrounded by ten oxygen atoms. Here the existence of less stable hydrogen bonds may be postulated: $N_{III}-O_V = 2.92$ A. However, the average $(NH_m)_{III}-O$ distance is considerably greater than $(NH_n)_{II}-O$ (3.08 A as against 2.71 A. The $(NH_m)_{III}$ group is in a larger cavity and has a greater coordination number that $(NH_n)_{II}$. As was pointed out by G. B. Bokii, this fact suggests that the ammonia molecule and not the ammonium ion plays the role of this "clathrate" group.

The perchlorate groups form hydrogen bonds with the $(NH_3)_I$ groups contained in the $[Cu(NH_3)_4]^{2+}$ complex. The N_I-O_{II} and N_I-O_{IV} distances are 3.00 and 2.97 A respectively. Apparently the tendency to form hydrogen bonds determines to a considerable extent the distribution of perchlorate groups along z. The considerable piezo effect observed in the crystals is probably associated with the presence of numerous hydrogen bonds.

The formally square environment of the Cu atoms is supplemented in the crystal to a bipyramidal one by $(NH_n)_{II}$ groups situated on the 4 axes half way between the Cu atoms. However, the distance $Cu-(NH_n)_{II} = 3.75$ A is so large that it is difficult to suppose the existence of a chemical bond (electron exchange) between $(NH_n)_{II}$ groups and Cu atoms. The position of the $(NH_n)_{II}$ groups at points $00\frac{1}{2}$ is evidently determined by considerations of packing only: a fairly large cavity (in the form of a flattened tetrahedron), formed by the four O atoms of the perchlorate groups, is present here. Therefore, it may be assumed that in this compound the coordination of the copper atom is of the square type.

The question of purely "square" coordination around bivalent copper in organic compounds has been controversial until recently and has been solved positively only by the very latest investigations. Square coordination around a Cu^{II} atom was discovered in the recently revised structure of azurite [9], in certain copper silicates [10], and finally, in the complex tetrammine compound described in the present communication.

LITERATURE CITED

1. M. Bukovska and M. A. Porai-Koshits, Kristallografiya, 5, 137 (1960).
2. M. A. Porai-Koshits and M. Bukovska, Kristallografiya, 6, 381 (1961).
3. M. A. Porai-Koshits and G. N. Tischenko, Kristallografiya, 4, 239 (1959).
4. M. Bukovska and M. A. Porai-Koshits, Kristallografiya, 5, 140 (1960).
5. D. W. J. Cruickshank, Acta crystallogr., 3, 72 (1950).
6. M. A. Porai-Koshits, Tr. Inst. Kristallografii AN SSSR, 3, 305 (1954).
7. B. K. Vainshtein, Zh. eksperim. i teor. fiziki, 27, 44 (1954).

8. B. K. Vainshtein, Structure Determination by Electron Diffraction [in Russian] (Izd. AN SSSR, Moscow, 1956).
9. G. Gattow and J. Zeman, Acta crystallogr., 11, 866 (1958).
10. A. Pabst, Acta crystallogr., 12, 733 (1959).

All abbreviations of periodicals in the above bibliography are letter-by-letter transliterations of the abbreviations as given in the original Russian journal. *Some or all of this periodical literature may well be available in English translation.* A complete list of the cover-to-cover English translations appears at the back of this issue.

STERIC HINDRANCES AND CONFORMATION OF MOLECULES

COMMUNICATION 6.* CRYSTAL AND MOLECULAR STRUCTURE OF 4,4°-DICHLOROACENAPHTHENE**

R. L. Avoyan and Yu. T. Struchkov
Institute of Heteroorganic Compounds, Academy of Sciences, USSR
Translated from Zhurnal Strukturnoi Khimii, Vol. 2, No. 6,
pp. 719-733, November-December, 1961
Original article submitted June 1, 1961

A complete x-ray structural investigation of 4,4°-dichloroacenaphthene was performed. Bond lengths and valence angles were determined to within ± 0.02 A and ± 1° by means of a three-dimensional electron density series. Steric hindrances between chlorine atoms, the distance between which in the ideal model is 2.77 A, lead to appreciable distortion of the angles (maximum, 5.5°) and slight disturbance from planarity (up to 0.05 A) of the molecule. Because of this difference between the real and the ideal conformation the intramolecular Cl . . . Cl distance increases to 3.12 A. The equilibrium distances between the atoms not bonded by valences were found from the intermolecular distances, and the lattice energy was calculated.

1. INTRODUCTION

Interest in the structure of this compound is due to the considerable influence of steric hindrance between chlorine atoms on the conformation of the molecule. In the ideal model (i.e., when the C–Cl bond is the bisector of the internal and hence the external C–C–C valence angle) the chlorine atoms in the molecule are 2.77 A apart (Fig. 1), whereas in other structures studied [1] the equilibrium distance for nonbonded chlorine atoms is Cl . . . Cl ≥ ≥ 3.60 A. Moreover, on the side of the naphthalene nucleus opposite to the chlorine atoms (which are mutually repelled and thereby tend to push apart the C_4 and C_4' carbon atoms in the peri-positions) there is a bridge of two methylene groups, CH_2-CH_2. This bridge draws together the other peri-atoms, C_1 and C_1'; i.e., it in a sense continues the deforming action of steric hindrances between the chlorine atoms on the naphthalene nucleus, and thereby favors even greater deformation of the latter.

Our purpose was quantitative determination of the real conformation of the molecule; i.e., the deformations in comparison with the acenaphthene molecule itself [3] which result from steric hindrances. The main characteristics of the real conformation of the 4,4°-dichloroacenaphthene molecule are given in a brief communication [4]; in this paper we describe the course of the investigation and present the results in detail. Replacement of chlorine atoms in the 4,4°-dichloroacenaphthene molecule by other halogen atoms and the consequent changes in the conformation of the acenaphthene nucleus should reveal definite conformational relationships; we are therefore carrying out a complete structural investigation of 4-chloro-4°-bromo- and 4,4°-dibromoacenaphthene.

2. EXPERIMENTAL

4,4°-Dichloroacenaphthene consists of fine colorless needles (with the needle axis corresponding to the c axis), easily obtained from a mixture of acetic acid and ethyl alcohol; m.p. 169-170°; the substance is quite stable in air. The crystals belong to the monoclinic system. The unit cell constants are:

$a = 15.37_3 \pm 0.01_2$ A $V = 956 + 9$ A³
$b = 9.45_3 \pm 0.00_3$ A $d_{x\text{-ray}} = 1.57$ g/cc
$c = 7.47_3 \pm 0.01_2$ A $d_{meas.} = 1.52 \pm 0.01$ g/cc
$\beta = 118°24' \pm 40'$ $N = 4$

* For communication 5 of this series, see [1].

** We adopted a numbering convention for the atoms which differs from the usual chemical convention [2], but is more convenient in the structural sense. The two systems are compared in Fig. 1. In the structural system 5,6-dichloroacenaphthene is called 4,4°-dichloroacenaphthene.

The identity periods were determined from oscillation x-ray patterns, and the monoclinic angle β was found from the shift of spots of the 0 0 *l* type on reciprocal-lattice diagrams of nonzero layer lines (rotation axis c) relatively to the center of rotation of this film; copper radiation was used for this purpose.

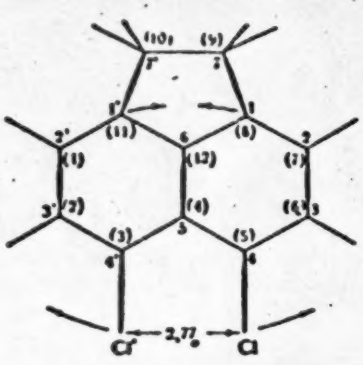

Fig. 1. Ideal model of the dichloroacenaphthene molecule. The "structural" system of atom numbering is used (the usual chemical numbering is given in parenthesis).

Photographs of six layer lines (hk0-hk5), containing 632 nonzero reflections, were taken by rotation about the c axis in a reciprocal-lattice camera with unfiltered molybdenum radiation.

The oscillation diagram obtained about the long direction of the crystal (the c axis) was symmetrical; there were two lines of symmetry in the hk0 trace, and one in each of the other hkL traces (L = 1, 2, . . .). Moreover, among the reflections of the general type hk*l*, only reflections with h + k = 2n were present, and among reflections of the h0*l* type, only those with *l* = 2n. It is evident from this that the crystal belongs to the 2/m C−/c diffraction class of the monoclinic system, which includes the C2/c and Cc space groups. Moreover, since the identity period b = 9.45$_5$ A agrees fairly well with the size of the molecule along its twofold axis of symmetry ($d_{mol} \approx R_{CH_2} + d_{CH_2-C_1} + d_{C_1-C_4} + d_{C_4-Cl} + R_{Cl} \approx 1.80 + 1.47 + 2.80 + 1.71 + 1.80 = 9.59$ A; see Fig. 2), we chose the C2/c space group as the most probable. The entire subsequent course of the structure analysis confirmed this choice (incidentally, measurement of the piezo effect gave a negative result). Data on the space group and the number of molecules in the cell lead to the conclusion that the molecule occupies a special position on the twofold in the molecule.

The spot intensities on the diagrams were assessed visually by comparison with a standard scale; the precision was not worse than 10%. The polarization and Lorentz factors were taken into account in calculations of the structure factors from the intensities. The absorption factor was disregarded, as it introduces an error (~12%) comparable with the error in the intensity estimations.

3. APPROXIMATE STRUCTURE DETERMINATION

As the molecule is in a special position, its position in the unit cell could roughly be determined by geometrical analysis based on the principle of closest molecular packing.

In this case it was necessary to determine the parameters corresponding to the two remaining degrees of freedom of the molecule, i.e.: 1) the angle of rotation ω about the y axis, and 2) the position of the molecule among the y axis; for example, the coordinate y_0 of the center of the naphthalene nucleus. For geometrical analysis we used the ideal plane molecular model shown in Fig. 2 (it was assumed that all the valence angles in the naphthalene nucleus and also the C−C−Cl and C−C−H angles are 120°; the length of the C−C bond is 1.40 A in the naphthalene nucleus, 1.54 A in the CH_2-CH_2 bridge, and 1.52 A in CH_2-C; C−H = 1.08 A, C−Cl = 1.72 A; the intermolecular radii are $R_H = 1.20$; $R_C = 1.80$; $R_{Cl} = 1.80$ A).

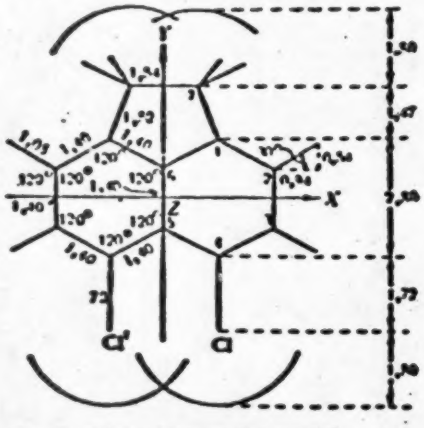

Fig. 2. Molecular model used for geometrical analysis of the structure.

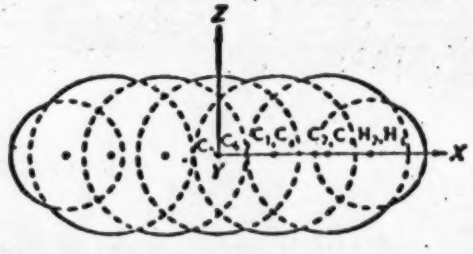

Fig. 3. Projection of the molecule along the twofold axis.

For solving the first part of the problem, we considered the packing possibilities of molecular projection along the 2 axes (Fig. 3) on the x0z projection of the cell. Only two molecular arrangements were found possible (an ambiguous solution): the 0x axis of the molecule forms either the angle $\omega_I = 12°$ or $\omega_{II} = 59°$ with the 0x axis of the cell; in each case the 0x axis of the molecule forms the same angle, 16.5°, with the normal to the 0x axis of the cell (Fig. 4). Therefore, the x coordinates of the atoms in the molecule should coincide and the z coordinates should differ in these two variants (Table 1).

To solve the second part of the problem, that of orientation of the molecule (location of the coordinate y_0 for the center of the nucleus), we examined contacts between molecules which are joined by the inversion centers $1(^1/_4\ ^1/_4\ ^1/_4)$ and $1(^1/_4\ ^3/_4\ ^1/_4)$ and which are situated on neighboring twofold axis (Fig. 2). This part of the problem is solved uniquely if a molecule A situated on a "given" twofold axis $[0y\ ^1/_4]$ is in simultaneous contact with two molecules ("upper" B and "lower" C) on a "neighboring" twofold axis $[^1/_2\ y\ ^1/_4]$ which are linked by c translation. On the basis of the intermolecular distances $H_3(A) \ldots Cl(C)$ and $H_2(A) \ldots C_2(B)$ (assumed to be 3.00 Å), which more than any others diminish the range of possible displacement of molecule A along the y axis, we calculated the position y_0 of the center of the nucleus for variant I by the following calculation:

Contact $Cl(C) \ldots H_3(A)$	Contact $C_2(B) \ldots H_3(A)$
$\Delta^2_{xz} = 7{,}43$; $(\Delta y)^2 = d^2 - \Delta^2_{xz} =$	$\Delta^2_{xz} = 3{,}64$; $(\Delta y)^2 = d^2 - \Delta^2_{xz} =$
$= 9{,}00 - 7{,}43$; $\Delta y = \pm 1{,}25$;	$= 9{,}00 - 3{,}64$; $\Delta y = \pm 2{,}31$;
hence $y_0 = 5{,}12$ or $3{,}87$ Å	hence $y_0 = 5{,}02$ or $7{,}33$ Å

Evidently the first solutions for y_0 from the two contacts are in good agreement. Hence, $y_0 = 5.0_7 \pm 0.0_5$ Å. The same solution is obtained for variant II. Approximate coordinates of the atoms in the molecule were thus found with values of z in two variants (Table 1).

TABLE 1. Atomic Coordinates Found by Geometrical Analysis

Atom	x	y	z_I	z_{II}	Atom	x	y	z_I	z_{II}
Cl	0,09	0,21	0,28	0,37	C_4	0,09	0,39	0,28	0,37
C_1	0,09	0,68	0,28	0,37	C_5	0	0,46	1/4	1/4
C_2	0,17	0,61	0,32	0,50	C_6	0	0,61	1/4	1/4
C_3	0,17	0,46	0,32	0,50	C_7	0,06	0,84	0,27	0,33

Geometrical analysis was accompanied by structure determination by objective methods of x-ray diffraction analysis. Since the c axis is the short axis, structure determination was started with the xy0 projection. This projection of the P(u,v) interatomic function gave the coordinates x and z of the chlorine atom: x = 0.108; z = 0.223. They approximate to the coordinates found by geometrical analysis, thus confirming the latter.

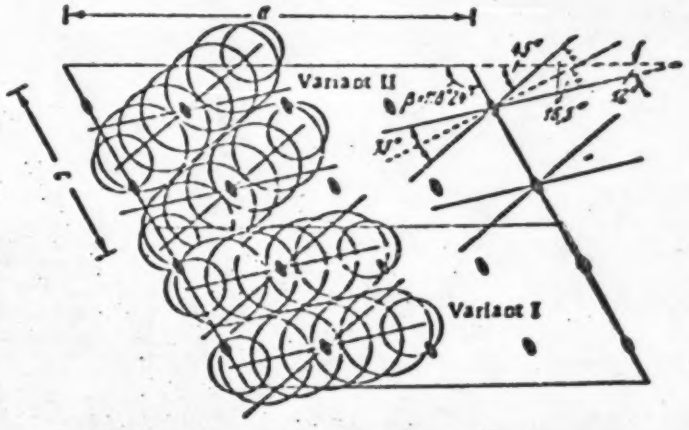

Fig. 4. Packing of molecular projections on the ac face of the cell. Two possible packing variants are shown.

The coordinates of the chlorine atom found from the projection of the P(u,v) interatomic function and the coordinates of the independent carbon atoms determined by geometrical analysis were used for calculation of the structure amplitudes F_{hk0} (in this first calculation the atomic curves were assumed similar), with subsequent calculation of the electron density distribution in the xy0 projection. This first approximation of $\rho(xy0)$ resolved the Cl, C_1, C_2, C_4, and C_8 atoms. The maxima of the C_3 and C_5 atoms coalesced with the maxima of the corresponding atoms in the neighboring molecule. Figure 6 shows that in this projection molecules linked by a center of symmetry are superposed to a considerable extent; this led to the above-mentioned coalescences. For the second calculation of F_{hk0} the coordinates of the C_3, C_5, and C_7 atoms were determined geometrically (from the C_2-C_3, C_5-C_6 and C_1-C_7 bond lengths in the structure of acenaphthene itself [3]).

In the subsequent three calculations of F_{hk0} the individual atomic curves for Cl and C given by Viervoll and Ögrim [5] were used; for C_7 (carbon atom of the CH_2 group) the N curve was used, as in the first approximation the CH_2 group can be regarded as a single scattering center. The same atomic curves were subsequently used for calculation of structure amplitudes of the general form F_{hkl}; however, in this case the C atomic curve was used for C_7, and the curve in [5] was used for hydrogens. The coordinates of the maxima in the projection were subsequently found by interpolation by the method of least squares, with approximation of the form of the maximum by an exponential function [6]. The same method for exact location of the maxima was used in the three-dimensional case.

Two more approximations of the electron-density projection were then calculated. In the last of these (Fig. 6) all the carbon atoms in the molecule are resolved and there are "projections" roughly corresponding to the calculated positions of the hydrogen atoms.

TABLE 2. Final Results for the xy0 Projection

Atom	x	y	Height of maximum in el/A²	Atom	x	y	Height of maximum in el/A²
Cl	0,109	0,220	27,1	C_4	0,090	0,397	8,8
C_1	0,073	0,095	8,4	C_5	0	0,473	8,3
C_2	0,168	0,627	8,3	C_6	0	0,618	9,1
C_3	0,168	0,480	12,9*	C_7	0,055	0,849	8,3

*High value due to partial superposition of maxima (Fig. 6).

The final atomic coordinates found from the projection are given in Table 2. Final calculations of the structure amplitudes F_{hk0} were then performed with the hydrogen atoms taken into account; their coordinates were taken (C–H = 1.08 A; C–C–H = 120°). The reliability factor was 19.4% (with the hydrogen atoms disregarded, 22.3%), whereas in the first calculation of F_{hk0} it was 39.6%. If we also reject several strong reflections which are apparently influenced by extinction, we have $R_{hk0} = 16.6\%$, and with zero reflections ignored $R_{hk0} = 16.0\%$.

4. STRUCTURE REFINEMENT

Three-dimensional electron-density synthesis was used for further refinement of the coordinates and, in particular, for determination of the third coordinate z.

TABLE 3. Approximate Values of z

Atom	z	Atom	z
Cl	0.30	C_4	0.30
C_1	0.29	C_5	1/4
C_2	0.33	C_6	1/4
C_3	0.33	C_7	0.28

For determination of the signs of the structure amplitudes of the general type it was necessary to have approximate values of z; i.e., to know the slope of the molecule relative to the xy0 plane. Geometrical analysis gave two possible slope angles: 12 and 45° (Fig. 4). Assuming that the length of the C_7-C_1 bond is 1.54 A (as in acenaphthene itself [3]), we can also find the slope angle ω from x_{C_7}:

$$\omega = \arccos \frac{2x_{C_7}}{1{,}54} = \pm 11{,}5°.$$

We therefore took $\omega \approx 12°$, varied this value by steps of 0.5°, and compared the calculated values of F_{hkl} and F_{hkl} with the experimental values. The best agreement was found with $\omega = 13°$. The values of the coordinate z for this orientation are given in Table 3.

Thus, the x, y coordinates found by two-dimensional electron-density synthesis and the z coordinates found by trial and error were used for the first calculation of F_{hkl} structure amplitudes with individual atomic curves taken into account.

Before calculation of the three-dimensional distribution of electron density, $\rho(xyz)$, it was necessary to reduce to a common scale the structure amplitudes of the reflections in different traces. For this purpose we compared the calculated and measured structure amplitudes:

$$KF_{meas.} = F_{calc.} \exp(-B \sin^2\theta/\lambda^2).$$

Values of the factor K for conversion into absolute units and of the temperature factor B for all the traces were found by the method of least squares. At this stage the divergence factors were fairly large; for example, $R_{hkl} = 21\%$, $R_{hks} = 36\%$.

TABLE 4. Final Values of the Atomic Coordinates and Electron Density Maxima [for Hydrogen Atoms, Coordinates Found from the Second ρ (xyz) Series are Given in Parentheses, and Calculated Ideal Coordinates are without Parentheses]

Atom	x	y	z	ρ_{max} in el/A³	
				found	calculated
C_1	0,1003	0,2200	0,2591	29,2	
C_2	0,080	0,689	0,273	9,0	8,4
C_3	0,164	0,632	0,296	7,5	8,0
C_4	0,168	0,582	0,301	7,4	8,3
C_5	0,089	0,502	0,279	8,8	8,8
C_6	0	0,564	1,4	9,1	9,2
C_7	0	0,614	1,4	9,8	9,0
C_8	0,052	0,848	0,259	7,7	7,3
H_2	0,22₆ (0,228)	0,72₆ (0,694)	0,32₅ (0,350)	1,1	1,2
H_3	0,22₃ (0,206)	0,55₆ (0,570)	0,28₂ (0,329)	1,2	1,2
H_4^1	0,11₂ (0,103)	0,59₆ (0,900)	0,37₂ (0,286)	1,2	1,2
H_4^2	— (0,050)	— (0,895)	— (0,124)	—	1,2

TABLE 5. Bond Lengths and Valence Angles

Bond lengths	Å	Valence angles	°	Bond lengths	Å	Valence angles	°
C_1-C_2'	1,55	$C_2'C_1C_3$	104,9	C_3-C_4	1,42	$C_4C_3C_5$	122,2
C_2-C_3	1,47	$C_1C_2C_8$	109,7	C_4-C_1	1,75	$C_1C_4C_5$	114,6
C_3-C_4	1,38	$C_1C_4C_5$	109,8	C_4-C_5	1,40	$C_3C_4C_1$	124,1
C_4-C_5	1,42	$C_4C_5C_6$	118,4	C_2-H_2	1,25	$C_3C_2C_1$	113,8
C_5-C_6	1,38	$C_5C_6C_7$	119,0	C_3-H_3	1,01	$C_4C_3C_4'$	130,9
C_6-C_7	1,40	$C_6C_7C_8$	121,4	C_2-H_4	1,00		

We did not calculate the entire $\rho(xyz)$ distribution over an independent region of the cell; it was sufficient for solution of the structural problem to perform the calculation for a number of sections parallel to the c axis and close to the centers of the maxima. The coordinates obtained from the three-dimensional synthesis were used in a second calculation of structure amplitudes; the method of least squares was used to refine the factor K for conversion of individual results to an absolute scale and the temperature factor: $B = 3.0 \pm 0.2$ A² (variation for different layer lines). The divergence factors diminished considerably: $R_{hkl} = 15\%$, $R_{hks} = 22\%$.

The second approximation of the electron density was then calculated; as before, a range of sections was taken. The cell edge a was divided into 120 parts, b into 60, and c into 48. The coordinates found from the second approximation are given in Table 4. In this approximation we attempted to detect maxima corresponding to hydrogen atoms; accordingly, we calculated a number of sections which clearly revealed the maxima of the H_2, H_3, and

H_7^1 atoms; i.e., only the H_7^2 atom was not found. The detection of three hydrogen atoms out of four shows that the precision in the structure determination was fairly high. Obviously, the positions of the hydrogen atoms are very approximate, but the average bond length C–H = 1.09 ± 0.09 Å almost coincides with the tabulated value.

It was decided to end the set structure refinement at this stage, because the second calculation of F_{hkl} changed only 17 signs of weak reflections (about one half of these were too weak for estimation), while calculations of the divergence factor without zero reflections from the coordinates of the second approximation gave the good value R_{hkl} = = 11% (with zero reflections, 14%).

Hydrogen atoms for which ideal calculated coordinates were taken were considered in this calculation of F_{hkl}.

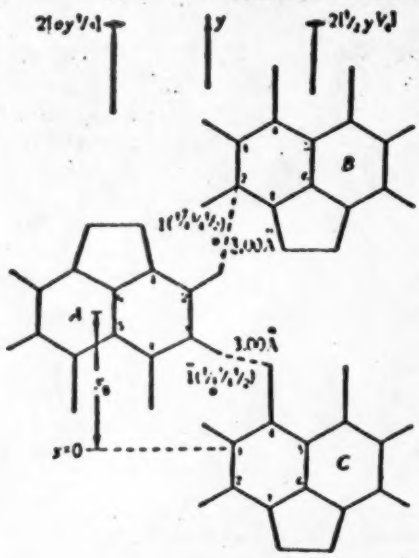

Fig. 5. Contacts of molecules on neighboring twofold axis.

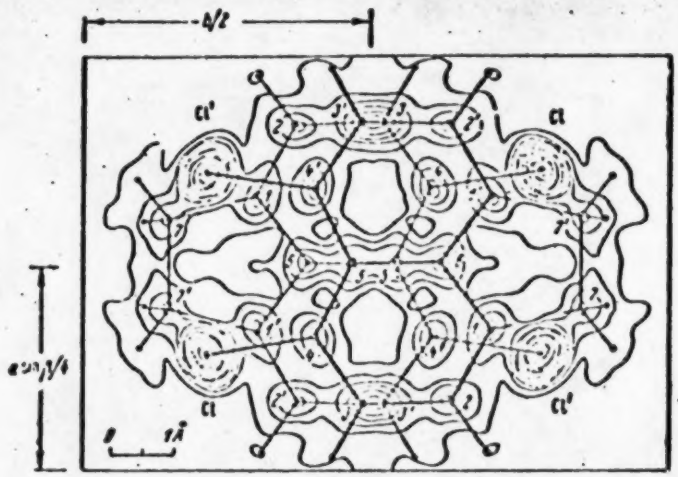

Fig. 6. Final (third) approximation for $\rho(xy0)$. Lines of equal density are drawn at intervals of 2 el/Å^2; the first corresponds to 0 el/Å^2.

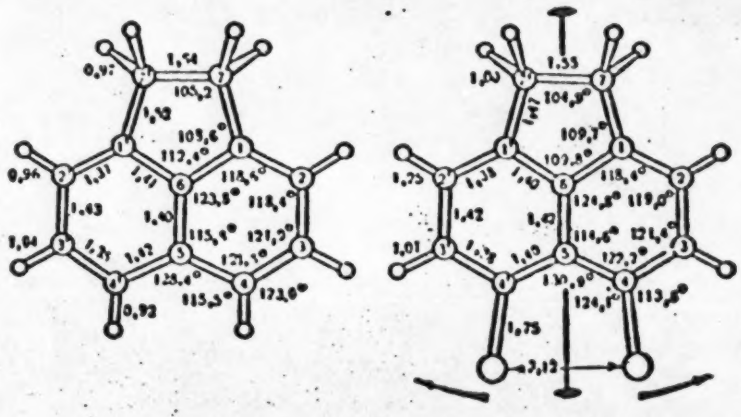

Fig. 7. Comparison of bond lengths and valence angles in the molecules of acenaphthene (left) from data in [3] and of 4,4'-dichloroacenaphthene (right).

5. PRECISION OF THE RESULTS

With the parameters characteristic of our structure, $B = 3.0\ A^2$, $\Delta F \approx R = 0.11$, $s_{max} = 0.65$, the precision in determination of bond lengths, calculated from B. K. Vainshtein's formula [7], is C–Cl ± 0.01$_4$, C–C ± 0.02$_4$, C–H ± ± 0.15 A. The errors in the coordinates, $\Delta x \approx \Delta y \approx \Delta z \approx \pm 0.01_4$ A for C, and ± 0.00$_3$ A for Cl, lead to the following errors in valence-angle determinations, calculated from the Darlow formula [8]: C–C–C ± 1.0° and C–C–Cl ± 0.8°.

The heights of the maxima ρ_{max} for all the atoms (except H$_1^3$) were found from the formula: $\rho_{max} = \rho(xyz)\exp(A_1x^2 + A_2y^2 + A_3z^2 + A_4xy + A_5yz + A_6zx + A_7x + A_8y + A_9z)$ with the aid of the final atomic coordinates. Here $\rho(xyz)$ is the experimental value of the electron density at a point with coordinates xyz relatively to the maximum; A_1 to A_9 are constants found by the method of least squares. The values found for ρ_{max} are given in Table 4 and Fig. 8 (with asterisks). For assessment of the error in electron-density determinations we assumed that the differences between the heights of the maxima are due to rotational oscillations of the molecule in the crystal about the center of gravity. The heights of the electron-density maxima of atoms of a given kind should then depend on the distance r from the center of gravity, in accordance with the formula $\rho(r) = \rho_0 - kr^2$, where ρ_0 is the height of the maximum in absence of rotational oscillations, and k is a constant. The values of ρ_0 and k for the carbon atoms were found by the method of least squares. Table 4 also gives values of $\rho_{max} = \rho(r)$ for carbon atoms calculated from this formula. Comparison of ρ_{meas} with ρ_{calc} shows that the average error is 6% and the maximum error is 12%. Thus, the precision of the electron-density determination is fairly high.

6. STRUCTURE AND CONFORMATION OF THE MOLECULE

The bond lengths and valence angles found from the final atomic coordinates are given in Table 5 and Fig. 7.

With the exception of C_1–C_7, the C–C bond lengths in the acenaphthene [3] and 4,4'-dichloroacenaphthene almost coincide; the observed differences may be attributed to the chemical influence of chlorine atoms on the nucl us. On the other hand, owing to considerable steric hindrance between the chlorine atoms, the valence angles in the two molecules differ considerably (Fig. 7). By their mutual repulsion the chlorine atoms in effect subject the molecule to the action of a pair of forces (arrows in Fig. 1) which should, for example, increase the C_4–C_5–C_5', C_5–C_4–Cl valence angles and decreases the Cl–C_4–C_3, C_1–C_6–C_1' angles. This is fully confirmed by experiment. As was to be expected, the greatest increase (5.5°) is found in the C_5C_4Cl angle. However, since the molecule is a single system, the influence of steric hindrance spreads further, i.e., to the aromatic nucleus, deforming the angles in it (maximum deformation 2.6°). As the result of these valence-angle deformations the Cl. . .Cl distance increases from 2.77 A (when the external C–C–Cl valence angles are equal) to 3.12 A but still remains considerably less than ≈3.8 A double the intermolecular radius of chlorine (see below).

Moreover, as the result of steric hindrance the molecule ceases to be planar; one chlorine atom rises above the median plane of the nucleus while the other sinks below it. The planarity of the nucleus itself is disturbed. For determination of the out-of-plane characteristics of the molecule we calculated the deviations of the atoms (apart from the hydrogen atoms) from the median plane passing through the twofold axis of symmetry and the carbon atoms C_2, C_3, C_5, and C_6. In a rectangular system of coordinates (0x° yz, where 0x° is the normal to the z axis) the equation of this plane, found by the method of least squares, is of the form:

$$0{,}3486x + 0{,}9373y = 0.$$

Deviations of the atoms from this median plane are given in Table 6 and Fig. 8 (values in parentheses).

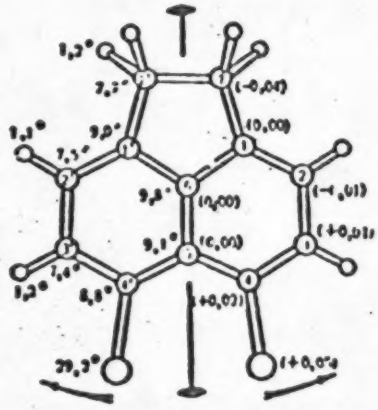

Fig. 8. Heights of electron-density maxima (el/A^3) and deviations (in A) of atoms from the median plane.

Although these values (apart from the deviations of Cl and C_3) are close in magnitude to the experimental error, they are fully consistent with the hypothesis [9] that in presence of considerable steric hindrances between substituents the benzene ring tends to assume the chair conformation (analogously to the cyclohexane nucleus). This tendency is weaker in condensed aromatic systems (because of the presence of a long conjugation chain) but it nevertheless persists. The same relationship was found for other aromatic molecules with large steric hindrances, such as peri-dihalonaphthalenes. A "side" view of the 4,4'-dichloroacenaphthene molecule, i.e., along the median plane and the normal to the twofold axis, is shown in Fig. 9 (deviations from the median

plane are magnified deliberately). The angle formed by C–Cl bond with the median plane of the molecule is 1°49' (in 1,4,5,8-tetrachloronaphthalene [9] it is 5°57').

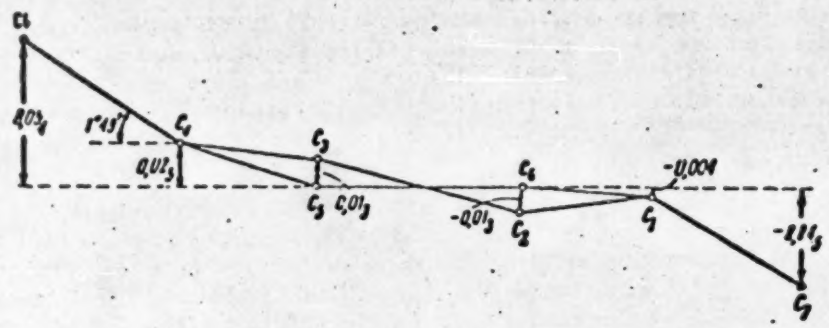

Fig. 9. Side view of the 4,4'-dichloroacenaphthene molecule.

When the conformations of 4,4'-dichloroacenaphthene and peri-dihalogenated naphthalenes are compared, it is also necessary to take into consideration the influence of the CH_2-CH_2 bridge. It has already been noted that this bridge "pulls together" the C_1 and C_1' atoms of the naphthalene nucleus and so facilitates its deformation by Cl...Cl steric effects. This explains why the Cl...Cl distance in the 4,4'-dichloroacenaphthene molecule is 3.12 A, whereas in 1,4,5,8-tetrachloronaphthalene [9] it is 2.98 A; accordingly, the valence angle distortion is greater and the disturbance of planarity is less in the former than in the latter.

TABLE 6. Deviations of Atoms (in A) from the Median Plane

Atom	Deviation	Atom	Deviation
Cl	0.05_4	C_4	0.02_5
C_1	-0.00_4	C_5	0.00_8
C_2	-0.01_3	C_6	0.00_8
C_3	0.01_3	C_7	-0.04_5

7. INTERMOLECULAR AND EQUILIBRIUM DISTANCES

The molecular packing in the crystal is shown in Figs. 10 and 11. Each molecule is surrounded by the 20 neighbors listed in Table 7 (I is the "original" molecule; II-XXI are the neighbors).

However, the original molecule I "touches" (i.e., the corresponding intermolecular distances do not exceed the equilibrium values) only 12 neighboring molecules, namely: II, III, V, VII-XIII, XV and XVI. Therefore, the molecular coordination number in this structure is 12.

For a complete characterization of the molecular packing in the crystal and for finding the equilibrium intermolecular distances and the lattice energy we calculated all the intermolecular distances not exceeding 5.0 A. This applied to the distances between a given molecule and 14 of its neighbors (in addition to those in contact with it, molecules VI and XIV). These distances are given in Table 8, which contains only symmetrically independent distances; the number of such distances is specially indicated. Certain characteristic short distances are also shown in Figs. 12 and 13.

The equilibrium intermolecular distances were calculated by the method of minimalization of the effective lattice energy, described in [1]. The expression for the interaction energy of nonbonded atoms is:

$$U(R/R_0) = -A(R_0/R)^6 + B\cdot 10^3 \exp[-\alpha(R/R_0)],$$

where U is in kcal per mole of interactions (the number of interactions is equal to the Avogadro number), and R_0 (equilibrium distance) and R (the given intermolecular distance) are in A. The constants A, B, and α for interactions of various atom pairs are given in Table 9; data for "mixed" Cl...C, Cl...H and C...H interactions, not given in the literature, were found by the combination rule [10].

The constant α was taken as 13.60 as this value is in good agreement with most literature data for the interactions in question whereas the form of the potential curve, according to [14], is relatively insensitive to the value taken for α. The $U(R/R_0)$ curves for interactions of various types are given in Fig. 14.

In analogous structures we found [1] a distinct relationship between the intermolecular radius and the angle formed by the corresponding interatomic vector with the plane of the molecule; therefore, for analysis of the distances we divided the 14 molecules in the coordination sphere into the following groups: 1) molecules II and XV; the

interatomic vectors joining them to the "original" molecule I form angles $\varphi = 90 \pm 20°$; 2) molecules VI, VIII, X, XII, XIV and XVI; $\varphi = 45° \pm 20°$; 3) molecules III, V, VII, IX, and XIII; $\varphi = 0° \pm 20$.

TABLE 7. Numbering and Symmetry Relations of the Molecules

Molecule	Coordinates	Symmetry relation to the original molecule
I	x, y, z	—
II	$\bar{x}, \bar{y}+1, \bar{z}$	$\bar{1}(0\frac{1}{2}0)$
III	$x, y-1, z$	$-\mathbf{b}$
IV	$\bar{x}, \bar{y}, \bar{z}$	$\bar{1}(000)$
V	$\bar{x}-\frac{1}{2}, y-\frac{1}{2}, \bar{z}+\frac{1}{2}$	$2_1[-\frac{1}{4}\, y\, \frac{1}{4}]$
VI	$x-\frac{1}{2}, \bar{y}+\frac{1}{2}, z-\frac{1}{2}$	$n(x\frac{1}{4}z)$
VII	$\bar{x}-\frac{1}{2}, y+\frac{1}{2}, \bar{z}+\frac{1}{2}$	$2_1[-\frac{1}{4}\, y\, \frac{1}{4}]$
VIII	$x-\frac{1}{2}, \bar{y}+\frac{1}{2}, z-\frac{1}{2}$	$n(x\frac{1}{4}z)$
IX	$x, y+1, z$	$\mathbf{b}$
X	$\bar{x}, \bar{y}+2, \bar{z}$	$\bar{1}(010)$
XI	$\bar{x}+\frac{1}{2}, y+\frac{1}{2}, \bar{z}+\frac{1}{2}$	$2_1[\frac{1}{4}\, y\, \frac{1}{4}]$
XII	$x+\frac{1}{2}, \bar{y}+\frac{1}{2}, z-\frac{1}{2}$	$n[x\frac{1}{4}z]$
XIII	$\bar{x}+\frac{1}{2}, y-\frac{1}{2}, \bar{z}+\frac{1}{2}$	$2_1[\frac{1}{4}\, y\, \frac{1}{4}]$
XIV	$x+\frac{1}{2}, \bar{y}+\frac{1}{2}, z-\frac{1}{2}$	$n[x\frac{1}{4}z]$
XV (II)*	$\bar{x}, \bar{y}+1, \bar{z}+1$	$\bar{1}(0\frac{1}{2}\frac{1}{2})$
XVI (X)*	$\bar{x}, \bar{y}+2, \bar{z}+1$	$\bar{1}(01\frac{1}{2})$
XVII (VI)*	$x-\frac{1}{2}, \bar{y}+\frac{1}{2}, z+\frac{1}{2}$	$n(x\frac{1}{4}z)$
XVIII (VIII)*	$x-\frac{1}{2}, \bar{y}+\frac{1}{2}, z+\frac{1}{2}$	$n(x\frac{1}{4}z)$
XIX (XII)*	$x+\frac{1}{2}, \bar{y}+\frac{1}{2}, z+\frac{1}{2}$	$n(x\frac{1}{4}z)$
XX (XIV)*	$x+\frac{1}{2}, \bar{y}+\frac{1}{2}, z+\frac{1}{2}$	$n(x\frac{1}{4}z)$
XXI (IV)*	$\bar{x}, \bar{y}, \bar{z}+1$	$\bar{1}(00\frac{1}{2})$

* These molecules are taken out of the positions indicated in parenthesis by $\underline{c}$ translation and cannot be shown in Figs. 10 and 12.

The equilibrium distances R_e were determined separately for each group of molecules; the results are given in Table 10, which also contains the shortest intermolecular distances for all the types.

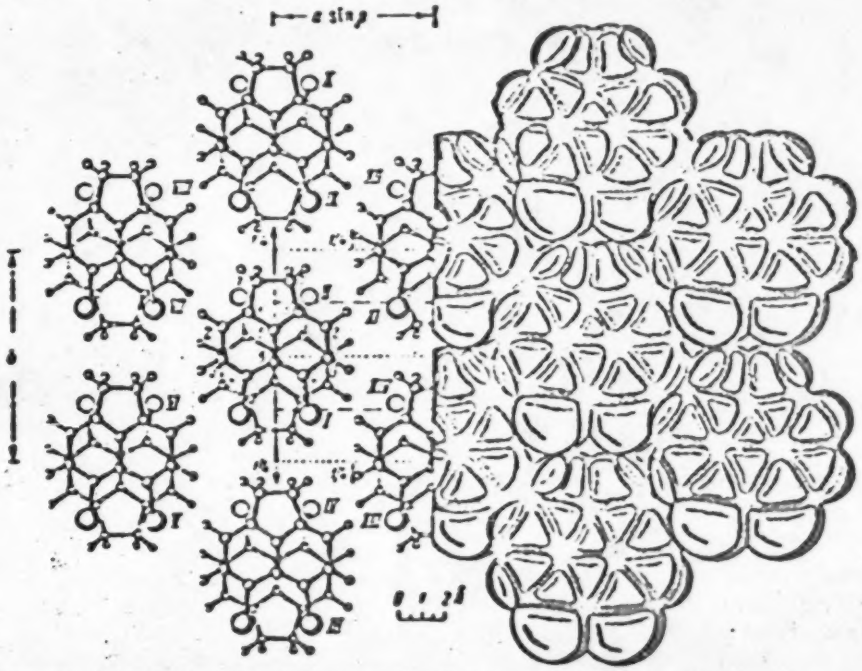

Fig. 10. Projection of the structure on the ab face. On the right the molecules are framed in the intermolecular radii.

TABLE 8. Intermolecular Distances d in A

Atoms	n*	d	d'**	Atoms	n*	d	d'
Cl'(I)—Cl(VI)	2	4,00	>5	C_4(I)—C_2'(II)	2	4,36	4,55
Cl (I)—C_2(II)	2	4,64	>5	C_4(I)—C_2(II)	2	4,28	>5
Cl(I)—C_2'(II)	2	4,28	3,74	C_4(I)—C_4(II)	2	4,20	>5
Cl(I)—C_3(II)	2	3,90	>5	C_5(I)—C_3(II)	1	3,80	3,80
Cl(I)—C_4'(II)	2	3,75	3,92	C_5(I)—C_6(II)	2	3,81	3,81
Cl(I)—C_2(II)	2	3,72	>5				
Cl(I)—C_2'(II)	2	3,70	4,05	C_6(I)—C_2(II)	2	4,58	>5
Cl'(I)—C_3(II)	2	4,48	>5	C_6(I)—C_4'(II)	2	4,55	4,86
Cl(I)—C_3(II)	2	4,65	>5	C_6(I)—C_6(II)	1	4,31	4,31
Cl(I)—C_6(II)	2	3,90	4,75	C_1'(I)—C_2'(V)	4	4,82	>5
Cl(I)—C_2(III)	4	3,60	>5	C_1(I)—C_2'(VIII)	2	3,81	>5
Cl(I)—C_2'(III)	4	4,22	>5	C_1(I)—C_1'(VIII)	2	4,81	>5
Cl'(I)—C_3(III)	4	4,05	>5	C_1(I)—C_2'(VIII)	2	4,78	>5
Cl'(I)—C_2'(V)	4	3,91	>5	C_2(I)—C_2'(VIII)	2	4,12	>5
Cl'(I)—C_3'(V)	4	4,40	>5	C_2'(I)—C_2(VIII)	2	3,69	>5
Cl'(I)—C_3(VI)	2	3,84	>5	C_2(I)—C_2'(VIII)	2	4,65	>5
Cl'(I)—C_4(VI)	2	4,36	>5	C_2(I)—C_2'(VIII)	2	4,20	>5
Cl'(I)—C_2(VI)	2	4,69	>5	C_3'(I)—C_2(X)	2	4,71	>5
C_3(I)—C_6(II)	2	4,58	>5	C_2(I)—C_2(X)	2	>5	4,46
C_3(I)—C_3(II)	2	3,83	4,55	Cl(I)—H_2'(II)	2	4,73	3,59
C_3(I)—C_4'(II)	2	3,87	3,85	Cl(I)—H_2^1(II)	2	4,74	4,08
C_3(I)—C_2'(II)	2	4,66	3,92	Cl(I)—$H_2^{1'}$(II)	2	3,13	4,72
C_3(I)—C_4(II)	2	3,82	>5	Cl(I)—H_2^2(II)	2	3,10	>5
C_3(I)—C_3(II)	2	4,52	>5	Cl(I)—$H_2^{2'}$(II)	2	4,74	3,21
C_2(I)—C_4(II)	2	4,25	>5	Cl'(I)—H_3(II)	2	4,86	>5
C_2(I)—C_4(II)	2	4,33	>5	Cl(I)—H_3^1(III)	4	3,11	>5
C_2(I)—C_2(II)	2	3,77	>5	Cl(I)—H_3^2(III)	4	3,28	>5
C_2(I)—C_4'(II)	2	3,49	4,30	Cl(I)—H_2^1(III)	4	4,16	>5
C_2(I)—C_3'(II)	2	3,88	3,90	Cl(I)—$H_2^{2'}$(III)	4	4,17	>5
C_2(I)—C_3'(II)	2	4,69	>5	Cl'(I)—H_3'(V)	4	2,98	>5
C_3(I)—C_2'(II)	2	4,75	>5	Cl'(I)—H_3'(V)	4	3,99	>5
C_3(I)—C_3'(II)	2	3,75	3,75	Cl'(I)—H_3(VI)	2	3,06	>5
C_3(I)—C_4'(II)	2	3,66	4,43	Cl'(I)—H_2(VI)	4	4,81	>5
C_3(I)—C_3(II)	2	3,73	>5	C_1'(I)—H_3(II)	2	4,97	>5
C_3(I)—C_4(II)	2	3,80	>5	C_2(I)—H_3'(II)	2	4,16	3,65
C_3(I)—C_4(II)	2	4,42	>5	C_3(I)—H_3'(II)	2	4,20	3,68
C_4(I)—C_3'(II)	2	4,30	3,49	C_3(I)—H_3'(II)	2	4,43	3,91
C_4(I)—C_4'(II)	2	4,17	4,17	C_3(I)—$H_3^{1'}$(II)	2	4,54	>5
C_4(I)—C_5(II)	2	3,75	4,51	C_3(I)—H_3^2(II)	2	4,90	>5
C_4(I)—C_4(II)	2	3,53	4,33				

* n is the number of distances (symmetrically equivalent) per molecule.
** d' is the distance to a molecule taken out of the original position with obligatory translation c; see Table 7.

TABLE 8 (continued)

Atoms	n	d	d'	Atoms	n	d	d'
$C_4(I)-H_2^{\cdot}(II)$	2	4,91	3,69	$C_3^{\cdot}(I)-H_3^1(VIII)$	2	4,41	>5
$C_4(I)-H_3^{1'}(II)$	2	4,15	>5	$C_2^{\cdot}(I)-H_3^2(VIII)$	2	3,15	>5
$C_4(I)-H_3^{2'}(II)$	2	3,94	>5	$C_2^{\cdot}(I)-H_3^3(VIII)$	2	4,48	>5
$C_4(I)-H_2(II)$	2	4,91	>5	$C_2^{\cdot}(I)-H_3(VIII)$	2	4,96	>5
$C_3(I)-H_3(II)$	2	4,32	>5	$C_3^{\cdot}(I)-H_3(VIII)$	2	3,96	>5
$C_3(I)-H_3(II)$	2	4,26	>5	$C_2(I)-H_3(VIII)$	2	4,93	>5
$C_4(I)-H_3^{2'}(II)$	2	4,23	>5	$C_2(I)-H_3^{1'}(X)$	2	3,94	>5
$C_4^{\cdot}(I)-H_3^{2'}(II)$	2	4,01	>5	$C_3(I)-H_3^{1'}(X)$	2	4,82	>5
$C_4(I)-H_3(II)$	2	4,16	>5	$C_2^{\cdot}(I)-H_3^{1'}(X)$	2	4,87	4,90
$C_4(I)-H_2(II)$	2	4,99	>5	$C_2^{\cdot}(I)-H_3^{2'}(X)$	2	3,67	>5
$C_3^{\cdot}(I)-H_2(II)$	2	4,71	>5	$C_3^{\cdot}(I)-H_3^{2'}(X)$	2	>5	3,51
$C_4^{\cdot}(I)-H_2(II)$	2	3,97	>5	$C_3(I)-H_3^{2'}(X)$	2	>5	4,79
$C_3^{\cdot}(I)-H_3(II)$	2	3,90	>5	$C_3^{\cdot}(I)-H_3^{2'}(X)$	2	>5	4,68
$C_3^{\cdot}(I)-H_3(II)$	2	4,66	>5	$H_2(I)-H_3^{\cdot}(II)$	2	3,90	3,93
$C_4(I)-H_3^1(III)$	4	4,79	>5	$H_3(I)-H_3^{1'}(II)$	2	4,29	>5
$C_4(I)-H_3^2(III)$	4	4,91	>5	$H_3^{\cdot}(I)-H_3^{1'}(V)$	4	3,59	>5
$C_4^{\cdot}(I)-H_2^{\cdot}(V)$	4	3,79	>5	$H_2^{\cdot}(I)-H_3^{2'}(V)$	4	3,16	>5
$C_2^{\cdot}(I)-H_3^{\cdot}(V)$	4	3,54	>5	$H_2^{\cdot}(I)-H_3(VIII)$	2	2,67	>5
$C_3^{\cdot}(I)-H_3^{\cdot}(V)$	4	4,73	<5	$H_2^{\cdot}(I)-H_3^1(VIII)$	2	2,62	>5
$C_4^{\cdot}(I)-H_3^{\cdot}(V)$	4	3,93	>5	$H_2^{\cdot}(I)-H_3^2(VIII)$	2	4,02	>5
$C_2^{\cdot}(I)-H_3^{\cdot}(V)$	4	3,69	>5	$H_2^{\cdot}(I)-H_3^3(VIII)$	2	4,47	>5
$C_3^{\cdot}(I)-H_2^{1'}(V)$	4	4,46	>5	$H_2(I)-H_3^3(VIII)$	4	4,44	>5
$C_3^{\cdot}(I)-H_3^{2'}(V)$	4	4,18	>5	$H_3^{\cdot}(I)-H_3^1(VIII)$	2	2,83	>5
$C_3^{\cdot}(I)-H_2^{\cdot}(V)$	4	3,47	>5	$H_3^{\cdot}(I)-H_3^2(VIII)$	2	4,18	>5
$C_4^{\cdot}(I)-H_3(VI)$	2	4,27	>5	$H_3(I)-H_3^2(VIII)$	2	4,56	>5
$C_3^{\cdot}(I)-H_3(VI)$	2	4,61	>5	$H_3^1(I)-H_3^{1'}(VIII)$	2	4,96	>5
$C_2^{\cdot}(I)-H_3(VIII)$	2	3,03	>5	$H_3^{1'}(I)-H_3^1(X)$	2	4,15	4,1
$C_3^{\cdot}(I)-H_3(VIII)$	2	3,24	>5	$H_3^{1'}(I)-H_3^2(X)$	2	2,92	>5
$C_2^{\cdot}(I)-H_3(VIII)$	2	3,38	>5	$H_3^{1'}(I)-H_3^{1'}(X)$	2	4,52	>5
$C_3^{\cdot}(I)-H_2(VIII)$	2	3,96	>5	$H_3^{1'}(I)-H_3(X)$	2	4,74	>5
$C_4^{\cdot}(I)-H_3(VIII)$	2	4,82	>5	$H_3^{2'}(I)-H_3^2(X)$	2	4,24	4,24
$C_4(I)-H_3(VIII)$	2	4,28	>5	$H_3^{2'}(I)-H_3^{2'}(X)$	2	>5	3,95
$C_3(I)-H_3(VIII)$	2	4,53	>5	$H_3^{2'}(I)-H_3^{2'}(X)$	2	>5	2,65
$C_4(I)-H_3(VIII)$	2	4,93	>5				
$C_3^{\cdot}(I)-H_3(VIII)$	2	4,73	>5				

These equilibrium distances were used for finding the intermolecular radii for all the groups of molecules:

Group of molecules	Intermol. radius in A		
	Cl	C	H
1	1,92	1,94	1,28
2	1,91	1,90	1,25
3	2,00	1,93	1,15

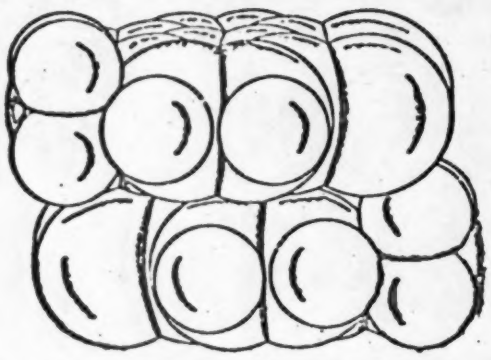

Fig. 11. Close packing of molecules (I and II) linked by a center of symmetry.

The "missing" equilibrium distances for Cl...Cl and H...H interactions were calculated from these values. These equilibrium distances and the interaction energy curves for nonbonded atoms (Fig. 14) were used for calculating the effective lattice energy, which was found to be 22.5 kcal/mole. As in the case of hexachlorobenzene [1], most of this energy is due to interactions involving chlorine atoms, i.e., in this instance Cl...C interactions. Atomic attraction at distances exceeding 5.00 A, which was not taken into account, introduces a correction not exceeding 5-10% into the value found for the lattice energy [15].

We define the energy $W(R/R_e)$ of steric hindrance as the increase of molecular energy due to contraction of the distances between nonbonded atoms in comparison with the equilibrium distances. Then the energy of steric hindrance of an ideal molecule with the distance Cl...Cl = 2.77 A is $W(2.77/3.90) = 10.9$ kcal/mole is Cl...Cl = 3.12 A sustained $W(3.12/3.90) = 2.4$ kcal/mole. Therefore, the deformation of valence angles and loss of planarity which were noted above lower the energy of steric hindrance by 8.5 kcal/mole.

TABLE 9. Values of the Constants A, B, and α

Interaction	A	B	α	Literature
Cl . . . Cl	0,706	2,598	13,00	[11]
C . . . C	0,147	0,523	13,00	[12]
H . . . H	0,095	0,338	13,00	[13]
Cl . . . C	0,322	1,156	13,00	—
Cl . . . H	0,259	0,921	13,00	—
C . . . H	0,118	0,421	13,00	—

TABLE 10. Equilibrium (R_e) and Shortest Intermolecular Distances in A

Group of molecules	R_e				Shortest distance					
	Cl...Cl	Cl...H	C...C	C...H	Cl...Cl	Cl...C	Cl...H	C...C	C...H	H...H
1	3,86	3,22	3,88	>*)	>5,00	3,70	3,10	3,49	3,62	3,90
2	3,83	3,15	>	>	4,00	3,60	2,98	4,82	3,47	2,62
3	4,00	3,15	3,85	3,15	>5,00	3,84	3,05	3,69	3,63	3,16

*The symbol > denotes that the corresponding distances are certinly greater than the equilibrium values.

8. MOLECULAR PACKING

The structure of 4,4'-dichloroacenaphthene is formed by layers of the symmetry $2_1{}^r[2_1]$, which are only permissible in respect to density. One such layer is shown in Fig. 10; the coordination number in the layer is six. However, superposition of the layers (by the centers of symmetry) proceeds with much closer packing (see Fig. 11), so that

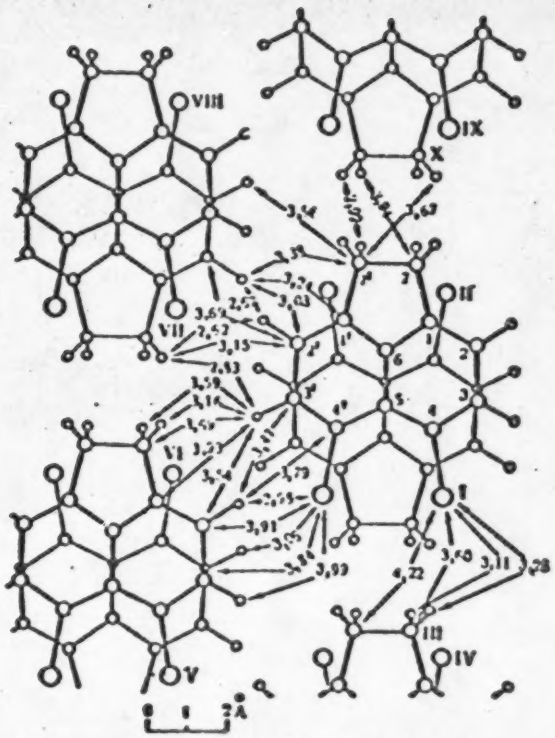

Fig. 12. Short intermolecular distances in the layer.

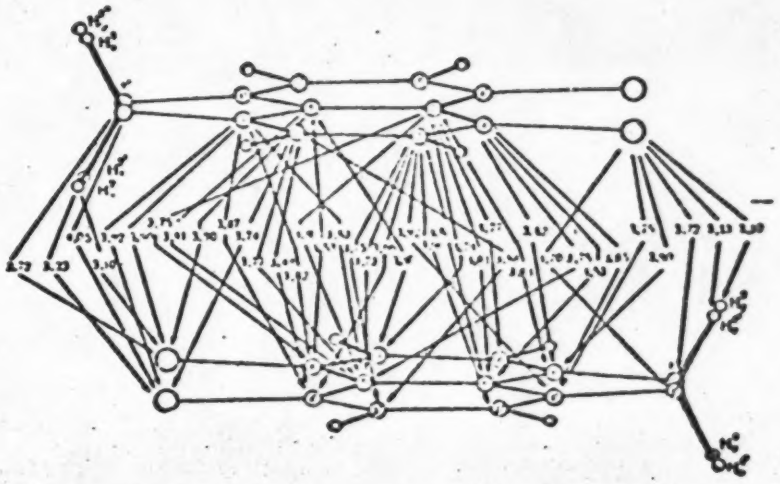

Fig. 13. Short intermolecular distances for molecules linked by a center of symmetry.

the structure as a whole has the very high packing factor k = 0.75, although it belongs to the specific group C2/c which is not the closest for molecules in special positions with twofold symmetry, but merely limitingly close [16].

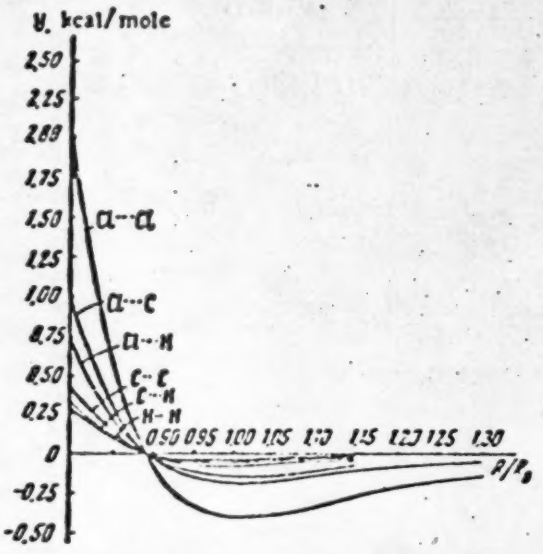

Fig. 14. Interaction energy curves for atoms not linked by valence bonds.

In conclusion, the authors thank Prof. A. I. Kitaigorodskii for his constant interest and valuable comments, and V. A. Koptyug for supplying the sample for investigation.

LITERATURE CITED

1. L. N. Strel'tsova and Yu. T. Struchkov, Zh. strukt. khimii, 2, 4, 312 (1961).
2. A. P. Terent'ev, A. N. Kost, A. M. Tsukerman, and V. F. Potapov. Nomenclature of Organic Compounds [in Russian] (Izd. AN SSSR, Moscow, 1955) p. 200.
3. H. W. W. Ehrlich, Acta crystallogr., 10, 699 (1957).
4. G. L. Avoyan and Yu. T. Struchkov, Zh. strukt. khimii, 2, 1, 67 (1961).
5. H. Viervoll and O. Ögrim, Acta. crystallogr., 2, 277 (1949).
6. Yu. T. Struchkov and T. L. Khotsyanova, Izv. AN SSSR, Otd. khim. n., 5, 821 (1960).
7. B. K. Vainshtein, Zh. éksperim. i teor. fiziki, 27, 1, 44 (1954).
8. S. F. Darlow, Acta crystallogr., 13, 687 (1960).
9. M. A. Davydova and Yu. T. Struchkov, Zh. strukt. khimii, 2, 1, 69 (1961).
10. E. Mason and W. Rice, J. Chem. Phys., 22, 522 (1954).
11. T. L. Hill, J. Chem. Phys., 16, 399 (1948).
12. A. D. Crowell, J. Chem. Phys., 29, 446 (1958).
13. L. S. Bartell, J. Chem. Phys., 32, 827 (1960).
14. A. I. Kitaigorodskii. Dokl. AN SSSR, 137, 116 (1961).
15. A. I. Kitaigorodskii and K. V. Mirskaya. Kristallografiya, 6, 4, 507 (1961).
16. A. I. Kitaigorodskii, Organic Crystal Chemistry [in Russian] (Izd. AN SSSR, Moscow, 1955) pp. 116, 121, 128.

All abbreviations of periodicals in the above bibliography are letter-by-letter transliterations of the abbreviations as given in the original Russian journal. *Some or all of this periodical literature may well be available in English translation.* A complete list of the cover-to-cover English translations appears at the back of this issue.

INTERNAL ASYMMETRY IN COMPLEX COMPOUNDS

II. CERTAIN RESULTS AND DISCUSSION

I. B. Bersuker

Institute of Chemistry, Academy of Sciences of the Moldavian, SSR
Translated from Zhurnal Strukturnoi Khimii, Vol. 2, No. 6,
pp. 734-739, November-December, 1961
Original article submitted October 24, 1960

In continuation of the previous communication, this paper contains the results of numerical calculations of internal asymmetry in certain hydrated complexes of transition metals of the first long period. The role of dynamic effects (caused by the existence of three equivalent asymmetric configurations of the complex) in experimental determination of internal asymmetry is elucidated. It is shown (qualitatively) that for each method of measurement there is a temperature (or, more correctly, a temperature range) below which the complex is seen to be asymmetric and above which the asymmetry is not revealed as the result of averaging over all the asymmetric configurations. Comparison with experimental data for the crystalline state showed that the theoretical results are in qualitative agreement with experimental data.

1. INTRODUCTION

In the previous communication [1] we considered internal asymmetry in six-coordinated ionic (high-spin, or "spin-free") complexes of transition metals, which arises because of the asymmetry of the ψ-cloud of the incomplete $\underline{d}$-electron shell of the central ion. A qualitative explanation of this asymmetry can also be derived from the Jahn–Teller theorem.

According to Eqs. 23, 27, and 32 [1], for point-dipole ligands the internal asymmetry, i.e., the difference between the lengths of two diagonals of the octahedron, is:

$$\xi = (2\mu/21K_1)\cdot[2F_2^*(R_{02}) - 5F_4^*(R_{02})] \quad (1)$$

for the electron configurations $\underline{d}^1$ and $\underline{d}^6$,

$$\xi = (\mu/14K_1)\,[12F_2^*(R_{02}) + 5F_4^*(R_{02})] \quad (2)$$

for $\underline{d}^4$ and $\underline{d}^9$, and

$$\xi = (\mu/70K_1)\,[24F_2^*(R_{02}) - 25F_4^*(R_{02})] \quad (3)$$

for $\underline{d}^2$ and $\underline{d}^7$.

Here μ is the effective dipole moment of the ligand, R_{02} is the equilibrium distance from the central ion to the ligands which form a regular square, $F_n^*(R)$ is determined by Eq. (12) [1] (the primes represent derivatives) and contains the parameter α of the effective nuclear charge for the $\underline{d}$-electron, and $K_1 = k_{11} - 2k_{12} + k_{14}$, where k_{ij} represents the force constants corresponding to changes in the absolute values of the distances between the ligands and the central ion [during their motion along three mutually perpendicular axis, see Eq. (5) [1]; the ligands are numbered so that the diagonals of the octahedron are formed by the pairs 1-4, 2-5, and 3-6].

Analogous equations, (22), (26), and (31) [1] were derived for ligands which are point ions.

In this communication, which is to be regarded as a continuation of the preceding one, we discuss the application of the results obtained to the study of certain physicochemical properties of complexes. The optical properties are not considered as they will be dealt with in the next communication.

2. CERTAIN NUMERICAL RESULTS FOR INTERNAL ASYMMETRY

It is necessary to know the parameters of the complex which are listed above for calculation of the numerical

values of ξ from Eqs. (1-3) and from (22), (26), and (31) [1]. Not all of them are well known and the force constants have been studied the least. However, a simplification is possible for the latter.

First, it can be shown that $K_1 = k_{11} - 2k_{12} + k_{14}$ is equal to the coefficient of the retracting force acting on ligand 1 in its motion when the ligand pair 1 and 4 approaches and one of the pairs 2 and 5 or 3 and 6 moves away from the central ion remaining all the time on mutually perpendicular axis; the absolute displacements from the equilibrium positions are the same for all ligands. Such motion corresponds to normal vibration of type e_g [2]. We can therefore put:

$$K_1 = M\omega^2, \tag{4}$$

where M is the reduced mass of ligand 1 and ω is the circular frequency of the e_g vibration.

For determination of the effective dipole moment μ (for dipole ligands) we can assume that $\mu_1 = \mu_1 + \mu_2$, where μ_1 is the constant dipole moment of the ligand and μ_2 is the dipole moment induced by the field of the central ion and of the remaining ligands. If we disregard the slight difference of μ_2 for ligands situated at the ends of the long and short diagonals respectively, we have:

$$\mu_2 = \beta\left(\frac{e}{R_0^2} - \frac{4\mu_1}{8R_0}\right)\Big/\left(1 + \frac{4\beta}{8R_0^3}\right). \tag{5}$$

Here e is the charge of the central ion, β is the polarizability of the ligand, and R_0 is the equilibrium distance between the ligand and the central ion.

Table 1 gives the results of numerical calculations from Eqs. (1)-(3) for internal asymmetry in certain hydrated complexes of transition metals of the first long period.

TABLE 1. Numerical Values for Internal Asymmetry in Certain Hydrated Complexes of Transition Metals of the First Long Period

Complex	Electron configuration of central ion	$\xi = 2(R_{01} - R_{02})$ in A	Complex	Electron configuration of central ion	$\xi = 2(R_{01} - R_{02})$ in A
$Ti(H_2O)_6^{3+}$	d^1	0,26	$Mn(H_2O)_6^{3+}$	d^4	0,65
$Fe(H_2O)_6^{3+}$	d^5	0,24	$Cu(H_2O)_6^{2+}$	d^9	0,79
$Co(H_2O)_6^{3+}$	d^6	0,27	$V(H_2O)_6^{3+}$	d^2	0,024
$Cr(H_2O)_6^{3+}$	d^3	0,73	$Co(H_2O)_6^{2+}$	d^7	0,0026

It was assumed in all cases that $R_{02} = 2$ A, and α was determined from the corresponding ionization potentials for 3d-electrons. For the induced dipole moment we found, from Eq. (5), the value $\mu_2 = 0.28$ a.u. for the bivalent central ion and $\mu_2 = 0.61$ a.u. for the trivalent ion (the constant dipole moment of the water molecule $\mu = 0.72$ a.u.).

We do not know the exact values for the frequencies ω of type e_g vibrations necessary for calculation of K_1. According to available data [3,4] ω for a bivalent central ion is of the order of 200-250 cm^{-1}. This frequency should be higher for a complex with a trivalent central ion. In order not to make the calculated value of ξ too high, we took $K_1 = 0.6 \cdot 10^5$ dynes/cm for the bivalent complex (which approximately corresponds to a frequency of 250 cm^{-1}) and $K = 0.9 \cdot 10^5$ dynes/cm for the trivalent.

It follows from Table 1 that the electron configuration d^3 and d^8 give the greatest internal asymmetry. This is to be expected from the general form of Eqs. (1)-(3) if it is taken into account that $F_D^0(R_{02})$ are positive. The value of ξ is appreciably less for configurations d^1 and d^6 than for d^3 and d^8, but it is still fairly considerable comprising about 10% of the length of the undistorted diagonal. The value of ξ for the d^5 and d^7 electron configuration is very small and may be neglected in the present approximation.

3. ROLE OF DYNAMIC EFFECTS. TEMPERATURE TRANSITION

Before we compare the results with experimental data it is necessary to consider an important consequence of the existence of different directions of distortion of the configurational octahedron as the result of internal asymmetry and to take into account the dynamic effects to which it leads.

In our investigation of internal asymmetry we emphasized that for ligands of the same kind it is quite immaterial which of the three diagonals of the equilibrium octahedron is longer or shorter than the other two; there are consequently three possibilities for a tetragonal distortion of the octahedron. For each of these possibilities there is a minimum of the potential energy surface as a function of the interatomic distances [1], and therefore one equilibrium configuration.

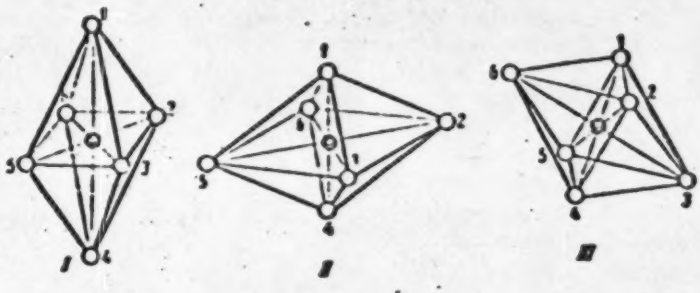

For example, for the cases of $\underline{d}^9$ and $\underline{d}^4$ the three equilibrium configurations of the elongated octahedron corresponds to the following three relationships between the distances R_{0i} of the ligands to the central ion [1]:

$$\left.\begin{array}{ll} \text{I.} & R_{01} = R_{06},\quad R_{02} = R_{04} = R_{03} = R_{05},\quad R_{01} > R_{02}, \\ \text{II.} & R_{02} = R_{04},\quad R_{01} = R_{03} = R_{06} = R_{05},\quad R_{02} > R_{01}, \\ \text{III.} & R_{03} = R_{05},\quad R_{01} = R_{06} = R_{02} = R_{04},\quad R_{03} > R_{01}. \end{array}\right\} \qquad (6)$$

Three analogous equilibrium configurations are obtained for the complexes in every case of internal asymmetry. The figure shows three such equilibrium configurations for an elongated octahedron. It is easy to see that in the absence of external fields defining some particular direction in space the three equilibrium configurations are mutually equivalent.

In connection with the existence of several (in our case, three) equivalent configurations in the system the question which naturally arises is, would one of these configurations be revealed by experimental measurements, or do they all appear simultaneously. In the latter case the measured quantities should be average values for all the equivalent configuration states.* The answer to this question depends on the character of the potential barrier between equivalent configurations. If this barrier is high enough, it is reasonable to speak of quasistationary states corresponding to each of the configurations and of the probability of transitions between them (mainly by the tunnel effect). This gives rise to the concept of the life τ of each configuration, and the reciprocal quantity–the transition frequency ω'. Suppose that the complex is subjected to an external influence characterized by a certain frequency ω. Then there are three possibilities with regard to the appearance of individual configurations:

1) $\omega \gg \omega'$. In this case one configuration of the complex appears, because there is not enough time for transitions between different configurations during interaction with the external field.

2) $\omega \ll \omega'$. In this case the measured quantity is averaged over all the three states of the equivalent configurations since the frequency of the transitions between them is considerably higher than the characteristic frequency of the external influence.

3) $\omega \sim \omega'$. This is a case of a special kind of interaction of a resonance character between the complex and the external field.

It is easy to see that internal asymmetry can be detected directly only if condition 1) is satisfied; i.e., when $\omega \gg \omega'$. For a given state of a complex, i.e., at given ω', it depends on the frequency ω of the external influence whether this condition is satisfied. It follows that the possibility of detecting internal asymmetry depends on the measurement method used. In other words, internal asymmetry may be manifested in some effects and not in others.

At the same time, the manifestation of internal asymmetry also depends on the state of the complex; in particular, on the temperature. Indeed, as the temperature rises the probability of a transition across the potential barrier between two equilibrium configurations increases, and consequently the transition frequency ω' also increases. Therefore, it may happen that with a given method of measurement the condition $\omega \ll \omega'$. And since internal asymmetry is not directly detected when $\omega \ll \omega'$ we conclude that the asymmetric complex passes into the symmetrical state (averaged over the three states of asymmetry) with rise of temperature.

* Similar problems arise in many molecular systems having two or more equivalent equilibrium considerations (e.g., the inversion vibrations of ammonia and hindered rotations in organic molecules).

Thus, for each method of measurement there should be a certain temperature (or, more correctly, a temperature range) below which the inner asymmetry of the complex appears and above which it is not directly manifested. This temperature range of transition of the complex from the asymmetric into the symmetric state differs with different measurement methods; the higher the frequency ω characteristic of the given measurement method, the higher will this temperature range lie. For example, at a given temperature internal asymmetry may be manifested in electron absorption spectra but not in infrared spectra or radio wave absorption.

It must be pointed out that although internal asymmetry is manifested directly only if the condition $\omega \gg \omega$ is satisfied, it may be detected indirectly even when $\omega \ll \omega$, because although the state averaged over the three equivalent configurations is symmetric it is not identical with the configuration state of a regular octahedron.

When $\omega \approx \omega^*$, it is possible to determine from resonance effect the frequency ω^*, which not only gives indication of the existence of several equivalent configurations (and therefore of internal asymmetry) but also makes it possible to assess the nature of the barrier between them. A more detailed (quantitative) treatment of some questions touched upon here is to be found in our publication [24]. Certain experimental data which confirm our results are examined below.

4. COMPARISON WITH EXPERIMENTAL DATA FOR THE CRYSTALLINE STATE

Direct determination of the aymmetric configurations of complexes by diffraction methods is possible only for the crystalline state. However, our investigation of internal asymmetry in free complexes is, strictly speaking, inapplicable to the crystalline state. In particular, if the influence of the second coordination sphere is fairly large and insufficiently symmetrical, the three equilibrium configurations resulting from internal asymmetry become nonequivalent so that there may be one predominant direction of asymmetry with a value of ξ differing from the value for free complexes. However, if the influence of the second coordination sphere is small in comparison with interactions within the first (as is to be expected in most cases), then the qualitative and, in certain instances, quantitative results obtained for free complexes may be transferred to the states of these complexes in the crystal lattice. It is evident that, at the best, agreement in order of magnitude only is to be expected here between calculated and experimental data.

Table 2 gives certain experimental data obtained by diffraction analysis of crystalline structures.

TABLE 2. Experimental Data on Internal Asymmetry for Certain Crystal Structures with Transition Metals

Crystal	Configurational octahedron	Electron configuration of central ion	Central ion–ligand equilibrium distances in A			$\xi = 2(R_{\text{ax}} - R_{\text{eq}})$ in A	Reference
			R_x	R_y	R_z		
$CuCO_3Cu(OH)_2$	CuO_6	d^9	2,41	2,01	2,01	0,80	[5]
$CuSO_4 \cdot 5H_2O$	CuO_6	d^9	2,3	2,00	2,00	0,60	[6]
CuF_2	CuF_6	d^9	2,27	1,93	1,93	0,68	[8]
K_2CuF_4	CuF_6	d^9	1,95	2,08	2,08	−0,26	[9]
K_2CuCl_3	$CuCl_6$	d^9	2,65	2,30	2,30	0,70	[10]
$CuCl_2$	$CuCl_6$	d^9	2,95	2,30	2,30	1,30	[11]
$CuBr_2$	$CuBr_6$	d^9	3,18	2,40	2,40	1,56	[12]
MnF_3	MnF_6	d^4	2,09	1,91	1,79	0,60–0,36	[13]
$MnO(OH)$	MnO_6	d^4	2,30	1,85–1,92		0,90–0,68	[14]

Comparison of these data with our results leads to the following conclusions. 1) In agreement with the predictions of the internal asymmetry theory, certain ions become surrounded by an asymmetric equilibrium arrangement of similar ligands. 2) So far this asymmetry has been discovered only for ions with d^9 and d^4 electron configurations (Cu^{2+} and Mn^{3+}); the theoretical explanation of this is that in these cases the extent of internal symmetry (and hence the height of the potential barrier between the equivalent configurations and the life of each) is fairly large, whereas in other cases it is appreciably less (see Table 1). 3) In the case of Cu^{2+} (d^9) the equilibrium configuration of the ligands in the first coordination sphere is a tetragonally distorted octahedron. Despite the view [7] that Cu^{2+} ions form only elongated octahedrons, the example of the K_2CuF_4 crystal shows that these octahedrons can also be foreshortened in accordance with the theoretical predictions; in the case of the Mn^{3+} ion (d^4) all three diago-

nals of the octahedron are different which is inconsistent with the theory. 4) The calculated and experimental differences between the lengths of two diagonals of the deformed octahedron are in good agreement in order of magnitude [for example, compare the calculated values for the configurational octahedron around Cu^{2+} in the free $Cu(H_2O)_6^{2+}$ complex with experimental data for almost similar octahedrons in the crystals of $CuSO_4 \cdot 5H_2O$ and $CuCO_3 \cdot Cu(OH)_2$].

Let us now consider the experimental evidence for the temperature transition from the asymmetric into the symmetric state; the relevant data are given in Table 3.

TABLE 3. Examples of Temperature Transitions of Certain Complexes from the Asymmetric into the Symmetric State

Crystal	Configurational octahedron	Electron configuration of central ion	Temp. range for transition from asymmetric to symmetric state	Measurement method	Literature
$CuSiF_6 \cdot 6H_2O$	$Cu(H_2O)_6$	$\underline{d}^9$	20–60°K	Radio-frequency absorption	[15]
$3Cu(NO_3)_2 \cdot 2Bi(NO_3)_3 \cdot 24H_2O$	$Cu(H_2O)_6$	$\underline{d}^9$	20–60°K	"	[15]
$Cu(BrO_3)_2 \cdot 6H_2O$	$Cu(H_2O)_6$	$\underline{d}^9$	12–20°K	"	[15]
Interstitial Ni^+ ion in germanium crystal		$\underline{d}^9$	25–50°K	"	[16]
$CuFe_2O_4$	CuO_6	$\underline{d}^9$	760°C		[17] [18] [19]
Mn_2O_3					
$ZnMn_2O_4$	MnO_6	$\underline{d}^4$	1000°C	Diffraction	[20]
Mn_3O_4					

In every case the configurational octahedron is tetragonally distorted at temperatures below the range indicated in the table, and becomes regular at temperatures above that range. However, the regular octahedron is detected as the result of averaging over the asymmetric configurations.

This was first discovered for the g-factor of copper fluosilicate hexahydrate [21]: it was shown that the high-temperature value of $g=2.25$, does not agree with the value of g for octahedral environment of the copper ion (where it should differ substantially from 2.25). Abragam and Pryce [22] showed that this result can be explained on the assumption that the environment of the Cu^{2+} ion is not cubic, but measurement of g results in averaging over a certain symmetry parameter.

According to [23], the low-temperature anisotropy of the g-factor can be explained on the assumption that it is the consequence of internal asymmetry and that rise of temperature results in averaging over all possible asymmetric configurations. This explanation of the origin of the temperature transition of complexes from the asymmetric into the symmetric state does not account for the dependence of the transition temperature on the method of measurement used. Until this has been explained it remains incomprehensible why, with complete isotropy of the g-factor even at 60°K, internal asymmetry is manifested, for example, in electron absorption, at considerably higher temperatures (also compare the transition temperatures with different measurement methods, given in Table 3).

A qualitative interpretation of all these problems is given in this paper. It would be interesting to obtain quantitative agreement between theory and experiment.

In conclusion, the author thanks A. V. Ablov for discussions.

LITERATURE CITED

1. I. B. Bersuker, Zh. strukt. khimii, 2, 350 (1961).
2. G. Gerzberg, Vibrational and Rotational Spectra of Polyatomic Molecules [Russian translation] (Izd. inostr. lit., 1949).
3. L. Schultz, J. Chem. Phys., 10, 194 (1942).

4. J. Darnaschun, Z. phys. Chem., B16, 81 (1932).
5. A. F. Wells, Acta. crystallogr., 4, 200 (1951).
6. C. A. Beevers and H. Lipson, Proc. Roy. Soc., A146, 570 (1934).
7. U. Öpik and M. H. L. Pryce, Proc. Roy. Soc., A238, 425 (1957).
8. C. Billy and H. M. Haendler, J. Amer. Chem. Soc., 79, 1049 (1957).
9. K. Knox, J. Chem. Phys., 30, 991 (1959).
10. A. F. Wells, J. Chem. Soc., 1662 (1947).
11. A. F. Wells, J. Chem. Soc., 1670 (1947).
12. L. Helmholz, J. Amer. Chem. Soc., 69, 886 (1947).
13. M. A. Hepworth and K. H. Jack, Acta crystallogr., 10, 345 (1957).
14. M. J. Buerger, Z. Kristallogr., A95, 163 (1936).
15. B. Bleaney and K. D. Bowers, Proc. Phys. Soc., A65, 667 (1952).
16. G. W. Ludwig and H. H. Woodbury, Phys. Rev., 113, 1014 (1959).
17. L. Weil, E. F. Bertaut, and L. Bochirol, J. Phys. Radium, 11, 208 (1950).
18. E. Prince and R. G. Treuting, Acta crystallogr., 9, 1025 (1956).
19. S. Miyahara and H. Ohuishi, J. Phys. Soc. Japan, 12, 1296 (1956).
20. B. Mason, Amer. Mineralogist, 32, 426 (1947).
21. B. Bleaney and D. J. E. Ingram, Proc. Phys. Soc., A63, 408 (1950).
22. A. Abragam and M. H. L. Pryce, Proc. Phys. Soc., A63, 409 (1950).
23. A. D. Liehr and C. J. Ballhausen, Ann. Phys. (USA), 3, 304 (1958).
24. L. B. Bersuker, Optika i spektroskopiya, 11, 319 (1961).

All abbreviations of periodicals in the above bibliography are letter-by-letter transliterations of the abbreviations as given in the original Russian journal. *Some or all of this periodical literature may well be available in English translation.* A complete list of the cover-to-cover English translations appears at the back of this issue.

BRIEF COMMUNICATIONS

ELECTRON PARAMAGNETIC RESONANCE OF COMPLEXES OF VANADIUM CHLORIDE WITH ORGANOALUMINUM COMPOUNDS

S. V. Shulyndin, N. N. Tikhomirova, A. E. Shilov, and A. K. Shilova

Institute of Chemical Physics, Academy of Sciences, USSR
Translated from Zhurnal Strukturnoi Khimii, Vol. 2, No. 6, pp. 740-741, November-December, 1961
Original article submitted August 5, 1961

Reactions of quadrivalent vanadium compounds with alkyl derivatives of aluminum yield soluble derivatives of bivalent vanadium, which are active catalysts of ethylene polymerization [1]. Elucidation of the structure of these catalytic complexes is necessary for an understanding of the mechanism of the polymerization catalysis. Considerable aid in this respect may be obtained by investigations of electron paramagnetic resonance (EPR) spectra, as the effect is usually easy to observe at room temperature with bivalent vanadium compounds [2].

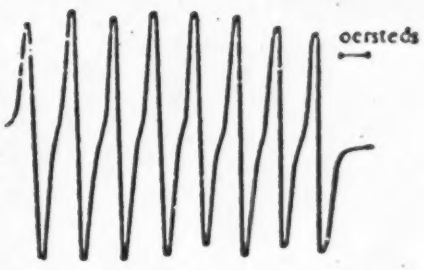

Fig. 1

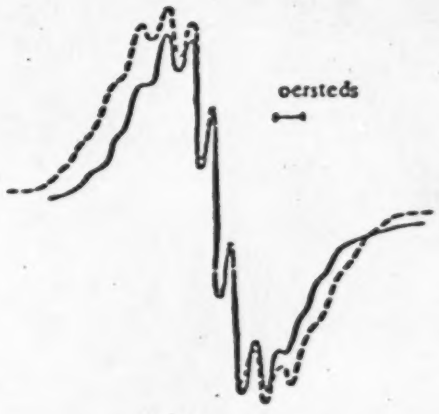

Fig. 2

In this note we present EPR data on the reaction products of VCl_4 and organoaluminum compounds in benzene solution. The reaction of excess $Al(C_2H_5)_3$ or $Al(iso\text{-}C_4H_9)_3$ with VCl_4 is almost instantaneous and yields dark-colored solutions which are apparently true solutions because they do not exhibit the Tyndall effect. If the amount of AlR_3 is insufficient a brown precipitate is formed; this is probably due to formation of trivalent vanadium compounds.

Figure 1 shows the EPR spectrum of a solution obtained by the reaction of $Al(C_2H_5)_3$ with VCl_4 in benzene. The whole spectrum ($g = 1.992$, width 510 oersteds) is split into eight equal lines as the result of interaction of the unpaired electron with the vanadium nucleus ($I = 7/2$). Each of the eight lines is resolved into an odd number of components; seven of these are especially distinct but two or three weak lines can also be seen at the edges so that the total number of components in each line may be 11 or 13. The hyperfine structure of each of the eight lines in the spectrum of Fig. 1 is shown in Fig. 2.

Among the elements present in the system (in addition to vanadium) which cause the main splitting, H, Al, and Cl atoms have spins other than zero: 1/2, 5/2, and 3/2 respectively. The spectrum of the reaction product obtained with triethylaluminum with all its hydrogen atoms replaced by deuterium ($I = 1$) completely coincides with the spectrum in Fig. 2 so that the splitting cannot be attributed to interaction of the unpaired electron with the proton. The

Al atoms cannot account for the observed hyperfine line structure either. In fact, splitting at one Al atom should give six equal components, and although splitting at two Al atoms does give 11 components their intensity ratio (1:2:3:4:5:6:5:4:3:2:1) differs entirely from that observed in the spectrum of Fig. 2. The most probable explanation is that the observed hyperfine structure is caused by interaction of the unpaired electron with four Cl atoms (I = 3/2). This should lead to splitting into 13 lines with intensities in the proportions of 1:4:10:20:31:40:44:40:31:20:10:4:1.

The dash line in Fig. 2 is the calculated spectrum for interaction with four Cl nuclei.* It is seen that the theoretical spectrum is very close to the observed one. Therefore it is probable that after reduction the bivalent vanadium atom remains linked to four equivalent chlorine atoms. This can be explained by the formation of a structure with bridge bonds, for example:

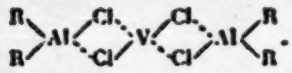

It is still too early to deduce the participation of the presumed complex in the polymerization process. It may be that the active catalyst is not this complex but other particles in equilibrium with it; for example:

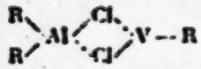

[1]

LITERATURE CITED

1. W. L. Carrick, J. Amer. Chem. Soc., 80, 6455 (1958); W. L. Carrick et al., J. Amer. Chem. Soc., 82, 3883 (1960); W. L. Carrick, A. G. Chasar, and J. J. Smith, J. Amer. Chem. Soc., 82, 5319 (1960).
2. D. Ingram, Spectroscopy at Radio and Microwave Frequencies [Russian translation] (Izd. inostr. lit., Moscow, 1959); S. A. Al'tshuler and B. M. Kozyrev, Electron Paramagnetic Resonance [in Russian] (Fizmatgiz, Moscow, 1961).

All abbreviations of periodicals in the above bibliography are letter-by-letter transliterations of the abbreviations as given in the original Russian journal. *Some or all of this periodical literature may well be available in English translation.* A complete list of the cover-to-cover English translations appears at the back of this issue.

---

* The lines were taken as Gaussian. A correction was applied for the difference between the moments of Cl^{35} and Cl^{37} nuclei. The spectrum in Fig. 2 is calculated for a ratio of 0.62 between hyperfine splitting and line width.

INFRARED SPECTRA AND STRUCTURE OF STRONTIUM SILICATES

A. N. Lazarev, T. F. Tenisheva, Mao Chih-chun, and N. A. Toropov

Institute of Silicate Chemistry, Academy of Sciences of the USSR, Leningrad

Translated from Zhurnal Strukturnoi Khimii, Vol. 2, No. 6, pp. 741-743, November-December, 1961
Original article submitted August 5, 1961

Only two crystalline compounds are known in the systems $SrO-SiO_2$ corresponding in composition to the orthosilicate $2SrO \cdot SiO_2$ and the metasilicate $SrO \cdot SiO_2$. The structure of these compounds has not been determined fully by x-ray diffraction; only the unit cell constants were determined [1, 2]. We have investigated the infrared spectra of these silicates in order to establish the structure of the complex silicate anions. The figure shows transmission (T) curves, while the table contains the frequencies of the absorption maxima, and an attempt is made at an approximate interpretation of the "internal" vibration frequencies of the anions.

Frequencies in Infrared Spectra of Strontium Silicates*

$Sr_2(SiO_4)$		$Sr_3(Si_2O_7)$	
Frequency, cm^{-1}	Assignment; $SiO_4(T_d)$	Frequency, cm^{-1}	Assignment; Si_2O_7 (D_{3h})
–		–	E'' (in) / A''_2 } ν_{as} (O–SiO–)
968 v.s., db?	$\nu_3(F_2)$	1078 v.s.	
940 s.		980 v.s.	E'** / A'_2 (in) } ν_{as} (SiOSi)
908 v.s.		–	
885 s.		930 v.s. db?	E'** / A'_1 (in) } ν_s (O–SiO–)
838 m		–	
	$\nu_1(A_1)$ (in)	714 v.s.	E'' / A'_2 (in) } ν (SiOSi)
		–	
532 m	δ (SiO)	551 s	δ (SiO)
510 s	and	484 m	and
495 m	ν (SrO)	443 s	ν (SrO)

*Abbreviations: v.s.) very strong; s) strong; m) moderate; w) weak; db) double; in) vibration inactive in the infrared spectrum.

**Assignment of the 980 and 930 cm^{-1} band to the ν_{as}(SiOSi) and ν_s(O–SiO–) vibrations is formal in character, as the two vibrations, which belong to the same symmetry type, interact strongly because the frequencies are very close.

Strong absorption in the 1000-800 cm^{-1} region with an absence of bands in the 800-600 cm^{-1} region brings the spectrum of $2SrO \cdot SiO_2$ close to the spectra of orthosilicates (in particular, δ-Ca_2SiO_4 [3]) and appears to confirm the presence of "isolated" $[SiO_4]^{4-}$ ions. The presence of three strong bands between 800 and 1000 cm^{-1} may be attributed to splitting of a triply degenerate valence vibration of the SiO_4 tetrahedron by the internal field of the crystal. The other valence vibration of the tetrahedron (fully symmetric) is not usually observed in the infrared spectrum.

The composition of strontium metasilicate $SrO \cdot SiO_2$, suggests that the most probable structure of the complex anion is in the form of infinite $[SiO_3]_\infty$ chains or $[SiO_3]_n$ rings. Liebau [2] postulated the existence of $[SiO_3]_3^{6-}$ ring anions because of the similarity of the unit cell constants of strontium metasilicate, pseudowollastonite, and strontium germanate crystals, the structure of which had been established by x-ray structural analysis. The spectrum of strontium metasilicate, shown in the figure, is very similar to the spectrum of pseudowollastonite which we considered earlier [4] and, like the latter, it has a very small number of bands (four or five) in the frequency region of Si–O valence vibrations. This indicates a high degree of symmetry in the anion and makes it possible to assign the frequencies (see table) in accordance with Liebau's hypothesis of the existence of $[Si_3O_9]^{6-}$ ring anions. It was assumed in assignment of the frequencies that the anion has D_{3h} symmetry. The table shows that our hypothesis [3-5] that the 750-600 cm^{-1} region (or the 800-550 cm^{-1} region) is quasicharacteristic for ν_s (SiOSi) vibrations (i.e., corresponding to the valence symmetrical vibration of the isolated SiOSi group) is confirmed in the present instance.

It must be noted, however, that it is somewhat arbitrary to assign the 551 cm^{-1} band to deformational vibrations of the anion, as it cannot be assumed in advance that the frequency of the valence vibration of the anion cannot appear in this region. For example, this band may be associated with the fully symmetric ν_s(SiOSi) vibration which, in contrast to the degenerate ν_s(SiOSi) vibration (of the E" symmetry type) relates to type A_1'', inactive in the infrared spectrum if the anion symmetry is D_{3h}. When the anion symmetry is lowered to C_{3h}, i.e., if the ring is nonplanar this is no longer forbidden. Thus, the problem of assignment of the 551 cm^{-1} band reduces to the choice between the plane (D_{3h}) and nonplane (C_{3v}) configurations of the ring anion. The most reliable criterion for this choice could be provided by Raman spectroscopy: if the ring is nonplanar in form there should be a polarized line at about 550 cm^{-1}; otherwise in the ν_s(SiOSi) frequency region a polarized line which does not coincide with any of the absorption bands should appear. However, the determination of the Raman spectrum of microcrystalline $Sr_3(Si_3O_9)$ involves considerable difficulties. We shall therefore restrict ourselves to certain considerations which indicate that the plane form of the ring is the more probable. First, even if the ring of three silicon-oxygen tetrahedrons is planar the SiOSi angle is not very large ($\sim 130°$). Therefore the transition to a nonplanar form, involving an inevitable further decrease of the SiOSi angle, seems improbable. Second, if the SiOSi angle is not large we may expect somewhat higher frequencies for ν_s(SiOSi) vibrations and therefore the frequency of 551 cm^{-1} is too low to be assigned to vibrations of this type. (Prima's [6] approximate estimate of the vibration frequencies of the A_1'' type, with only the dynamic valence coefficients taken into account, performed with the aid of secular equations, gave a value for the ν_s(SiOSi) vibration frequency about 10% higher than the ν_s(SiOSi) frequency of type A_1 of the pyroxene chain calculated in the same approximation [7]). If the 551 cm^{-1} frequency cannot be assigned to valence vibrations of the anion there are no grounds for assuming that the anion is nonplanar.

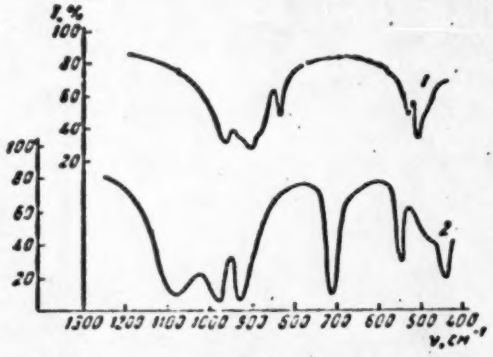

The foregoing interpretation of the spectrum and views on the form of Si_3O_9 rings in strontium metasilicate are equally applicable to pseudowollastonite, the infrared spectrum of which contains a band at 565 cm^{-1}, corresponding to the 551 cm^{-1} band in the spectrum of $Sr_3(Si_3O_9)$.

LITERATURE CITED

1. O. Daniel. Z. Kristallogr., 104, 348 (1942).
2. F. Liebau. Neues Jb. Miner., 94, 1209 (1960).
3. A. N. Lazarev. Optika i spektroskopiya, 9, 195 (1960).
4. A. N. Lazarev and T. F. Tenisheva. Optika i spektroskopiya, 12, 27 (1962).
5. A. N. Lazarev and T. F. Tenisheva. Optika i spektroskopiya, 10, 79 (1961).
6. A. M. Prima. Optika i spektroskopiya, 9, 452 (1960).
7. B. I. Stepanov and A. M. Prima. Optika i spektroskopiya, 5, 15 (1958).

STRUCTURE OF $K_2OsO_4 \cdot 2H_2O$

M. A. Poral-Koshits, L. O. Atovmyan,
and V. G. Andrianov

N. S. Kurnakov Institute of General and Inorganic Chemistry,
Academy of Sciences USSR
Translated from Zhurnal Strukturnoi Khimii, Vol. 2, No. 6,
pp. 743-744, November-December, 1961
Original article submitted July 1961

Various structures have been attributed to the compound of the composition $K_2OsO_4 \cdot 2H_2O$; they comprise $K_2[OsO_4] \cdot 2H_2O$ with tetrahedral complex ions and $K_2[OsO_4(H_2O)_2]$ [1], $K_2H_4[OsO_6]$ [2], $K_2[OsO_2(OH)_4]$ [3] with octahedral complex ions. The last of these formulas was put forward by G. B. Bokii, L. O. Atovmyan, and T. S. Khodashova on the basis of the general hypothesis that a tendency to form stable groupings of the MX_2, MX type with light atoms (mainly oxygen and nitrogen), supplemented by other ligands in the complex, is a characteristic feature of the chemistry of complex compounds of heavy metals such as U, W, Mo, Cr, Os, Ru, etc. Shortening of M–X distances in various groupings indicates an increase of bond multiplicity in them [4, 5, 6].

A structural investigation of $K_2OsO_4 \cdot 2H_2O$ was undertaken in order to verify this hypothesis; in contrast to the other three alternative structures, the presence of $[OsO_2(OH)_4]^{2-}$ complexes presupposes considerable "compression" of the Os coordination octahedron along one of its axes.

Crystals of $K_2OsO_4 \cdot 2H_2O$, prepared as described in [7], belong to the tetragonal-bipyramidal type of symmetry; the {101} faces are the most developed. The lattice constants are: $a = 5.56 \pm 0.02$, $c = 9.44 \pm 0.05$ A (results obtained with the KFOR camera with NaCl standard); $d_{pycn} = 4.04$ g/cc, $N = 2$. Space group $I4/m$.

Values of $|F(hkO)|^2$ and $|F(hOl)|^2$ were obtained by visual assessment of intensities (by blackening), with the Lorentz and polarization factors taken into account. The KFOR camera with MoK_α radiation was used; the specimens selected were isometric crystal fragments with linear dimensions not exceeding 0.15 mm.

The general structure motif was determined from Patterson projections, and the atomic coordinates were refined from electron density projections and the difference projection $\sigma(xz) - \sigma_K(xz)$ with subtraction of the K atom, occupying a nonparametric position, the maximum of which partially overlaps with the maximum corresponding to one of the oxygen atoms. The divergence factors are $R_{hk0} = 0.12$ [64 reflections, $(\sin\vartheta/\lambda)_{max} = 1.08$]; $R_{h0l} = 0.13$ [94 reflections, $(\sin\vartheta/\lambda)_{max} = 1.08$]; zero reflections and the strongest 020,200, 040,400, 002, 004,101 reflections, considerably distorted by extinction, were disregarded. The atomic positions and coordinates are:

Atom	Position	x	y	z	Atom	Position	x	y	z
Os	2 (a)	0	0	0	O_I	4 (d)	0	0	0,186
K	4 (d)	½	0	¼	O_{II} (OH	8 (h)	0,298	0,398	0

The interatomic distances (in A) calculated from these coordinates are given below; asterisks indicate distances between atoms in the same complex.

Os — O_I = 1,77*	K — K = 3,92 (and 4,72)
Os — O_{II} = 2,03*	O_I — O_{II} = 2,70* and 3,54
Os — K = 3,61	O_{II} — O_{II} = 2,88*, 2,79 and 3,20
K — O_I = 2,81	O_I — O_I = 3,10 (and 5,20)
K — O_{II} = 2,82	

The Os atom, situated at the intersection of the fourfold axis with the m plane, is octahedrally surrounded by two O_I atoms on the fourfold axis and four O_{II} atoms in the m plane. The distances $Os-O_I = 1.77$ A, the distance $Os-O_{II} = 2.03$ A. The first is close to the Os–O distance in $K_2[OsO_2Cl_4]$ [8], which is 1.85 A, indicating the presence of the osmyl group with O = Os = O double bonds, and the second corresponds to the length of the Os–OH single bond. Thus, the deformation of the octahedron (which is flattened) and the distances both indicate the presence of tetrahydroxyosmyl ions and make it possible to assign conclusively the formula $K_2[OsO_2(OH)_4]$ to the compound.

The $[OsO_2(OH)_4]^{2-}$ complexes and K^+ ions are packed in accordance with the antifluorite pattern. Therefore the structure of $K_2[OsO_2(OH)_4]$ is genetically linked to the structure type of cubic potassium chloroplatinate and tetragonal $[Pt(NH_3)_4Cl_2]Cl_2$ [9] and $K_2[OsO_2Cl_4]$ [8]. The further lowering of symmetry in $K_2[OsO_2(OH)_4]$ (transition from 14/mmm to 14/m) is evidently due to a nonlinear arrangement of the oxygen bonds in the hydroxyl groups.

Rotation of the complexes in the m plane is determined by the need for close packing of $Os(OH)_4$ "squares" or possibly by a tendency to hydrogen bonding (along the perimeter of the square) between OH groups of four neighboring complexes in the same m plane (the distance OH–OH = 2.79 A). It is possible, however, that the OH bonds are taken out of the sections z = 0 and $z = 1/2$: either all in one direction (with lowering of the symmetry to 4), or by pairs in opposite directions ($\bar{4}$ symmetry), or else statistically (with retention of 4/m symmetry). In this case hydrogen bonds are not formed; this is shown by the fact that the OH–O distances are 3.54 A (the distance OH – O = 2.74 A is the distance within the complex).

It is the authors' pleasant duty to offer their gratitude to Corresponding Member of the Academy of Sciences USSR, G. B. Bokii whose valuable advice was of considerable assistance in the investigation.

LITERATURE CITED

1. R. Charonnat. Pascal Traité de Chimie Minerale, Paris, t. 2, p. 352 (1932).
2. A. Werner. New Views in the Field of Inorganic Chemistry [Russian translation] (L. 1936) p. 113.
3. G. B. Bokii, L. O. Atovmyan, and T. S. Khodashova. Dokl. AN SSSR, 128, 1, 78 (1959).
4. L. O. Atovmyan and G. B. Bokii. Zh. strukt. khimii, 1, 4, 501 (1961).
5. G. B. Bokii and L. O. Atovmyan. Zh. strukt. khimii, 2, 3, 308 (1961).
6. V. M. Volkov and M. E. Dyatkina. Dokl. AN SSSR, 31, 2, 351 (1960).
7. A. Retgers. Z. phys. chem., 8, 74 (1891); 10, 531 (1892).
8. J. L. Hoard and J. D. Grenko. Z. Kristallogr., A87, 100 (1936).
9. G. B. Bokii and M. A. Porai-Koshits. Izv. Sektora platiny, IONKh AN SSSR, 24, 52 (1949).

All abbreviations of periodicals in the above bibliography are letter-by-letter transliterations of the abbreviations as given in the original Russian journal. *Some or all of this periodical literature may well be available in English translation.* A complete list of the cover-to-cover English translations appears at the back of this issue.

STEREOCHEMISTRY OF FOUR-COORDINATED SPIN-FREE INTERNAL COMPLEX COMPOUNDS OF Co(II) AND Ni(II) WITH o-HYDROXYALDEHYDES

V. V. Zelentsov and V. K. Trunov

Moscow Physicotechnical Institute
M. V. Lomonosov Moscow State University
Translated from Zhurnal Strukturnoi Khimii, Vol. 2, No. 6,
pp. 745-746, November-December, 1961
Original article submitted December 30, 1960

There is no doubt that, if no electron pairing occurs, four-coordinated complex compounds of Co(II) have tetrahedral structure. The magnetic method of stereochemical investigation can be applied with success to complex Co(II) compounds. In the $^4F_{1/2}$ ground state the magnetic moment of Co(II) is determined by three unpaired electrons. The "spin only" value of the magnetic moment is 3.88 μ_B. However, it has been found experimentally that the effective magnetic moments of bivalent-cobalt complexes in which there is no enforced electron pairing are considerably above this value and lie in the region of 4.2-5.2 μ_B. This is attributable to the greater or lesser contribution of the orbital component to the magnetic moment of the complex. The contribution of the orbital component depends both on the stereochemistry of the complex and on the ligand field. Figgis and Nyholm [3] showed that tetrahedral complexes have smaller magnetic moments than complexes of octahedral structure. This is understandable if we consider the influence of the ligand field on the magnitude of the orbital component [4]. In fact in octahedral Co(II) ($d_\gamma^2 d_\varepsilon^5$) complexes redistribution of electron density occurs in the d_ε orbitals under the influence of an external field, whereas there should be no such redistribution in ($d_\gamma^4 d_\varepsilon^3$) tetrahedral complexes because each d_ε^3 orbital is occupied by only one electron. Therefore the crystal field "freezes" the orbital component of the magnetic moment to a greater extent in tetrahedral than in octahedral complexes.

Investigations of the magnetic susceptibility of tetrahedral complexes of bivalent cobalt [2] showed that the magnetic moments of these complexes are in the 4.26-5.00 μ_B range and depend on the nature of the ligands: the weaker the ligand field the less is the orbital component suppressed. Complexes of the CoI_4^{2-} type have the largest moments, and compounds in which the cobalt atom is surrounded by four oxygen atoms (CoO) have the smallest.

Whereas there is no doubt about the tetrahedral structure of four-coordinated high-spin cobalt complexes, in the case of nickel (II) a tetrahedral structure has so far been reliably demonstrated only for complexes of nickel with triphenylphosphine and similar compounds [5-7]. The structure of nickel complexes with o-hydroxyaldehydes has not been finally settled. It is known that these internal complex compounds are paramagnetic with magnetic moments of 3.04-3.15 μ_B [8]. A tetrahedral structure has been postulated for Ni salicylaldehydate because it is isomorphous with zinc salicylaldehydate [9].

Compound	Temperature, °K	$\chi_T \cdot 10^6$	$\chi_{Co^{2+}} \cdot 10^6$	$\mu_{eff.} \cdot \mu_B$
Cobalt bis(4-methyl-2-hydroxybenzaldehydate) $(C_8H_7O_2)_2Co$	296	23.4	8283	4.45
Cobalt bis(5-chloro-2-hydroxybenzaldehydate) $(C_7H_4O_2Cl)_2Co$	295	19.7	7480	4.22
Cobalt bis(5-bromo-2-hydroxybenzaldehydate) $(C_7H_4O_2Br)_2Co$	291	18.4	8635	4.50
Cobalt bis(2-hydroxy-1-naphthaldehydate) $(C_{11}H_7O_2)_2Co$	296	17.85	7350	4.20

Study of the magnetic susceptibility of internal complexes of cobalt with o-hydroxyaldehydes showed that, as was to be expected, electron pairing does not occur during complex formation. The effective magnetic moments of all four internal complexes at room temperature are in the range of 4.20-4.50 μ_B.

Study of the magnetic susceptibility of internal complexes of bivalent cobalt leads to the conclusion that they all have tetrahedral structure with $4s4p^3$ bonds.

We have shown [8] that the magnetic moment of nickel bis(4-methyl-2-hydroxybenzaldehydate) at room temperature is 3.05 μ_B. For confirmation of the view, based on magnetic data, that the structure of nickel bis(4-methyl-

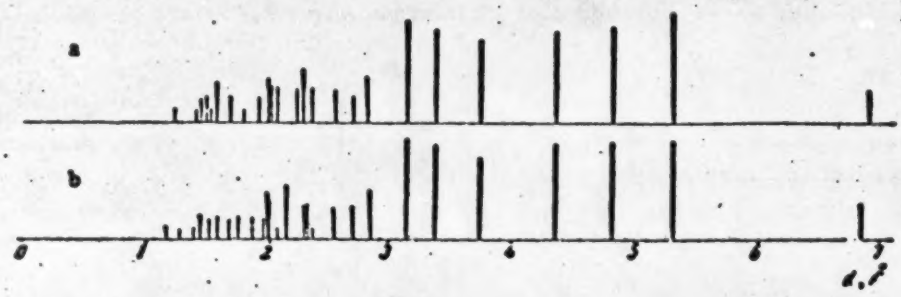

2-hydroxybenzaldehydate) is tetrahedral we obtained powder diagrams of the internal complexes of cobalt (Fig., a) and nickel (Fig., b) with 4-methyl-2-hydroxybenzaldehyde. Comparison of the powder diagrams shows that the two compounds are completely isostructural. Assuming that the tetrahedral structure of cobalt (II) bis(4-methyl-2-hydroxybenzaldehydate) is established, we also propose a tetrahedral structure for nickel bis(4-methyl-2-hydroxybenzaldehydate) on the basis of the above data.

EXPERIMENTAL

Internal complex compounds of Co(II) were synthesized by the interaction of an alcoholic solution of the appropriate aldehyde with aqueous cobalt acetate solution (2 : 1 mole ratio), followed by heating on a boiling water bath for 30 minutes. The orange microcrystalline substances were filtered off, washed with alcohol, dried to constant weight at 100-105°, and analyzed for Co as $CoSO_4$ or Co_3O_4:

	Found Co, %		Calculated Co, %
$(C_8H_7O_2)_2Co$	18,03;	17,96	17,90
$(C_8H_6O_2Cl)_2Co$	16,06;	16,11	15,93
$(C_8H_6O_2Br)_2Co$	12,71;	12,80	12,84
$(C_{11}H_7O_2)_2Co$	14,50;	14,63	14,69

Magnetic susceptibility was measured at room temperature by Faraday's method.

LITERATURE CITED

1. R. H. Holm and F. A. Cotton. J. Chem. Phys. 31, 788 (1959).
2. R. H. Holm and F. A. Cotton. J. Chem. Phys. 32, 1168 (1960).
3. B. N. Figgis and R. S. Nyholm. J. Chem. Soc. 12 (1954).
4. R. S. Nyholm. J. Inorg. and Nucl. Chem. 8, 401 (1958).
5. L. M. Venanzi. J. Inorg. and Nucl. Chem. 8, 137 (1958).
6. N. S. Lill, R. S. Nyholm, and P. Pauling. Nature 182, 168 (1958).
7. F. A. Cotton and D. M. L. Goodgame. J. Amer. Chem. Soc. 82, 2967 (1960).
8. V. V. Zelentsov, I. A. Savich, and B. V. Evdokimov. Nauchn. dokl. vyssh. shkoly. Khimiya i khim. tekhnol. 672 (1958).
9. D. H. Carfiss, F. K. C. Lile, and E. C. Lingafelter. Acta crystallogr. 5, 388 (1952).

STRUCTURES DERIVED FROM THE CaF_2–CeO_2 CUBIC TYPE

Yu. A. Pyatenko

Institute of Mineralogy, Geochemistry, and Crystal Chemistry
of the Rare Elements
Translated from Zhurnal Strukturnoi Khimii, Vol. 2, No. 6,
pp. 746-748, November-December, 1961
Original article submitted August 5, 1961

The discovery of the mineral calzirtite and determination of its crystal structure [1, 2] considerably extended our knowledge of structures derived from the cubic fluorite (CaF_2) – cerianite (CeO_2) type. Calzirtite corresponds to the approximate formula $2CaO \cdot 5ZrO_2 \cdot 2TiO_2 = Ca_2Zr_5Ti_2O_{16}$ and is a new representative of the class of subtractive structures which may be derived from the simple CaF_2–CeO_2 motif by removal of some of the anions from the primitive cubic packing. N. V. Belov [3] gives the formula M_4X_{8-x} for derived structures of this type; when $x = 0$ we have the original CaF_2, CeO_2, ThO_2 and UO_2 structures; $x = 1$ corresponds to the structure type of the mineral pyrochlore, $A_2B_2X_7$, and, finally, $x = 2$ corresponds to the structures of Sb_2O_3, As_2O_3, Y_2O_3 and certain others. Whereas in the structure of CeO_2 ($x = 0$) all the Pauling polyhedrons are cubes, in the case of pyrochlore ($x = 1$) there are equal numbers of cubes and octahedrons, and structures with $x = 2$ contain octahedrons only [3]. All these derived structures have cubic symmetry with unit cells having edges twice the length of the edge of the CeO_2 cell. Calzertite has tetragonal symmetry and is the first noncubic representative of these derived structures. Both the lattice parameters of calzirtite (a = 15.30, c = 10.20 A) are multiples of 5.1 A; this, in its turn, is very close to the value of a in the cubic structures of CaF_2, CeO_2, etc. If we compare calzirtite with pyrochlore we note that the ratios of total cations to anions in the formulas of these minerals are approximately equal ($^9/_{16} \approx {}^4/_7$). This means that in the formation of both derived structures from the original cubic packing almost equal numbers of oxygen atoms per given volume are removed. Therefore, pyrochlore and calzirtite provide an example of two different structural types determined only by the pattern in which equal numbers of oxygen atoms are removed from the original packing. Whereas in the case of pyrochlore the characteristic distribution of vacant places in the packing while lowering the symmetry of the structure still leaves it cubic ($Fm3m \rightarrow Fd3m$), in the case of calzirtite the change is sharper: $Fm3m \rightarrow I4_1/acd$. The pyrochlore structure contains Pauling polyhedrons of two kinds: cubes and octahedrons. In calzirtite these polyhedrons are supplemented by seven-pointed polyhedrons (cubes with one vertex missing). The appearance of a third type of polyhedron favors complication of the cationic composition; this occurs in the case of calzirtite $Ca_2Zr_5Ti_2O_{16}$, in the structure of which Ca atoms occupy cubes, $^4/_5$ of the total number of Zr atoms are in the seven-point polyhedrons,* and the Ti atoms are in octahedrons. It should be noted that the example of calzirtite confirms the distinct tendency of Zr atoms to sevenfold coordination in oxide structures [4].

Let us consider the principal characteristics of these derived structures. The main feature is a three-dimensional checkerwork distribution of Pauling polyhedrons which is equivalent to exact or almost exact location of the cations at the points of a face-centered F-lattice. A consequence of this is that the lattice constants of the derived structure are multiples of the same quantity, the constant a of this F-lattice. The numbers of filled and empty polyhedrons are equal. In real derived structures the ideal (cubic) packing of the anions may be deformed to a considerable extent; however, this merely distorts the shape of the polyhedrons without changing the coordination numbers of the cations. Since the most probable polyhedrons in the formation of these derived structures are cubes, seven-pointed polyhedrons, and octahedrons, these structures are formed the most readily with the participation of cations characterized by coordination numbers of 8, 7, and 6.

We note further that the ratio p of the total number of cations to the number of anions in the formula of the compound forming a derived structure must be in the range $^1/_2 \leq p \leq {}^2/_3$. When $p = {}^1/_2$ we have the original structure of the CeO_2 type, and when $p = {}^2/_3$ we have a derived structure in which all the polyhedrons are octahedrons.

* The remaining Zr atoms are statistically distributed in cubes with Ca atoms.

The next characteristic feature of M_4X_{8-x} structures in which X = O is the complexity of the cationic composition with relatively high cation valence. Indeed, it follows from the general formula M_4O_{8-x} ($0 \leq x \leq 2$) that the valence of the cation M can be a whole number only when x = 0 or x = 2 (+4 and +3 respectively). All other values of x correspond to nonintegral values of the valence M. In real structures such "fractional" valence may represent merely a certain average valence of several kinds of cations present simultaneously in the structure.

It is quite obvious that the formation of a particular derived structure is determined both by the number of vacancies in the original anionic packing and by their distribution motif. However, this is not in itself sufficient for unique definition of the structure type, because the same distribution motif of vacancies in the packing is in general associated with two theoretically possible types of subtractive structure. Thus, in the pyrochlore structure the empty polyhedrons continuing the filled cubes and octahedrons are exclusively seven-pointed figures. The second ("complementary") structure type possible within the framework of a given anion packing is obtained if these seven-pointed figures are filled with cations and the cubes and octahedrons are left empty. It is obvious that the number of seven-pointed figures is equal to the sum of the cubes and octahedrons. If the centers of these cubes and octahedrons coincide with the points of two 16-fold positions of the Fd3m [5], then the centers of the seven-pointed figures are points of one 32-fold xxx complex. In accordance with the foregoing, cations of several kinds should be distributed statistically at these points. In this case we have a new derived structure corresponding to the formula $(M', M'', \ldots)_4X_7$ and not $A_2B_2X_7$ (pyrochlore). A similar consideration of the oxygen packing forming the basis of the calzirtite structure type shows that in the calzirtite cell the numbers of filled Pauling cubes, seven-pointed figures, and octahedrons are 24, 32, and 16 respectively (a total of 72 polyhedrons). If we now imagine these polyhedrons to be empty and those adjacent to them by their faces filled, we have a new structure. In the cell of this new derived structure all the Pauling octahedrons are empty, and the numbers of occupied cubes and seven-pointed figures are 8 and 64. Unfortunately, no concrete examples of these two "complementary" structures have been reliably established. In these structures seven-pointed polyhedrons are either the only polyhedrons (in the first) or are greatly predominant (in the second). It is therefore likely that these structures should be characteristic of compounds such as those with a predominance of zirconium atoms, which have a marked tendency to sevenfold coordination. In addition, as the "average" cation valences in these derived structures cannot be whole numbers, at least one other type of cation with a valence less than +4 must be present. Therefore one pair suitable for formation of such "complementary" structure is, for example, the pair Zr + Ca.

The formation of derived structures close to those discussed above probably occurs during the so-called stabilization of the high-temperature cubic modification of ZrO_2. It is known [6] that the cubic modification of pure ZrO_2 (CaF_2–CeO_2 structure type) is stable only at temperatures above 1400°. The monoclinic modification of zirconium dioxide (baddeleyite) exists at normal temperatures. However, ZrO_2 heated in presence of relatively small amounts of MgO, CaO, etc., retains a cubic structure even at low temperatures [7]. This property is of practical use, as it is utilized for raising the mechanical endurance of refractory ceramics. The nature of this effect is probably the following. The solid-state reaction of ZrO_2 with a small amount of CaO leads to the formation of a compound of the type $(Zr, Ca)_4O_{8-x}$. This compound should correspond to one of the theoretically possible subtractive structures similar to those considered in this paper. Therefore the "stabilization" of cubic ZrO_2 is none other than the formation of an independent structure type, only formally related to the fluorite-cerianite type, to which the high-temperature modification of ZrO_2 belongs.

We may note in conclusion that in a study of the phase diagram of the systems CaO–ZrO_2–TiO_2 only one ternary compound, $CaZrTi_2O_7$, was detected [8]; these workers missed the compound $Ca_2Zr_5Ti_2O_{16}$, which is a synthetic analog of our calzirtite. This compound falls into the composition region defined by these workers as "the field of cubic ZrO_2." In accordance with what was said earlier in this paper, this region should be defined as the region of derivatives of the CaF_2–CeO_2 cubic structure type which may include noncubic representatives.

LITERATURE CITED

1. T. B. Zdorik, G. A. Sidorenko, and A. V. Bykova. Dokl. AN SSSR 137, 3, 681 (1561).
2. Yu. A. Pyatenko and Z. V. Pudovkina. Kristallografiya 6, 2, 196 (1961).
3. N. V. Belov. Miner. sb. L'vovsk. geol. obshch. 4, 21 (1950).
4. N. V. Belov. Kristallografiya. 5, 3, 460 (1960).
5. H. R. Gärtner. Neues Jahrb. Min., Beil.–Bd. 61, 1 (1930).
6. A. E. Van Arkel. Physica 4, 286 (1924).
7. O. Ruff and F. Ebert. Z. anorgan. und allgem. Chemie 180, 19 (1929).
8. L. W. Coughanow, R. S. Roth, S. Marzullo, and F. E. Sennett. J. Res. Nat. Bur Standards 54, 4, 191 (1955).

PHASE DIAGRAM OF THE ALUMINUM – BORON SYSTEM

V. T. Serebryanskii and V. A. Épel'baum

L. Ya. Karpov Scientific Research Institute of Physical Chemistry
Translated from Zhurnal Strukturnoi Khimii, Vol. 2, No. 6,
pp. 748-750, November-December, 1961
Original article submitted July 14, 1961

According to the literature, the aluminum-boron system includes the compounds AlB_2, AlB_{12} [1, 2] and AlB_{10} [3]; AlB_{12} exists in several crystalline modifications [4, 5]. The conditions for preparation of these borides have been studied repeatedly [1, 2, 6, 7]. However, mainly mixtures of various phases with a predominance of one particular phase were obtained in these investigations. Only Felten [8] succeeded in obtaining AlB_2 as the main reaction product by sintering of the elements. According to [9] the compound AlB_2 is formed as the result of a peritectic reaction at 1350°; according to [7] it decomposes at 1100°. There are no data in the literature on the conditions for the existence of other aluminum boride phases.

In this communication we present the results of the first stage in the study of the equilibrium diagram involving investigation of the phase diagram and conditions for formation of aluminum borides from the elements over a wide concentration range at temperatures up to 1400°.

EXPERIMENTAL

The boron-containing specimens were prepared from the pure elements (Al – 99.99%, B – 99.5%). The powders were mixed thoroughly, formed into rods, and put in a corundum boat into a quartz tube contained in a tubular furnace. First the system was evacuated and the specimens were heated in vacuum for 30 minutes at about 400°. Pure argon was then passed through and the temperature was raised to the required level. The optimum synthesis conditions (temperature and heating time) were chosen in accordance with the composition. The phase composition of the specimens was investigated by the x-ray method. Some were also investigated by the thermographic method in V. A. Nedumov's VNTA-1 apparatus for high-temperature noncontact thermal analysis [10]. The pure phases were analyzed for aluminum and boron and their pycnometric densities were determined. The following conclusions were reached from the results of the experiments.

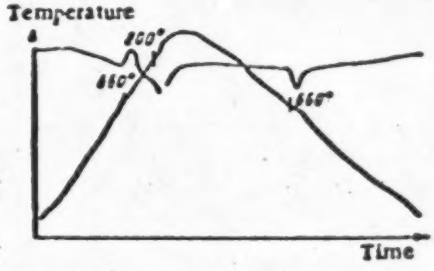

Fig. 1. Thermogram for the interaction of aluminum and boron. Heating and cooling.

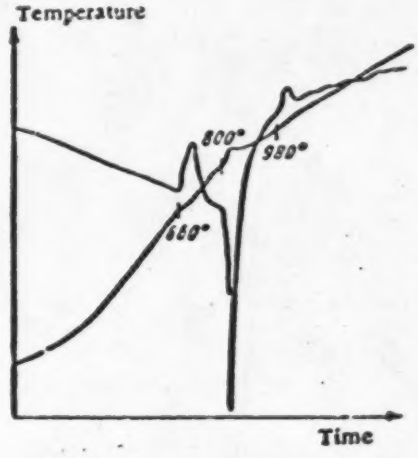

Fig. 2. Heating curve (up to 1400°) of a specimen of the original composition AlB_2.

1. Formation of AlB_2 begins even at 650°, but the reaction is not complete – the x-ray patterns contain lines corresponding to pure aluminum together with AlB_2 lines.

2. The most suitable temperature for formation of AlB_2 is 800°. At this temperature an original mixture corresponding to the composition AlB_2 gives a single-phase product after 15 hours of heating; this confirms the data in [8].

3. In view of the report [11] that AlB_2 is unstable at room temperature, we investigated the compound after it had been kept for 1½ years. No changes were found; i.e., AlB_2 is quite stable at room temperature.

The thermogram in Fig. 1 represents the interaction of aluminum and boron at temperatures up to 900° during heating and cooling at a rate of 20°/min. Several thermal effects are seen: an endothermic effect at 660° corresponding to fusion of aluminum; an exothermic effect at 800° representing the interaction of aluminum with boron. The cooling curve exhibits only one phase transition, at 660°, corresponding to crystallization of Al. No solid-state change indicating decomposition of AlB_2 was recorded on the cooling curve.

TABLE 1. Phase Composition in Relation to Specimen Composition and Synthesis Temperature

Original composition		Synthesis temperature									
% B	% Al	600°	700°	800°	900°	950°	1000°	1100°	1200°	1300°	1400°
28.9	71.1	AlB_2, Al				AlB_2 + Al	α-AlB_{12} + Al				
44.9	55.1										
55.0	45.0										
61.9	38.1										
70.9	29.1										
76.5	23.5	AlB_2 + Al		AlB_2		α-AlB_{12}	α-AlB_{12}				
80.3	19.7										
82.5	17.5										

TABLE 2. Powder Diagram of α-AlB_{12} (CuK_α Radiation)

Line No.	hkl	I	d(kX)	Line No.	hkl	I	d(kX)
1	110	w.	7.16	20	–	w.	1.722
2	111	v.v.w.	6.25	21	–	s.	1.681
3	112,200	w.	5.08	22	–	m.	1.544
4	211	m.	4.39	23	–	v.v.w.	1.512
5	202	v.v.s.	4.14	24	–	v.v.w.	1.482
6	212	s.	3.84	25	–	s.	1.435
7	221	v.v.w.	3.45	26	–	s.	1.395
8	222	v.v.w.	3.20	27	–	m.	1.362
9	302	m.	3.048	28	–	m.	1.324
10	312	v.v.w.	2.936	29	–	w.	1.293
11	320	w.	2.817	30	–	w.	1.118
12	322	m.	2.629	31	–	v.v.w.	1.062
13	224	w.	2.534	32	–	v.w.	0.928
14	215	v.s.	2.411	33	–	w.	0.915
15	225	s.	2.228	34	–	v.v.w.	0.904
16	–	s.	2.154	35	–	w.	0.828
17	–	w.	1.903	36	–	w.	0.828
18	–	s.	1.829	37	–	w.	0.777
19	–	w.	1.759	38	–	w.	0.776

Note: v.v.w. (very, very weak), v.w. (very weak), w. (weak), m. (medium), s. (strong), v.s. (very strong), v.v.s. (very, very strong).

4. On further increase of temperature AlB_2 begins to decompose. During prolonged heating the decomposition reaction begins at 950° and proceeds with liberation of aluminum. The x-ray patterns of specimens synthesized at this temperature contain reflections of AlB_2, Al, and AlB_{12}. Figure 2 is the thermogram for a specimen of the original composition AlB_2 heated to 1400°. In addition to two peaks, at 660 and 800°, corresponding to fusion of alumi-

num and formation of AlB_2, the differential curve also has a peak at 980° which corresponds to endothermic decomposition of AlB_2 as follows: $AlB_2 \rightarrow AlB_{12} + Al$.

The results of thermal analysis are confirmed by syntheses effected at various temperatures and with various concentrations of the original components; the results are given in Table 1. The table shows that at temperatures up to 900° AlB_2 is formed, and at 1000° and over only AlB_{12} is formed, regardless of the original composition. The powder diagram of AlB_{12} shows (Table 2) that this is α-AlB_{12}, i.e., the tetragonal modification [4] of the so-called "graphite-like boron." Indexing was performed only for the first 15 lines, as at large angles indexing becomes indefinite owing to the large cell dimensions. The identity periods are a = 10.15 and c = 14.29 A; the experimental pycnometric density is 2.62 g/cc. The boron and aluminum contents are 82.8 and 16.7%.

No other modifications of AlB_{12} were found in any of the experiments under the conditions specified. The conditions for formation of such modifications of AlB_{12}, and also of AlB_{12}, will be detailed in a future paper.

Our data on the formation and decomposition temperatures of AlB_2 are confirmed in [12], but the author of that paper obtained β-AlB_{12} as the final product; this requires further verification.

LITERATURE CITED

1. H. Biltz, Ber. 41, 2634 (1908); 43, 297 (1910).
2. H. Funk, Z. anorgan. Chem. 142, 269 (1925).
3. J. Cohn, J. Catz, A. Giardini, Z. Kristallogr. 111, 53 (1958).
4. F. Halla and H. Weil, Z. Kristallogr. 101, 435 (1939).
5. S. Naray-Szabo, Z. Kristallogr. 94, 367 (1936).
6. A. Binet du Jassoneix, Ann. Chim. phys. 17, 161 (1909).
7. P. Haenni, Rev. Metallurgie, 23, 342 (1926).
8. E. J. Felfen, J. Amer. Chem. Soc. 72, 5977 (1956).
9. W. Hofmann and W. Jäniche, Z. phys. Chem. 31, 214 (1936).
10. N. A. Nedumov, Zh. fiz. khimii 34, 184 (1960).
11. F. Lihl and P. Jenitschek, Z. Metallkunde 44, 414 (1953).
12. H. J. Becher, Z. anorgan. und allgem. Chem. 308, 13 (1961).

All abbreviations of periodicals in the above bibliography are letter-by-letter transliterations of the abbreviations as given in the original Russian journal. Some or all of this periodical literature may well be available in English translation. A complete list of the cover-to-cover English translations appears at the back of this issue.

INTERNATIONAL UNION ON CRYSTALLOGRAPHY

COMMISSION ON CRYSTAL STRUCTURE DATA

LIST OF 1957 PUBLICATIONS CONTAINING NEW DATA ON CRYSTAL STRUCTURES

Translated from Zhurnal Strukturnoi Khimii, Vol. 2, No. 6,
pp. 751-759, November-December, 1961

C. ORGANIC COMPOUNDS

1. Abrahams S. C., Cr. str. of diphenyl sulfoxide. Acta Cryst. 10, 417.
2. Almenningen A., Bastiansen O., and Harshbarger F. Some e. diffrn. studies of 1,4-dibromo-butyne-2. Acta Chem. Scand. 11, 1059.
3. Alver E. and Furberg S., Str. of cr. cytidylic acid b. Acta Chem. Scand. 11, 188.
4. Amorós J. L., Belgrano C., and Canut M. L. Estudios acerca de la dinámica reticular en crs. mol. V. Determn. directa de la amplitud de la oscilacion térmica. Publ. dept. cryst. mineral., Madrid 3, 5.
5. Amoros J. L. and Canut M. L. Thermal vibrations in dicarboxylic acids. Acta Cryst. 10, 794. (Abstracts of papers delivered at 4th Assembly and International Congress I. U. C., Montreal, July 1957).*
6. Andreeva N. S., Esipova N. G., and Millionova M. I. Chars of collagen str. Kristallografiya 2, 470.
7. Andresen A. F. Investn. of hexamethylene tetramine by n. diffrn. Acta Cryst. 10, 107.
8. Bacon G. E.,Mol. str. detn. by n. diffrn. Acta Cryst. 10, 844.
9. Bacon G. E., Unters. v. H Brücken mit Neutronenbeug. Angew. Chem. 69, 755.
10. Bacon G. E. and Curry N. A., N.-diffrn. study of K H bis-phenyl-acetate. Acta Cryst. 10, 524.
11. Bak B., Christensen D., Hansenygaard L., and Tannenbaum E. Microwave detn. of str. of trifluorobutyne. J. Chem. Phys. 26, 241.
12. Baker J. G., Jenkins D. R., Kenney C. N., and Sugden T. M. Microwave spectrum a. str. of trichloroacetonitrile. Trans. Faraday Soc. 53, 1397.
13. Baro R., Champagne M., Luzzati F., and Nicolaieff A. Détermn. de forme et dims. de la mol. de serumalbumine de boeuf en soln au moyen de la diffusion des r. X aux petits angles. "Mezinarodni symp. makromolekulami chemie, Praha, 1957." Československ. Společnost. Chem. 21.
14. Barss W. M. Str. of gaseous chloropicrin as determined by e. diffrn. J. Chem. Phys. 27, 1260.
15. Bartell L. S. and Bonham R. A. Str. of ethylene. J. Chem. Phys. 27, 1414.
16. Bastiansen O.and Cyvin S. J. Mol. vibrations a. standard deviation of interat. distances in benzene. Nature 180, 980.
17. Bastiansen O., Hedberg L., and Hedberg K. Reinvestn. of mol. str. of 1, 3, 5, 7 cyclooctatetraene by e. diffrn. J. Chem. Phys. 27, 1311.
18. Bauer J. Krystalografická data dihydroxybenzochinonu. Chem. listy 51, 511; Collection Czechoslov. Chem. Commun. 22, 1620 (Czech.).
19. Becker K. A., Plato K., and Plieth K. Röntgenograph. Str.-unters. v. 1,3-Di(p-brombenzal)-cyclopentanon-(2). Z. Elektrochem. 61, 96.
20. Beevers C. A. and Geachin P. Mc. D. Cr. str. of α-rhamnose monohydrate. Acta Cryst. 10, 227.
21. Bendit E. G. α-β-transformn. in keratin. Nature 179, 535.
22. Bennet J. E., Gibson J. F., Ingram D. J. E. E.-resonance studies of haemoglobin derivatives. I. Haemplane orientation. Proc. Roy. Soc., 240, 67.
23. Bireswan Banerjee and Priyadaranjan Ray. Complex compds. of bipositive Ag with pyridine carboxylic acids. J. Indian Chem. Soc. 34, 207.
24. Biswas S. G. and Sirkar S. C. X-ray anal. of str. of frozen toluene a. its soln. in alcohol at − 180° C. Indian J. Phys. 31, 141.

---

*Subsequently abbreviated as (Abstracts . . .).

25. Bodo G. X-ray study of cr. cytochrome c. Biochim. Biophys. Acta. 25, 428.
26. Bokij G. B. and Kukina G. A. Cr. chem. of complex divalent Pt compds. Acta Cryst. 10, 786. (Abstracts ...)
27. Bregman J., Fankuchen T., Katz J. L., Miksic M., Norman N., and Post B. X-ray diffrn. studies at low temps. Acta Cryst. 10, 801. (Abstracts . . .)
28. Broekema J., Havinga E. E., Wiebenga E. H. Refnt. of cr. strs. of $N(CH_3)_4J_3$. Acta Cryst. 10, 596.
29. Brotherton T. and Jeffrey G. A. Crystallogr. a. str. of some C_{19} cyclopropane fatty acids. J. Am. Chem. Soc. 79, 5132.
30. Brown G. M., Norment H. G. Jr., and Levy H. A. Cr. str. of 2,6-dimenthyl-γ-pyrone. Acta Cryst. 10, 806. (Abstracts . . .)
31. Brown T. L. and Rogers M. T. X-ray diffrn. data for methyl-a. ethyl-Li. Acta Cryst. 10, 465.
32. Brś L. Cr. str. of Pb a. thiourea inclusion compd. Acta Cryst. 10, 798. (Abstracts. . .)
33. Brś L. Cr. str. of 1-phenyl-2-mercapto-4-arabotetrahydroxibutylimidazol. Acta Cryst. 10, 814 (Abstracts...)
34. Brś L., Perez Rodriguez M., Roldan Gonzalez L. (I). Brś L., Cubero M., and Roldan Gonzalez L. (II). Estructura cr. del 2-fenil-2-mercapto-4-arabotetrahidroxibutilimidazol. I. Modifn. cr. A. II. Modifn. cr. B. Anales real soc. espaň. fis. y quim. (Madrid), 53A, 149; 155.
35. Bryden J. H. Cr. str. of azo-bis N-chloroformamidine. Program & Abstracts 15th Pittsburgh Diffrn. Conf. 6-8 Nov. 1957, 33.
36. Bryden J. H. Mol. configuration of 1,4-dimethyl-5-iminotetrazole. Acta Cryst. 10, 148.
37. Bryden J. H. Cr. str. of N-methylurea nitrate. Acta Cryst. 10, 714.
38. Bryden J. H. Cr. str. of aminoguanidine hydrochloride. Acta Cryst. 10, 677.
39. Bud'ko I. Ya and Frank-Kamenetskii V. A. U. c. and spg. gr. of curtisite (idrjalene). Zap. Vses. min. obshch. 86, 716.
40. Bullen G. J. U. c. pars. a. sp. gr. of bisacetylacetoneberyllium. Acta Cryst. 10, 143.
41. Bullough R. K. and Wheatley P. J. Stereochem. of mols. containing C = C = N gr. II. Cr. str. of N-methyl-sulphonyl 2-phenylsulphonylidineamine. Acta Cryst. 10, 233.
42. Burns J. H. and Wasen J. Cr. str. of arsenomethane. J. Am. Chem. Soc. 79, 859.
43. Canut M. L. Equipo para el estudio experimental de la difraccion de r. X. a baja temp. Publ. dept. crist. mineral., Madrid 3, 39.
44. Canut M. L. and Amorós J. L. Estudios acerca de la dinámica reticular en crs. mols. VI. Difracción difusa de los ácidos dicarboxilicos de la serie par: succinico y adipico. VII. Difracción difusa de los ácidos dicarboxilicos de la serie impar: pilémica. Publ. dept. crist. mineral., Madrid 3, 15; 27.
45. Carlström D. Cr. str. of α-chitin (poly-N-acetyl-glucosamine). J. Biophys. Biochem. Cytol. 3, 669.
46. Carter F. L. and Hughes E. W. Cr. str. of complexes cuprous chloride-1,6-heptadiyne. Acta Cryst. 10, 801 (Abstracts . . .)
47. Cavalca L., Nardelli M., and Coghi L. Str. del Cd chloride (DI) acetamide. Nuovo Cim., 6, 278 (Ital.)
48. Chackraburtty C. M. X-ray anal. of bivalent Ag nicotinate. Acta Cryst. 10, 128.
49. Chackrabutty C. M. X-ray measrts. on nettle fibres. Nature, 179, 776.
50. Chapman D., Crossley A., and Davies A. C. Str. of major component glyceride of cocoa butter, a. of major oleodisaturated glyceride of lard. J. Chem. Soc. 1502.
51. Chowdhury S. K. On size of intermicellar sps. a. capillaries in jute fibers as revealed by X-ray anal. Textile Research J., 27, 935.
52. Chowdhury S. K. On str. of alpha-cellulose obtained from jute fibres. Indian J. Phys. 31, 639.
53. Chowdhury S. K. X-ray diffrn. pat. a. micellar dims. of some substitute of jute fibre. Indian J. Phys. 31, 572.
54. Claster J. and Rabaud H. Str. cr. du 9-cyananthracene. Acta Cryst. 10, 804. (Abstracts. . .)
55. Corradini P. Sulla str. di alti polimeri amorfi di alfa-olefine con particolare riguardo al polietilene. Rend. ist. lombardo sci., Pt. I. Classe sci. mat. e nat. 91, 889 (Ital.)
56. Corradini P. Sulla str. cr. del succinilsuccinato di metile. Atti accad. nazl. Lincei, Rend., Classe sci.fis., mat. e nat. 22, 615 (Ital.).
57. Corradini P. Sulla str. cr. del trimero della esaidro-benzaldeide. Atti accad. nazl. Lincei, Rend., Classe sci. fis., mat. e. nat. 22, 504 (Ital.)
58. Coyne T., Pepinsky R., and Watanabe T. Cyclic configuration of aspartate ion in cr. str. of Zn, cobaltous a. nickelous aspartate trihydrate. Acta Cryst. 10, 438.
59. Crick F. H. C. and Kendrew J. C. X-ray anal. a. protein str. Advances Protein Chem. 12, 134.
60. Cromer D. T. Least-squares refnt. of str. of tetramethylpyrazine. J. Phys. Chem. 61, 254.
61. Crowder M. M., Morley K. A., and Taylor C. A. Direct str. detn. by opt.-transformn. methods. Nature 180,431.

62. Cruickshank D. W. J. Detailed refnt. of cr. a. mol. str. of anthracene. Acta Cryst. 10, 470.
63. Cruickshank D. W. J. Detailed refnt. of cr. a. mol. str. of naphthalene. Acta Cryst. 10, 504.
64. Crute M. B. Cr. str. of Ni tioporphyrin II. Acta Cryst. 10, 803 (Abstracts . . .)
65. Cubero M., Roldán L., Pérez Puente A. Estructura cr. del 1-fenil-2-mercapto-4-arabotetrahidroxibutil imidazol. Derivado bromado. Anales real soc. espan. fis. y quim. (Madrid), 53 A, 125.
66. Curien H., Gasperin M., Rimsky A., and Jaeger M. Données cristallogr. sur le dipicrate de nornicotine. Bull. soc. franc. minéral. et cryst. 80, 243.
67. Darlow S. F. Unters. mit Röntgenstrahlen an Ammoniumbifluorid u. Monokaliummaleat. Angew. Chem. 69, 755.
68. Dejace J. Note sur la str. cr. de la chloroacetamide. Acta Cryst. 10, 240.
69. Diamond R. X-ray diffrn. data for large aromatic mols. Acta Cryst. 10, 359.
70. Dietrich H. von, Zahn H., and Schmidt F. Elementarzelle d. cycl. nylon-oligomeren 1,8, 15, 22-tetra-aza-2, 7, 16, 21-tetra-oxocyclo-octacosan. Acta Cryst. 10, 477.
71. Dietrich H. von, Zahn H., and Spoor H. Elementarzelle v. 1,8-diaza-cyclo-tetradecan. Acta Cryst. 10, 468.
72. Donohue J. Bifurcated H bonds a str. of cycloserine hydrochloride. Acta Cryst. 10, 333.
73. Dornberger-Schiff K. Zur OD-Str. (Order-Disorder str.) d. purpurogallin. Acta Cryst. 10, 271.
74. Dulmage W. J. Mol. a. cr. str. of cellulose triacetate. J. Polym. Sci. 26, 277.
75. Dunitz J. D. Cr. str. of Cu dipyridine dichloride a. violet form of Co dipyridine dichloride. Acta Cryst. 10, 307.
76. Edgell W. F., Kinsey P. A., and Amy J. W. Microwave spectra a. str. of $CF_2 = CH_2$, $CF_2 = CHD$ a. $CF_2 = CD_2$. J. Am. Chem. Soc. 79, 2691.
77. Ehrlich H. W. W. Refnt. of cr. a. mol. str. of acenaphthene. Acta Cryst. 10, 699.
78. Eichhorn E. L. Cis-beta-ionylidine crotonic acid. Konikl. Ned. Akad. Wetenschap., Proc., Ser. B, 60, 33.
79. Eichhorn E. L. Str. of trans 4,4'-azopyridine-N-oxide. Acta Cryst. 10, 795. (Abstracts . . .)
80. Eichhorn E. L. and Hoogsteen K. Some pyridine-N-oxide derivatives. Acta Cryst. 10, 382.
81. Eller H., von. Sur la str. de la forme cr. triel. du sélénо-indigo. Compt. rend., 244, 1041.
82. Eller H., von. Sur le polymorphisme de l'indigo. Acta Cryst. 10, 807. (Abstracts . . .)
83. Ermolina A. V., Markova G. S., and Kargin V. A. E. diffrn. investn. of polymers. IV. Study of changes in the str. of polytrifluorochloroethylene in the cr. melting range. Kristallografiya 2, 623.
84. Ezaki H., Owada K., and Noguchi S. Transn. de phases et str. des savons. J. Chem. Soc. Japan 60, 883 (Jap.)
85. Feilchenfeld H. Bond length a. bond energy in hydrocarbons. J. Phys. Chem. 61, 1133.
86. Fenoglio M. Relazioni cristallogr.- str. tra il difenile ed una serie di suoi nuovi derivati. Nuovo Cim. 5, 765; 6, suppl. 1, 449 (Ital.)
87. Ferrari A., Cavalca L., Cingi M., and Magnano G. Esacloroantimoniati di alchilammonio. Gazz. chim. ital. 87, 651 (Ital.
88. Ferrari A., Nardelli M., and Tani M. E. Relazioni str. fra uranilacetati ed uranil-propionati di metalli alcalini. Gazz. chim. ital. 87, 1203 (Ital.)
89. Fischer E. W. Übermolekulare Ordnn. in Polyamiden u. Polyäthylen. Physik. Verhandl. 8, 213.
90. Flachsbart I. Git-konst. u. Raumgruppe v. Salol. Naturwissenschaften 44, 348.
91. Font Altaba M. Estudio analitico por r. X de la mol. de retamina. I. Cristalografia de bromhidrato de retamina. Publ. dept. cryst. mineral., Madrid 3, 33.
92. Foss O. X-ray crystallogr. data on miscellaneous S. compds. Acta Chem. Scand. 11, 1442.
93. Foss O. and Johnsen J. Str. of formamidine disulphide. Acta Chem. Scand. 11, 189.
94. Foss O. and Reistad T. Str. of cr. racem-1, 2-dithiane-3,6-dicarboxylic acid. Acta Chem. Scand. 11, 1427.
95. Foss O. and Schotte L. U. ct. a. sp. grt. of some carboxylic acid derivatives of 1,2-dithiolane, 1,2-dithiane, 1,2-diselenane a. 1,2-dithiepane. Acta Chem. Scand. 11, 1424.
96. Foss O. and Tjomsland O. Str. of cr. 1,2-dithiolane-4-carboxylic acid. Acta Chem. Scand. 11, 1426.
97. Fraser R. D. B. and MacRae T. P. Evidence of regularities in chem. str. of α-keratins. Nature 179, 732.
98. Frey-Wyssling A. Macromols. in cell str. Nature 179, 941.
99. Furberg S. and Hordvik A. Cr. a. mol. str. of β-arabinose. Acta Chem. Scand. 11, 1594.
100. Gafner G., Herbstein F. H., and Wybenga F. T. Crystallogr. data for three trimethylsteroids. Acta Cryst. 10, 603.
101. Galli M. Studio cristallogr.-str. sull'ossima del cheticineolo. Period. Miner. 26, 39 (Ital.).
102. Gee M., Jones F. T., and McCready R. M. Synth. of p-biphenylyl-β-D-glycopyranosiduronic acid a. its opt. a. crystallogr. props. J. Org. Chem. 22, 471.

103. Giacomello G., Bertinotti F., Liquori A., and Hameka H. E. a. mol. str. of azines. XVI^eme Congr. Internat. Chimie pure et appl. II. Chimie org. Paris, 1957, 318.
104. Giacomello G., Liquori A. and Ripamonti A. Str. cr. dell' 1-5-naftiridina. Atti accad. nazl. Lincei, Rend., Classe sci. fis., mat. e nat. 22, 418 (Ital.)
105. Gillier H. Str. du violurate de Rb. Compt. rend. 244, 2812; Acta Cryst. 10, 797 (Abstracts . . .)
106. Glusker J. P. Some details of X-ray anal. of hexacarboxylic acid obtained from vitamin B_{12}. Acta Cryst. 10, 810. (Abstracts . . .)
107. Glusker J. P., Patterson A. L., Love W., and Dornberg M. L. Cr. str. of monopotassium a. monorubidium salts of lactone of naturally occurring isocitric acid. Program & Abstracts 15th Pittsburgh Diffrn. Conf. 6-8 Nov. 1957, 35.
108. Goedkoop J. A. and MacGillavry C. H. Cr. str. of malonic acid. Acta Cryst. 10, 125.
109. Grant D. F. Cr. str. of hydroxydihydroeremophilone. Acta Cryst. 10, 498.
110. Grant W. K., Vos A., and Speakman J. C. Cr. str. of 2 : 3-dihydro-2 : 3-methylene-1 : 4-naphthaquinone. Acta Cryst. 10, 806. (Abstracts . . .)
111. Guerreschi L. Sulla str. del parafenolsolfonato di Ni idrato $(C_6H_5SO_4)_2Ni \cdot 8H_2O$. Period. Miner., 26, 243 (Ital.)
112. Hahn T. Str. chars. of amino acids a. carboxylic acids. Z. Krist. 109, 438.
113. Hahn T. and Buerger M. J. Cr. str. of diglycine hydrochloride, $2(C_2H_5O_2N) \cdot HCl$. Z. Krist. 108, 419.
114. Haisa M. and Itami H. X-ray diffrn. study of polyvinyl alcoholiodine syst. J. Phys. Chem. 61, 817.
115. Hanson J., Lowy J., Huxley H. E., Bailey K., Kay C. M., and Ruegg J. C. Str. of molluscan tropomyosin. Nature 180, 1134.
116. Happey F. Alpha helix in natural a. synth. polypeptides. Nature 179, 194.
117. Hargreaves A. Cr. str. of Zn p-toluene sulphonate hexahydrate. Acta Cryst. 10, 191.
118. Hargreaves A. Application of isomorphous-replacement method in detn. of centrosymmetric strs. Acta Cryst. 10, 196.
119. Hargreaves A. and Watson H. C. X-ray a. phys. study of β-naphthol. Acta Cryst. 10, 368.
120. Harker D., King M. V., Pignataro E. H., Adelman M. B., and Furnas T. C., jr. Shape of ribonuclease mol. as deduced from nine cr. modifns. Acta Cryst. 10, 816. (Abstracts . . .)
121. Harris C. M. and Stephenson N. C. Sixcovalent Pt(II) complexes containing nitrides coordinates through C = N bond. Chem. and Ind. (London), 426.
122. Hassel O. Str. of addition compds., especially those in which halogens act as e.-acceptors. Proc. Chem. Soc., Sept., 250.
123. Hassel O. and Rømming C. Str. of 1 : 1 compd. pyridine-iodo monochloride. Erratum. Acta Chem. Scand. 11, 195.
124. Havinga E. E. Bijdrage tot the kennis van de str. van polyhalogeniden. Proefschrift, Groningen, 28 (Dutch)
125. Havinga E. E. Refnt of str. of tetramethylammonium pentaiodide determined by Hach a. Rundle. Proefschrift, Groningen, 48.
126. Herbstein F. H. and Schoening F. R. L. On centrosymmetric mols. in non-centrosymmetric sp. grs. Acta Cryst. 10, 657.
127. Hennodsson Y. and Strandberg B. Cr. data of Cu-glycylglycine. Acta Cryst. 10, 434.
128. Hess K. Suprastr. bei hochpolymeren Stoffen (Fasern). XVI^eme Congr. Internat. Chimie pure et appl. I. Chimie phys. Chimie minér. Paris 1957, 110.
129. Hess K., Steinmann R., Kussig H., and Avisiers I. Einlager. v. J. u. Tl in d. gitterungeordneten u. gittergeordneten Bereiche v. Zellulosefasern; e. Beitrag zur Reaktionsweise v. Zellulose. Kolloid-Z. 153, 128.
130. Hinch R. J., jr., Kre J., jr. Crystal-logr. data. 163. Tetra-p-biphenylsilane. Anal. Chem. 29, 1550.
131. Hirshfeld F. L. and Schmidt G. M. J. Cr. a. mol. strs. of heterocyclic compds. III. α-phenazine near 80°K. J. Chem. Phys. 26, 923.
132. Iizukuri S. and Nikuri Z. Etudes par diffrn. des r X des amidons. II. Str. des cristallites du type "C". J. Agric. Chem. Soc., Japan 31, 525 (Jap.)
133. Hodgkin D. C., Kamper J., Lindsey J., Mackay M., etc. Str. of vitamin B_{12}. I. Outline of crystallogr. investn. of vitamin B_{12}. Proc. Roy Soc., Ser A, 242, 228.
134. Hodgkin D. C. and Oughton B. M. Possible mol. models for gramicidin S a. their relnsh. to present ideas of protein str. Biochem. J., 65, 752.
135. Hodgkin D. C., Webster M. S., and Dunitz J. D. Str. of calciferol Chem. a. Ind. (London), 34, 1148.
136. Holtzer A. and Rice S. A. Some particle scatg. fs. for rods with inhomogeneous mass distribns. Applications to mol. configuration of myosin. J. Am. Chem. Soc. 79, 4847.

137. Honjo G. and Watanabe M. Study of cellulose fibre by low-temp. specimen method of e. diffm. a. e. micr. Acta Cryst. 10, 818 (Abstracts . . .)
138. Hoppe W. D. Orientier. d. aromat. Ringsyst. in Phyllochlorinester. Z. Krist. 108, 355.
139. Hoppe W. D. Faltmolekulmeth. u. ihre Anwend. in d. röntgenograph. Konstitutionsanalyse v. Biflorin ($C_{20}H_{20}O_4$). Z. Elektrochem. 61, 1076.
140. Hoppe W. and Baumgartner F. Nachweis d. Stäbchengestalt u. Orientier.-best. d. organ. Kations in 1,5,N–N'-Dipyrrolidylpentamethlinperchloratkristallen mit diffuser Röntgenstreustrahl. Z. Krist. 108, 328.
141. Housty J. and Clastre J. Str. cr. de la forme triel. du paradichlorobenzène. Acta Cryst. 10, 695.
142. Huber M. Str. de la 5'-Bromo-5'-de-oxythymidine. Acta Cryst. 10, 129.
143. Hulme R. and Powell H. M. Str. of compds. of ferrocyanide. J. Chem. Soc. 719.
144. Inoue M. and Tabata Y. Etudes au micr. é. de la str. cr. de l'indigo naturel. J. Chem. Soc. Japan 60, 700 (Jap.)
145. Ishibashi M., Suito E., and Sekido E. Etudes sur les précipités des chélates métalliques. II. Obsn. au micr. é. de l'oxinate cuivrique. III. Compn. de l'oxinate cuivrique. IV. Etude de l'oxinate cuivrique à l'aide de la diffrn. des r. X. J. Chem. Soc. Japan, Pure Chem. Sect. 78, 1784 (Jap.)
146. Iwasaki M., Nagase S., and Kojima R. Mol. str. of 1,2-difluoro-1,1,2,2-tetrachloroethane. Bull. Chem. Soc. Japan 30, 230.
147. Jagannadham A. V. Sp. gr. of 1,8-Dihydroxyanthraquinone, $C_{14}H_8O_4$. Z. Krist. 108, 457.
148. Jagdish S., Khubchandani P. G., and Padmanabhan V. M. Cr. str. of Mg acetatetetrahydrate $Mg(CH_3COO)_2 \cdot 4H_2O$. Proc. Indian Acad. Sci., A 45, 117.
149. Jellinek F. Str. of muscarine. Acta Cryst. 10, 277.
150. Jensen L. H., Krimm S., Parrish R. G., and Wood D. L. Cr. str. of NmN'-hexamethylenebispropionamide. Acta Cryst. 10, 528.
151. Jerslev B. Cr. str. of oximes. Nature, 180, 1410.
152. Kag M. I. and Katz L. Cr. str. of α-Pimelic acid. Program & Abstracts 15th Pittsburgh Diffrn. Conf. 6-8 Nov. 1957, 34.
153. Karle I. L. Application of probability methods to p,p'-dimethoxybenzophenone. Acta Cryst. 10, 754 (Abstracts . . .)
154. Karle I. L., Hauptman H., Karle J., and Wing A. B. Cr. a. mol. str. of p,p'-dimethoxybenzophenone by direct probability method. Acta Cryst. 10, 481.
155. Katayama M. Polymorphism of chloroacetamide. Acta Cryst. 10, 468.
156. Kehl W. L. and Jeffrey G. A. Str. of 4-methyl 1-2 dithia-4-cyclopentene-3-thione. Acta Cryst. 10, 807 (Abstracts . . .)
157. Kehren M. and Rösch M. Röntgenograph. Unterss. an wasserfreien u. wasserhalt. Alkylpolyäthylenoxyden. I Literaturübersicht. II. Eigene Unterss. Fette Seifen, Anstrichmittel 59, 1; 80.
158. Kehren M. and Rösh M. Uber e. Feinstr.- syst. monosubstituierter Polyaethylenoxydderivate. Melliand Textilber. Dtsch. 38, 96.
159. Keller A. Note on single crs. in polymers; evidence for folded chain configuration. Phil. Mag. 2, 1171.
160. Keller A. and Maradudin A. Diffrn. of X-rays by fibres consisting of small crs.: application of theory to polyamides. Phys. and Chem. Solids 2, 301.
161. Keller A. and O'Connor A. Large periods in polyethylene: origin of low-angle X-ray scatrg. Nature 180, 1289.
162. Kendrew J. C. and Perutz M. F. X-ray studies of compds of biological interest. Ann. Rev. Biochem. 26, 327.
163. Khotsyanova T. L. Cr. strs. of diphenyliodonium halides. Kristallografiya, 2, 51.
164. Khotsyanova T. L. and Struchkov Yu. T. Cr. strs. of diphenylhalogenonium compds. Kristallografiya, 2, 384.
165. Khocjanova T. L. and Struckov J. T. Cr. str. of diphenylhalogenonium compds. Acta Cryst. 10, 796. (Abstracts . . .)
166. Kiessig H. D. Bedeut. v. Langperiodeninterferenzen für d. Str. v. Hochpolymeren. Angew. Chem. 68, 468.
167. Kiessig H. D. röntgenograph. Untress d. grossen Periode bei Cellulose. Angew. Chem. 69, 619; Papier, Das 11, 355.
168. Kilb R. W. and Pierce L. Microwave spectrum str., a. internal barrier of methyl silane. J. Chem. Phys. 27, 108.
169. Kimura K., Suzuki S., Kimura M., and Kubo M. Mol. str. of tropone. Phys. Rev. 27, 320.
170. Kitaigorodskii A. I. Conditions for formn. of solid solns. of org. compds. Dokl. AN SSSR 113, 604.
171. Klug A. and Finch J. T. X-ray studies on turnip yellow mosaic virus (TYMV). Acta Cryst. 10, 817 (Abstracts...)
172. Klug A., Finch J. T., and Franklin R. E. Str. of turnip yellow mosaic virus. Nature 179, 683.
173. Kolde T., Oda T., and Nitta I. On cr. str. of 2,2-dichloro-3,3-dimethylbutane. Bull. Chem. Soc. Japan 30, 198.

174. Koide T., Takeuchi S., Oda T., Yamada I., and Taguchi I. X-ray study on cr. str. of 2-chloro-2,3,3-trimethylbutane. Bull. Chem. Soc. Japan 30, 680.
175. Kooiman F. and Kreger D. R. X-ray obsns. on Tamarindus amyloid. Biochim. Biophys. Acta 26, 207.
176. Kratky O., Sekora A., and Breiner R. Röntgenograph. Studien zur Übermolekularen Str. v. Vinyon N, Makromol. Chem. 22, 115.
177. Krishna Murti G. S. R. Cr. str. of diphenyl at different temps. Indian J. Phys. 31, 1.
178. Krishna Murti G. S. R. Cr. str. of p-nitroaniline at different temps. Indian J. Phys. 31, 353.
179. Krishna Murti G. S. R. Cr. str. of anthranilic acid at different temps. Indian J. Phys. 31, 611.
180. Kruse F. H., Marsh R. E., McCullough J. D. Cr. str. of p, p'-dichlorodiphenyl diselenide a. p,p'-dichlorodiphenyl ditelluride. Acta Cryst. 10, 201.
181. Kuchitsu K. E. diffrn. investn. of mol. str. of 1,4-dichlorobutyne. I. Detn. of bond distances a. angles. II. Study of internal rotation by use of halos in small angle region. Bull. Chem. Soc. Japan, 30, 391; 399.
182. Kurdyumov G. M. and Semenenko K. N. Some props. of Be hydroxybenzoate. Vestn. Mosk. Univ. Ser. mat., mekh., astr., fiz., khim. 3, 265.
183. Kurland R. J. and Wilson E. B., jr. Microwave spectrum, str., dipole moment, a. quadrupole coupling consts. of formamide. J. Chem. Phys. 27, 585.
184. Kuroda K. Etude aux r. X des systs. binaires des mélanges d'amides gras. J. Chem. Soc. Japan 78, 239. (Jap.)
185. Labaw L. W. and Wyckoff R. W. G. Mol. striae from an indanthuene dye. Proc. Nat. Acad. Sci. U. S. 34, 1052.
186. Langridge R. et al. Mol. str. of deoxyribonucleic acid (DNA). J. Biophys. Biochem. Cytol., 3, 767.
187. Laurent T. C. I. On hydration of macromolecules. X-ray diffrn. studies on aqueous solns. of hyaluronic acid. II. Amorphous X-ray diffractogram of hyaluronic acid. Ark. Kemi. 11, 503; 513.
188. Legrand C. and Yovanovitch O. Etude radiocrist. de l'influence de l'eau sur la str. de divers amidons. Compt. rend. 245, 1553.
189. Lennox D. H. X-ray powder diffrn. pats. of some org. compds. Anal. Chem. 29, 1433.
190. Lerner R. G. and Dailey B. P. Microwave spectrum a. str. of propionitrile. J. Chem. Phys. 26, 678.
191. Lerner R. G., Dailey B. P., and Friend J. P. Microwave spectrum a. str. of formic acid. J. Chem. Phys. 26, 680.
192. Leung Y. C. and Marsh R. E. Cr. str. of L-leucyl-L-prolyl-glycine. Acta Cryst. 10, 815.
193. Lide D. R., jr. Str. of methylamine mol. I. Microwave spectrum of $CDND_2$. J. Chem. Phys. 27, 343.
194. Lingafelter E. C., Breazeale J. D., and Stewart J. M. Salicylaldehyde a. salicyldimine complexes of Cu (II) a. Ni (II) Acta Cryst. 10, 785. (Abstracts. . .)
195. Liquori A. M. Su alcune questioni riguardanti angoli e distanze di legame nelle mol. org. Nuovo Cim., 6, suppl. 1, 455 (Ital.)
196. Luzzati V. and Mustacchi H. Str. des stases mésomorphes d'un syst. binaire savon-eau. Acta Cryst. 10, 828. (Abstracts . . .)
197. Luzzati V., Mustacchi H., and Skoulios A. Etude de la str. des différentes phases des systs. savon-solvant polaire et savon-solvant nonpolaire. XVI^ème Congr. internat. Chimie pure et appl. I. Chimie phys. Chimie minér., Paris, 1957, 118.
198. Luzzati V., Mustacchi H., and Skoulios A. Str. of liquid-cr. phases of soap-water syst.: middle soap a. neat soap. Nature, 180, 600.
199. McCullough J. D., Bauer R. S., and Jacobs T. L. X-ray diffrn. study of polytetrafluoroallene. Chem. a. Ind. (London), 22, 706.
200. Malinovskii T. I. X-ray str. investn. of Co diparatoluidine dichloride. Kristallografiya 2, 734.
201. Mann D. E. and Lide D. R. Microwave spectrum of trimethylamine. Bull. Am. Phys. Soc. 2, 212.
202. Marsh R. E. Refnt. of cr. str. of glycine Acta Cryst. 10, 814. (Abstracts . . .)
203. Mason R. Mol. str. a. carcinogenic activity of 1,2 : 8,9 dibenzacridine. Nature 179, 465.
204. Mathieson A. McL. Simple adapter for rotation cameras to improve accuracy of measrt. of identity periods. Acta Cryst. 10, 351.
205. Mazzi F. and Garavelli C. La str. della oxalite $FeC_2O_4 \cdot 2H_2O$. Period. Miner. 26, 269.
206. Mazzi F., Jona F., and Pepinsky R. Preliminary X-ray study of non-ferroelectric phases of rochelle salt. Z. Krist. 108, 359.
207. Miksić M. G., Segerman E., and Post B. Str. transformn. of dimethyl acetylene at −120°C. Program & Abstracts 15th Pittsburgh Diffrn. Conf. 6-8 Nov. 1957, 53.
208. Millionova M. I. and Andreeva N. S. Diffraction pat. of collagen. Biofizika 2, 43.
209. Millionova M. I. and Andreeva N. S. Str. of mol. chains of collagen Biofizika 2, 294.

210. Milone M. and Borello E. Sulla str. della gliossima allo stato solido. Nuovo Cim. 5, 562; 6, Suppl. 1, 468 (Ital.)
211. Mitra G. B., Mitra S. K., and Basak M. G. X-ray diffrn. study of α-yohimbine $C_{21}H_{26}O_3N_2$. Z. Krist. 108, 385.
212. Murty B. V. R. At. form-f. curves for C a. O of > C = O bond of anthraquinone (25–35°C). Acta Cryst. 10, 146.
213. Nakatsu K., Shiro M., Saito Y., and Kuroya I. Studies on crs. of met. trisethylene-diamine-complexes. II. Cr. str. of Na D-tris-ethylene-diamine-Co(III) chloride hexahydrate 2D-[Co en 3] Cl_3 · NaCl. $6H_2O$. Bull. Chem. Soc. Japan 30, 158.
214. Nardelli M., Fraibanti A., Chierici I. Complessi fra cloruri di metalli bivalenti ed urea. Gazz. chim. ital. 87, 1226 (Ital.)
215. Nardelli M. and Chierici I. Complessi fra cloruri di metalli bivalenti e tioacetamide. Gazz. chim. ital. 87, 1478 (Ital.)
216. Natta G. and Corradini C. Application des r. X pour l'etude de la str. et compn. stéréoisomérique des polymères vinyliques concernant leurs props. technologiques Colloq. sur les bases scientifiques des essais relatifs aux élastomeres, aux fibres et aux plastiques, July 1957.
217. Natta G., Corradini P., and Cesari M. Determinazione quant della cristallinità del polipropilene. Atti accad. nazl. Lincei, Rend., Classe sci. fis., mat. e nat. 22, 11 (Ital.)
218. Nechitailo N. A. and Ravich G. B. Phase trans. in normal paraffin hydrocarbons with long chains. Uspekhi khimii 26, 640.
219. Nilsson M., Ryhage R., and Sydow E. von. Constituens of pollen II. Long-chain hydrocarbons a. alcohols. Acta Chem. Scand. 11, 634.
220. Noether H. D. X-ray diffrn. pat. a. u. c. dims. of some polymethylene sulfones. J. Polym. Sci. 25, 217.
221. Nowacki W., Bürki H., Bonsma G. F., and Jaggi H. Direkte Kristall-u. Molekülstr.-best. v. 7α-Bromcholesterylbromid, d. Alkaloids Erythralin-Hydrobromid u. d. Phthalsäure. Acta Cryst. 10, 809. (Abstracts...)
222. Nowacki W. and Jaggi H. D. Kr.-str. d. Phthalsäure, $C_6H_4(COOH)_2$. Z. Krist. 109, 272.
223. Nyburg S. G. and Hilton J. Cyclooctatetraene dimer, M. Pt. 38.5°; cr. mol. str. of Ag nitrate adduct. Chem. & Ind. (London), 31, 1072.
224. O'Connor R. T., Mod R. R., Murray M. D., Magne F. C., and Skau E. L. X-ray diffrn. of mol. compds. of long-chain saturated fatty acids. II. Some further obsns. on diffrn. of mol. compds. of acetamide a. long-chain saturated fatty acids. J. Am. Chem. Soc. 79, 5129.
225. Ohlberg S. M. and Scott S. C. Detn of glass trans. temp. of polythene by X-ray diffrn. Program & Abstracts 15th Pittsburgh Diffrn. Conf. 6-8 Nov. 1957, 12.
226. Okaya Y., Ahmed M. S., Pepinsky R., and Vand V. X-ray crystallogr. study of room temp. modifn. of monomethylammonium Al sulfate alum, (CH_3NH_3)-$[Al(H_2O)_6]$ $(SO_4)_2$ · $6H_2O$ · Z. Krist. 109, 367.
227. Okaya Y. and Pepinsky R. Cr. str. of triaminoguanidinium chloride$(NH_2$·$NH)_3C$·Cl. Acta Cryst. 10, 681.
228. Okaya Y. and Pepinsky R. X-ray crystallogr. of lycomarasmin Cu salt. Acta Cryst. 10, 138.
229. Okaya Y. and Pepinsky R. Cr. str. of ammonium acid phthalate. Acta Cryst. 10, 324.
230. Okaya Y., Pepinsky R., Takeuchi Y., Kurova H., Shimada A., Gallitelli P., Stemple N., Beevers A. X-ray anal. of some complex-ion strs. Acta Cryst. 10, 708 (Abstracts...)
231. Okuda T. and Price C. C. Polymorphic forms of 2-methylthio-4-amino-5-hydroxymethylpyrimidine. J. Org. Chem. 22, 1719.
232. Orgel L. E. and Dunitz J. D. Stereochem. of cupric compds. Nature 179, 462.
233. Oughton B. M. and Harrison P. M. Cr. str. of hex. L-cystine. Acta Cryst. 10, 479.
234. Parker K. D. and Rudall K. M. Silk of egg-stalk of green lace-wing fly. Str. of silk of chrysopa egg-stalks. Nature 179, 905.
235. Parsons J., Beher W. T., and Baker G. D. Steroid X-ray diffrn. powd. data. Anal. Chem. 29, 762.
236. Penco A. M. Ricerche cristallogr., ottiche e röntgenografiche sull'amide dell'acido carfen-1-carbonico. Period. Miner. 26, 12 (Ital.)
237. Pepinsky R. Some new X-ray a. n. studies of H bonding. "Simpozij o vodikovi vezi. Ljubljana, 1957." Ljubljana, Tiskarna "Toneta Tomsica."
238. Pepinsky R., Okaya Y., Eastman D. P., and Mitsui T. Ferro-electricity in glycine Ag nitrate. Phys. Rev. 107, 1538.
239. Pepinsky R., Okaya Y., and Mitsui T. Ferro-electricity in ammonium monochloroacetate. Acta Cryst. 10, 600.
240. Pepinsky R. et al. X-ray anals. of some biochem. important compds. Acta Cryst. 10, 811. (Abstracts ...)
241. Peterson J., Steinrauf L. K., and Jensen L. H. Cr. str. of L-cystine hydrochloride. Acta Cryst. 10, 814. (Abstracts...

242. Petitpas T. and Oberlin M. Str. de la cellulose II. Acta Cryst. 10, 818. (Abstracts...)
243. Petitpas T., Oberlin M., and Mering J. Chaine mol. de la cellulose II. Compt. rend. 244, 346.
244. Phillips D. C. and Ahmed F. R. Crystallogr. of acridine III. Str. of acridine II. Acta Cryst. 10, 809. (Abstracts...)
245. Poraj-Kojic M. A., Antzishkina A. S., Dickareva L. M., and Jukhno E. K. At.cr. str. of complex acido-amine Ni compds. Acta Cryst. 10, 784 (Abstracts...)
246. Prietzschk A. D. Kr-str. d. Polycarbonates aus 4,4'-Dioxydiphenyl-2,2-propan. Angew. Chem. 69, 269.
247. Przybylska M. and Marion L. Cr. a. mol. str. of annotinine bromohydrin. Canad J. Chem. 35, 1075.
248. Ramachadran G. N. and Santhanam M. S. Str. of elastin. Proc. Indian Acad. Sci. A 45, 124.
249. Ray L. Preliminary single-cr. X-ray a. opt. study of nor-harman, $C_{11}H_8N_2$. Acta Cryst. 10, 707.
250. Ray L. Sp. gr. a. u. c. of harmine, $C_{13}H_{14}ON_2$. Z. Krist. 108, 459.
251. Rérat C. Radiocristallographie. Etude radiocrist. du chlorhydrate de triméthylaminoxide. Compt. rend. 245, 704.
252. Rivett D. E. A. and Herbstein F. H. Revised mol. formulae for cucurbitacins. Chem. & Ind. (London), 393.
253. Robertson J. M., Rossmann M. G., and Trotter J. Str. of some higher condensed-ring hydrocarbons. Acta Cryst. 10, 803. (Abstracts...)
254. Robinson C. and Ward J. C. Liquid-cr. str. in polypeptides. Nature 180, 1183.
255. Roe D. A. and Heyn A. N. J. X-ray diffrn. pats. a. alpha-beta transformn. of protein extracted from human epidermis. Nature 179, 266.
256. Rolsten R. F. and Sisler H. H. X-ray a. infrared studies of addition compds of Ti tetrabromide with 1,4-dioxane, tetrahydrofuran a. tetrahydropyran. J. Am. Chem. Soc. 79, 1819.
257. Romain P. Contribution a l'etude de la str. de l'antipyrine: str. de la bromoantipyrine par les r. X (I). Bull. soc. chim. France 11-12, 1417.
258. Romers C., Shoemaker C. B., and Fischmann E. Studies on tautomerism. VI. Preliminary communication on mol. str. of α-3-methyl-6-chloroquinone-4-oxime a 3-chloroquinone-4-oxime in solid phase. Rec. trav. chim. Pays-Bas 76, 490.
259. Rose H. A. and Van Camp A. Note on crystallogr. of carbutamide (BZ-55). J. Am. Pharm. Assoc. Sci. Ed. 46, 452.
260. Rouault M. and Waziutynska Z. L. Str. de la mol de fulvène par diffrn. des électrons. Ann. Acfas 23, 112; Acta Cryst. 10, 804. (Abstracts...)
261. Rouault M. and St.-Arnaud C. Str. de la mol. $CH_2 = CH - C \equiv N$ par diffrn. des électrons. Canad. J. Phys. 35, 503.
262. Rundle R. E. and Corbett J. D. Concerning symmetry of benzenepositive ion complexes; unpositive third gr. ions. J. Am. Chem. Soc. 79, 757.
263. Ryhage R., Stenhagen E., and Sydow E. von. Mass spectrometric detn. of str. of phthiocerol. Acta Chem. Scand. 11, 180
264. Saito Y., Nakatsu K., Shiro M., and Kuroya H. Studies on crs. of met. trisethylenediamine complexes. III. Detn. of absolute configuration of opt. active complex ion $[Co\ en_3]^{3+}$ by means of X-rays. Bull. Chem. Soc. Japan 30, 795.
265. Sasada Y. and Nitta I. Cr. str. of 1-oxaazulan-2-one. Acta Cryst. 10, 806. (Abstracts...)
266. Sasada Y. and Nitta I. Refnt. of cr. str. of tropolone hydrochloride. Bull. Chem. Soc. Japan 30, 62.
267. Sasisekharan V. and Ramachadran G. N. Studies on collagen. II. Cylindrical lat. str. of collagen. Proc. Indian. Acad. Sci., A 45, 363.
268. Schmidt G. M. J., Hodgkin D. C., and Oughton B. M. Crystallogr. study of some derivatives of gramicidin S. Biochem. J. 65, 744.
269. Segal L. and Conrad C. M. Char. of cellulose derivatives by means of X-ray diffractometer. Am. Dyestuff Reptr., August, 1.
270. Sekino S. and Nishikawa T. Microwave spectrum of vinylidene chloride. J. Phys. Soc. Japan 12, 43.
271. Shearer H. M. M. and Robertson J. M. Str. of azulene. Acta Cryst. 10, 805. (Abstracts...)
272. Sheridan J. Mol. consts. a. str. of methyl cyanoacetylene from microwave spectra. Kurzreferate d. Vorträge auf d. Internat. Tag. d. Europ. Molekülspektroskopiker. Freiburg im Breisgau, 1957, 1.
273. Shibata I. Studies on mol. str. of bisacetylacetone-Ni (II) by e. diffrn. Bull. Chem. Soc. Japan 30, 753.
274. Shibata I. Studies on str. of bisacetylacetone-Ni (II) by X-ray powd. method Bull. Chem. Soc. Japan 30, 842.
275. Shintani R. and Nitta I. Cr. str. of diacetylhydrazine. Acta Cryst. 10, 795. (Abstracts...)
276. Shino R., Cruickshank D. W. J., and Cox E. G. Refnt. of cr. str. of pentaerythritol. Acta Cryst. 10, 794. (Abstracts...)

277. Sime J. G. and Abrahams S. C. Cr. str. of 4,4'-dichlorodiphenyl sulphone. Acta Cryst. 10, 807.
278. Simonsen S. H. and Pfluger C. E. U. c. dims. a. sp. grs. of Ni (II), Cu(II), a. Pd(II) salicylimines. Acta Cryst. 10, 471.
279. Simonsen S. H. and Pfluger C. E. Str. of 5-chlorosalicylaldoxime. Acta Cryst. 10, 473.
280. Simonsen S. H. and Pfluger C. E. U. c. dims. a. sp. grs. of Ni(II) a. Pd(II) 5-chlorosalicylaldoximates. Acta Cryst. 10, 536.
281. Skertchly A. R. B. Rapid obsn. of phase transformns in fibrous proteins using X-ray diffractometer. Nature 180, 802.
282. Smith A. E. Str. of stable ord. phases in mixed paraffins a. their reln to str. of pure n-paraffins. Acta Cryst. 10, 802. (Abstracts...)
283. Sobue H. and Mirato H. Str. fine de la cellulose étudiée par anal. aux r. X. J. Chem. Soc. Japan 60, 327. (Jap.)
284. Srivastava S. N. Sp. gr. of anthrone. Indian J. Phys. 31, 644.
285. Stora C. Str. et halochromie du bromure de triphénylméthyle. Compt. rend. 245, 1626.
286. Stora C. Ebauche de la str. du triphenylmethane Br. $(C_6H_5)_3C_3$-Br. Acta Cryst. 10, 797. (Abstracts...)
287. Struchkov Yu. T. X-ray str. investn. of heteroorganic compds. Stereochemistry of ferrocene and its derivatives. Zh. obshch. khim. 27, 2034.
288. Struchkov Yu. T. and Khotsyanova T. L. X-ray diffrn. investn. of crt. of some ferrocene derivatives. Kristallografiya 2, 382.
289. Struckov J. T. and Khocjanova T. L. X-ray investn. of crs. of some ferrocene derivatives. Acta Cryst. 10, 796. (Abstracts...)
290. Suito E. and Sekido E. Dimosphism a. cr. habits of Cu-oxinate precipitates. Proc. Japan Acad. 33, 196.
291. Sundaramma K., Vedam K., and Sundara Rao R. V. G. Preliminary report on str. of dibariumcupricformate. Current Sci. (India) 26, 315.
292. Sundara Rao R. V. G., Turley J. W., and Pepinsky R. Cr. str. of urea phosphate. Acta Cryst. 10, 435.
293. Sutor D. J. Cr. str. of caffeine a. theophyline. Acta Cryst. 10, 808. (Abstracts...)
294. Swalen J. D. Microwave spectra of acetone. Spectrochim. Acta 10, 229.
295. Sydow E. von. Molekylpackningen hos (−)-2-metyl-2-etyl-eikosansyra. Svensk. Kem. Tidskr. 69, 402. (Dutch).
296. Sydow E. von, Abrahamsson S., and Aleby S. Cr. str. of some long-chain compds. Acta Cryst. 10, 801. (Abstracts...)
297. Takeuchi Y. and Pepinsky R. Cr. str. of pyridinium reineckate. Z. Krist. 109, 29. Korrektion: Z. Krist. 110, 474, 1958.
298. Takeuchi Y. and Saito Y. Str. of reineckate complex ion. Bull. Chem. Soc. Japan 30, 319.
299. Tashpulatov Yu., Zvonkova Z. V., and Zhdanov G. S. X-ray str. investn. of Captax (2-mercaptobenzothiazole). Kristallografiya 2, 38.
300. Teare P. W. and Holmes D. R. Extra refls in X-ray diffrn pat of polyethylenes a. polymethylenes. J. Polym. Sci. 24, 496.
301. Thomas L. F., Heeks J. S., and Sheridan J. Microwave spectra of some mols containing $-CF_3$ a. $-SiF_3$ grs. Z. Electrochem. 61, 935.
302. Toussaint J. Etude radiocrist. du syst. $\underbrace{X-C_6H_4-C(=Y)-C_6H_4}$ avec X = (O,S), Y = (O,S). Bull. soc. roy. sci. Liége 26, 77.
303. Toussaint J. Strs. ordonnées et désordonnées par la trithioformaldéhyde. Bull. soc. roy. sci. Liége 26, 73.
304. Tramer A. and Wierzchowski K. L. Str. of carbonyl cyanide. Bull. acad. polon. sci., III, 5, 417.
305. Traub W., Hutchinson J. B., and Daniels D. G. H. X-ray studies of wheat protein complex. Nature 179, 769.
306. Trillat J.−J., Barbezat S., and Jacquot A. Etude aux r. X du polymorphisme des savons de Pb et de Cu par la méthode du cylindre tangent rotatif. Bull. soc. franc. mineral et crist. 80, 67.
307. Truter M. R. Co-ordination complexes involving ligands containing S. Acta Cryst. 10, 785. (Abstracts...)
308. Tsoucaris G. Radiocristallographie. Etude radiocrist. du chlorhydrate de pyridinoxyde. Compt. rend. 245, 703.
309. Turley J. W., Okaya Y., Vand V., and Pepinsky R. X-ray anal. of miscellaneous org. str. Acta Cryst. 10, 813. (Abstracts...)
310. Turley J. W. and Pepinsky R. Further refnt of cr. str. of cycloserine hydrochloride. Acta Cryst. 10, 480.
311. Ukaji T. Study on mol. str. of acrylylchloride by e. diffrn. Bull. Chem. Soc. Japan 30, 737.
312. Van Camp A. and Pfeiffer R. Note on crystallogr. a. X-ray diffrn. data for ethinamate. J. Am. Pharm. Assoc. Sci. Ed. 46, 571.
313. Van Camp A. and Rose H. A. Note on crystallogr. of alstonidine. J. Am. Pharm. Assoc., Sci. Ed. 46, 509.

314. Volarovich M. P. and Gusev K. F. Comparative x-ray str. investns. of peat, lignites, and sapropels. Tr. Mosk. torfyanogo Inst., No. 5, 3.
315. Wagner R., Fine J., Simmnons J. W., and Goldstein J. H. Microwave spectrum, str. a. dipole moment of "s-trans" acrolein. J. Chem. Phys. 26, 634.
316. Wallwork S. C. and Powell H. M. Cr. str. of phloroglucinol dihydrate. Acta Cryst. 10, 48.
317. Watase H. and Nitta I. Str. of kainic acid, most active component of digenea simplex Ag. I. Mol. a. cr. str. of Zn kainate dihydrate. Bull. Chem. Soc. Japan 30, 869.
318. Watase H., Osaki K., and Nitta I. Cr. str. of monocl. form of naphthazarin. Bull. Chem. Soc. Japan 30, 532.
319. Weiss A. and Weill'A. Str. u. Eigg. v. Gallerten einiger quecksilberorgan. Verbb. XVI^{eme} Congr. internat. Chimie pure et appl. I. Chimie phys. Chimie minér. Paris 1957, 118.
320. Wheatley P. J. Cr. a. mol. str. of pyrazine. Acta Cryst. 10, 182.
321. Williams P. P. Unstable modifn of aprobarbital. Nature 179, 1189.
322. Williams R. C. and Smith K. M. Crystallizable insect virus. Nature 179, 119.
323. Wilson F. C. and Shoemaker D. P. Mol. str. of bis-(cyclopentadienyl Mo tricarbonyl). J. Chem. Phys. 27, 809; Acta Cryst. 10, 783. (Abstracts...)
324. Witnauer L. P., Lutz D. A., Sasin G. S., and Sasin R. X-ray diffrn. powd. data of some thiol esters of long chain fatty acids. J. Am. Oil Chemists' Soc. 34, 71.
325. Wolf L. von and Baringhausen H. Uber Kr.-str.-unterss. an Th-tetrakis-(dibenzoylmethan). Chem. Tech. (Berlin) 9, 306.
326. Wolf L. von and Baringhausen H. Kristalldaten v. Th-tetrakis-(dibenzoylmethan) u. d. isomorphen Komplexen d. vierwert. Cr u. U. Acta Cryst. 10, 605.
327. Wolff P. M. de. On detn. of u. c. dims. from powd. diffrn. pats. Acta Cryst. 10, 590.
328. Wood E. A. and Holden A. N. Monocl. glycine sulfate: crystallogr. data. Acta Cryst. 10, 145.
329. Woolfson M. M. Efficient process for solving cr. str. by sign relnshs. Acta Cryst. 10, 116.
330. Worsham J. E. Jr., Levy H. A., and Peterson S. W. Positions of H atoms in urea by n. diffrn. Acta Cryst. 10, 319.
331. Wyckoff R. W. G., Bear R. S., Morgan R. S., and Carlstrom D. Opt. diffractometer for facilitation of X-ray diffrn. studies of macromol. strs. J. Opt. Soc. Am. 47, 1061.
332. Yokoi M. E. diffrn. investn. on mol. strs of some organosilicon compds. Bull. Chem. Soc. Japan 30, 100.
333. Zahn H. Grosse Ringe in Polyamiden. Angew. Chem. 69, 270.
334. Zalkin A. Cr. str. of tetra-n-propyl ammonium bromide. Acta Cryst. 10, 557.
335. Zaslov B. and Rundle R. E. Cr. str. of tetraphenylarsonium tetrachloroferrate (III) $(C_6H_5)_4AsFeCl_4$. J. Phys. Chem. 61, 270.
336. Zeil W. and Perommer J. F. Mikrowellenspektroskop. Messungen zur Kenntnis d. C−C-Abstandes in Gruppe $\geq C-C \equiv N$ v. Nitrilen. Z. Elektrochem. 61, 490.
337. Zubenko V. V. and Umanskii M. M. X-ray diffrn. detn. of thermal expan. of single crs. Kristallografiya 2, 508.
338. Zvonkova Z. V. Cr.-chem. investn. of the str. of some complex compds. Kristallografiya 2, 408.

CORRECTION

The third paragraph and scheme on p. 226 (Zh. strukt. khimii, 2, 2) should read as follows:

1) The latest work on the first of these problems, involving structural investigations of the compounds K[Pt(C_2H_4)Br_3]·H_2O [46], m cis-[Pt(C_2H_4)NH_3Br_2] [48], trans-[Pt($P(C_2H_5)_3$)$_2$BrH] [69], α-[$Pt_2(SCN)_2Cl_2(P(C_2H_7)_3)_2$] [70], provide data accurate enough to allow discussion of the relation between the Pt–ligand distance and the trans influence effect. The results (configuration of the complexes) and the most important distances in A are shown schematically below:

Compounds	Structure of complex and distances	Literature references
K[$PtC_2H_4Br_3$]·H_2O	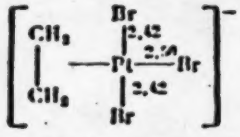	[46]
cis-[$PtC_2H_4NH_3Br_2$]	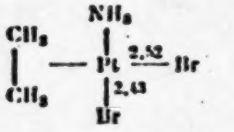	[48]
trans-[$Pt((C_2H_5)_3P)_2HBr$]	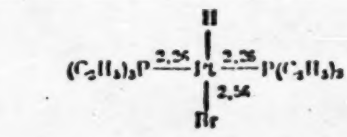	[69]
α-[$Pt_2(SCN)_2Cl_2((C_2H_5)_3P)_2$]	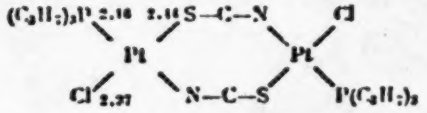	[70]

Soviet Journals Available in Cover-to-Cover Translation

ABBREVIATION	RUSSIAN TITLE	TITLE OF TRANSLATION	PUBLISHER	TRANSLATION BEGAN Vol.	Issue	Year
AÉ	Atomnaya énergiya	Soviet Journal of Atomic Energy	Consultants Bureau	1	1	1956
Akust. zh.	Akusticheskii zhurnal	Soviet Physics – Acoustics	American Institute of Physics	1	1	1955
	Antibiotiki	Antibiotics	Consultants Bureau	4	1	1959
Astr(on). zh(urn).	Astronomicheskii zhurnal	Soviet Astronomy–AJ	American Institute of Physics	34	1	1957
Avtom(at). svarka	Avtomaticheskaya svarka	Automatic Welding	British Welding Research Association (London)		1	1955
	Avtomatika i Telemekhanika	Automation and Remote Control	Instrument Society of America	27	1	1956
	Biofizika	Biophysics	National Institutes of Health*		1	1957
	Biokhimiya	Biochemistry	Consultants Bureau	21	1	1956
Byull. éksp(erim). biol. i med.	Byulleten' éksperimental'noi biologii i meditsiny	Bulletin of Experimental Biology and Medicine	Consultants Bureau	41	1	1959
DAN (SSSR) / Dokl(ady) AN SSSR	Doklady Akademii Nauk SSSR	The translation of this journal is published in sections, as follows:				
Life Sciences		Doklady Biochemistry Section	American Institute of Biological Sciences	106	1	1956
Life Sciences		Doklady Biological Sciences Sections (includes: Anatomy, biophysics, cytology, ecology, embryology, endocrinology, evolutionary morphology, genetics, histology, hydrobiology microbiology, morphology, parasitology, physiology, zoology sections)	American Institute of Biological Sciences	112	1	1957
Life Sciences		Doklady Botanical Sciences Sections (includes: Botany, phytopathology, plant anatomy, plant ecology, plant embryology, plant physiology, plant morphology sections)	American Institute of Biological Sciences	112	1	1957
Chemical Sciences		Proceedings of the Academy of Sciences of the USSR, Section: Chemical Technology	Consultants Bureau	106	1	1956
Chemical Sciences		Proceedings of the Academy of Sciences of the USSR, Section: Chemistry	Consultants Bureau	106	1	1956
Chemical Sciences		Proceedings of the Academy of Sciences of the USSR, Section: Physical Chemistry	Consultants Bureau	112	1	1957
Earth Sciences		Doklady Earth Sciences Sections (includes: Geochemistry, geology, geophysics, hydrogeology, mineralogy, paleontology, petrography, permafrost sections)	American Geological Institute	124	1	1959
Earth Sciences		Proceedings of the Academy of Sciences of the USSR, Section: Geochemistry	Consultants Bureau	106-123	1	1957-1958
Earth Sciences		Proceedings of the Academy of Sciences of the USSR, Sections: Geology	Consultants Bureau	106-123	1	1957-1958
Mathematics		Doklady Soviet Mathematics	The American Mathematics Society	131	1	1961
Physics		Soviet Physics–Doklady (includes: Aerodynamics, astronomy, crystallography, cybernetics and control theory, electrical engineering, energetics, fluid mechanics, heat engineering, hydraulics, mathematical physics, mechanics, physics, technical physics, theory of elasticity sections)	American Institute of Physics	106	1	1956
Physics		Proceedings of the Academy of Sciences of the USSR, Applied Physics Sections (does not include mathematical physics or physics sections)	Consultants Bureau	106-117	1	1956-1957
Derevoobrabot. prom-st'.	Derevoobrabatyvayushchaya promyshlennost'	Wood Processing Industry	Timber Development Association (London)		9	1959
Élektrosvyaz	Élektrosvyaz	Telecommunications	Massachusetts Institute of Technology*		1	1957
Entom(ol. obozr(enie)	Entomologicheskoe obozrenie	Entomological Review	American Institute of Biological Sciences	38	1	1959
Farmakol. (i) toksikol(ogiya)	Farmakologiya i toksikologiya	Pharmacology and Toxicology	Consultants Bureau	20	1	1957
FMM	Fizika metallov i metallovedenie	Physics of Metals and Metallography	Acta Metallurgica*	5	1	1957
Fiziol. zhurn. SSSR (im. Sechenova)	Fiziologicheskii zhurnal im. I. M. Sechenova	Sechenov Physiological Journal USSR	National Institutes of Health*		1	1957
Fiziol(ogiya) rast.	Fiziologiya rastenii	Plant Physiology	American Institute of Biological Sciences	4	1	1957
	Geokhimiya	Geochemistry	The Geochemical Society		1	1958
FTT	Fizika tverdogo tela	Soviet Physics–Solid State	American Institute of Physics	1	1	1959
Izmerit. tekh(nika)	Izmeritel'naya tekhnika	Measurement Techniques	Instrument Society of America		1	1959
Izv. AN SSSR, O(td). Kh(im). N(auk)	Izvestiya Akademii Nauk SSSR; Otdelenie khimicheskikh nauk	Bulletin of the Academy of Sciences of the USSR; Division of Chemical Sciences	Consultants Bureau		1	1952

continued

Izv. AN SSSR, O(td). T(ekhn). N(auk): Met(all). i top.	(see Met. i top.)					
Izv. AN SSSR Ser. fiz(ich).	Izvestiya Akademii Nauk SSSR: Seriya fizicheskaya	Bulletin of the Academy of Sciences of the USSR: Physical Series	Columbia Technical Translations		1	1954
Izv. AN SSSR Ser. geofiz.	Izvestiya Akademii Nauk SSSR: Seriya geofizicheskaya	Bulletin (Izvestiya) of the Academy of Sciences USSR: Geophysics Series	American Geophysical Union		1	1954
Izv. AN SSSR Ser. geol.	Izvestiya Akademii Nauk SSSR: Seriya geologicheskaya	Izvestiya of the Academy of Sciences of the USSR: Geologic Series	American Geological Institute		1	1958
Kauch. i rez.	Kauchuk i rezina	Soviet Rubber Technology	Research Association of British Rubber Manufacturers	18	1	1959
	Kinetika i kataliz	Kinetics and Catalysis	Consultants Bureau	1	3	1960
	Koks i khimiya	Coke and Chemistry USSR	Coal Tar Research Association (Leeds, England)		1	1958
Kolloidn. zh(urn).	Kolloidnyi zhurnal	Colloid Journal	Consultants Bureau	14	1	1952
	Kristallografiya	Soviet Physics – Crystallography	American Institute of Physics	2	1	1957
Metallov. i term. obrabot. metal:	Metallovedenie i termicheskaya obrabotka metallov	Metal Science and Heat Treatment of Metals		6	1	1958
	Metallurg	Metallurgist	Acta Metallurgica		1	1957
Met. i top.	Metallurgiya i topliva	Russian Metallurgy and Fuels	Eagle Technical Publications		1	1960
Mikrobiol.	Mikrobiologiya	Microbiology	American Institute of Biological Sciences	26	1	1957
OS	Optika i spektroskopiya	Optics and Spectroscopy	American Institute of Physics		6	1959
	Pochvovedenie	Soviet Soil Science	American Institute of Biological Sciences		1	1958
	Priborostroenie	Instrument Construction	British Scientific Instrument Research Association		1	1959
Pribory i tekhn. eksp(eriments)	Pribory i tekhnika eksperimenta	Instruments and Experimental Techniques	Instrument Society of America		1	1957
Prikl. matem. i mekh.	Prikladnaya matematika i mekhanika	Applied Mathematics and Mechanics	American Society of Mechanical Engineers		1	1958
PTÉ	(see Pribory i tekhn. éks.)					
	Problemy Severa	Problems of the North	National Research Council of Canada			
Radiotekh.	Radiotekhnika	Radio Engineering	Massachusetts Institute of Technology*	12	1	1957
Radiotekh. i élektronika	Radiotekhnika i élektronika	Radio Engineering and Electronics	Massachusetts Institute of Technology*	2	1	1957
	Stanki i instrument	Machines and Tooling	Production Engineering Research Assoc.		1	1959
	Stal'	Stal (in English)	Iron and Steel Institute		1	1959
Stek. i keram.	Steklo i keramika	Glass and Ceramics	Consultants Bureau	13	1	1956
Svaroch. proiz-vo	Svarochnoe proizvodstvo	Welding Production	British Welding Research Association		4	1959
Teor. veroyat. i prim.	Teoriya veroyatnostei i ee primeneniie	Theory of Probability and Its Applications	Society for Industrial and Applied Mathematics		1	1956
Tsvet. Metally	Tsvetnye metally	Nonferrous Metals	Primary Sources		1	1960
UFN	Uspekhi fizicheskikh Nauk	Soviet Physics – Uspekhi (partial translation)	American Institute of Physics	66	1	1958
UKh	Uspekhi khimii	Russian Chemical Reviews	The Chemical Society (London)		1	1960
UMN	Uspekhi matematicheskikh nauk	Russian Mathematical Surveys	London Mathematical Society	15	1	1960
Usp. fiz. nauk	(see UFN)					
Usp. khim(ii)	(see UKh)					
Usp. matem. nauk	(see UMN)					
Usp. sovr. biol.	Uspekhi sovremennoi biologii	Russian Review of Biology	Oliver and Boyd		48	1959
Vest. mashinostroeniya	Vestnik mashinostroeniya	Russian Engineering Journal	Production Engineering Research Assoc.		4	1959
Vop. gem. i per. krovi	Voprosy gematologii i perelivaniya krovi	Problems of Hematology and Blood Transfusion	National Institutes of Health*		1	1957
Vop. onk.	Voprosy onkologii	Problems of Oncology	National Institutes of Health*		1	1957
Vop. virusol.	Voprosy virusologii	Problems of Virology	National Institutes of Health*		1	1957
Zav(odsk). lab(oratoriya)	Zavodskaya laboratoriya	Industrial Laboratory	Instrument Society of America	25	1	1959
ZhAKh Zh. anal(it). khimii	Zhurnal analiticheskoi khimii	Journal of Analytical Chemistry USSR	Consultants Bureau	7	1	1952
ZhETF; Zh. eksperim. i teor. fiz.	Zhurnal éksperimental'noi i teoreticheskoi fiziki	Soviet Physics–JETP	American Institute of Physics	28	1	1955
ZhFKh Zh. fiz. khimii	Zhurnal fizicheskoi khimii	Russian Journal of Physical Chemistry	The Chemical Society (London)		7	1959
ZhMÉI Zh(urn). mikrobiol. épidemiol. i immunobiol.	Zhurnal mikrobiologii, épidemiologii i immunobiologii	Journal of Microbiology, Epidemiology and Immunobiology	National Institutes of Health*		1	1957
ZhNKh; Zh(urn). neorgan(ich). khim(ii)	Zhurnal neorganicheskoi khimii	The Russian Journal of Inorganic Chemistry	The Chemical Society (London)		1	1959
ZhOKh; Zh(urn). obshch(ei) khimii	Zhurnal obshchei khimii	Journal of General Chemistry USSR	Consultants Bureau	19	1	1949
ZhPKh; Zh(urn). prikl. khimii	Zhurnal prikladnoi khimii	Journal of Applied Chemistry USSR	Consultants Bureau	23	1	1950
ZhSKh; Zh(urn). strukt. khimii	Zhurnal strukturnoi khimii	Journal of Structural Chemistry	Consultants Bureau	1	1	1960
ZhTF; Zh(urn). tekhn. fiz.	Zhurnal tekhnicheskoi fiziki	Soviet Physics–Technical Physics	American Institute of Physics	26	1	1956
Zh(urn). vyssh. nervn. deyat. (im. Pavlova)	Zhurnal vysshei nervnoi deyatel'nosti (im. I. P. Pavlova)	Pavlov Journal of Higher Nervous Activity	National Institutes of Health*		1	1958

*Sponsoring organization. Translation through 1960 issues is a publication of Pergamon Press.

SIGNIFICANCE OF ABBREVIATIONS MOST FREQUENTLY ENCOUNTERED IN SOVIET PERIODICALS

FIAN	Phys. Inst. Acad. Sci. USSR
GDI	Water Power Inst.
GITI	State Sci.-Tech. Press
GITTL	State Tech. and Theor. Lit. Press
GONTI	State United Sci.-Tech. Press
Gosenergoizdat	State Power Press
Goskhimizdat	State Chem. Press
GOST	All-Union State Standard
GTTI	State Tech. and Theor. Lit. Press
IL	Foreign Lit. Press
ISN (Izd. Sov. Nauk)	Soviet Science Press
Izd. AN SSSR	Acad. Sci. USSR Press
Izd. MGU	Moscow State Univ. Press
LEIIZhT	Leningrad Power Inst. of Railroad Engineering
LET	Leningrad Elec. Engr. School
LETI	Leningrad Electrotechnical Inst.
LETIIZhT	Leningrad Electrical Engineering Research Inst. of Railroad Engr.
Mashgiz	State Sci.-Tech. Press for Machine Construction Lit.
MEP	Ministry of Electrical Industry
MES	Ministry of Electrical Power Plants
MESEP	Ministry of Electrical Power Plants and the Electrical Industry
MGU	Moscow State Univ.
MKhTI	Moscow Inst. Chem. Tech.
MOPI	Moscow Regional Pedagogical Inst.
MSP	Ministry of Industrial Construction
NII ZVUKSZAPIOI	Scientific Research Inst. of Sound Recording
NIKFI	Sci. Inst. of Modern Motion Picture Photography
ONTI	United Sci.- Tech. Press
OTI	Division of Technical Information
OTN	Div. Tech. Sci.
Sredizdat	Construction Press
TOE	Association of Power Engineers
TsKTI	Central Research Inst. for Boilers and Turbines
TsNIEL	Central Scientific Research Elec. Engr. Lab.
TsNIEL-MES	Central Scientific Research Elec. Engr. Lab.-Ministry of Electric Power Plants
TsVTI	Central Office of Economic Information
UF	Ural Branch
VIESKh	All-Union Inst. of Rural Elec. Power Stations
VNIIM	All-Union Scientific Research Inst. of Metrology
VNIIZhDT	All-Union Scientific Research Inst. of Railroad Engineering
VTI	All-Union Thermotech. Inst.
VZEI	All-Union Power Correspondence Inst.

NOTE: Abbreviations not on this list and not explained in the translation have been transliterated, no further information about their significance being available to us. —Publisher.